

Radiation Damage in Semiconductors

Mara Bruzzi

INFN, University of Florence, Italy

- ✓ Radiation environments and working principles
- ✓ Microscopic radiation damage
- ✓ Impact of Defects on HEP detector properties
- ✓ Macroscopic radiation damage (Si)
- ✓ Material Engineering (Si)
- ✓ Other examples: Dosimetry and Space solar Cells
- ✓ Conclusions



Typical working environments for radiation damage

Environment	Radiation type	Typical exposure
Fission reactor	0.1-5MeV n	$5 \times 10^{17} \text{ m}^{-2} \text{s}^{-1}$
Fusion reactor	0.1-14MeV n	$8 \times 10^{18} \text{ m}^{-2} \text{s}^{-1}$
Space	6eV photons	$10^{20} \text{ m}^{-2} \text{s}^{-1}$
	10keV-3MeV β	$5 \times 10^{12} \text{ m}^{-2} \text{s}^{-1}$
	1MeV-300MeV p	$4 \times 10^9 \text{ m}^{-2} \text{s}^{-1}$
Ion accelerator	15 MeV p	$6 \times 10^{16} \text{ m}^{-2} \text{s}^{-1}$
High energy physics experiments	n,p , pions	$10^{14}-10^{16} \text{ cm}^{-2}$
radiotherapy	X, e, p	10kGy

High Energy Physics Experiments

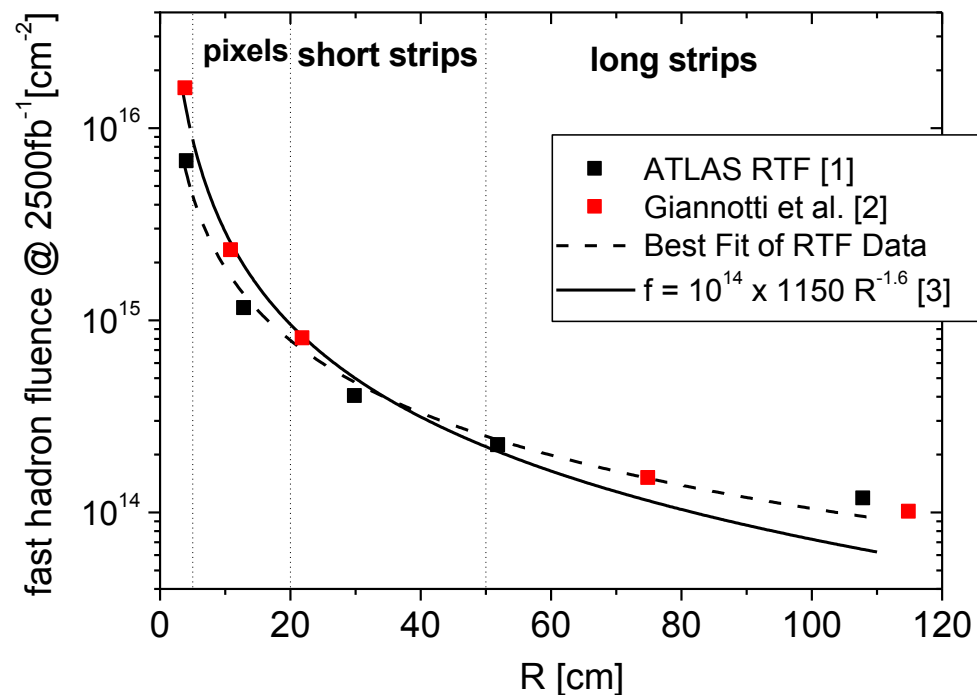
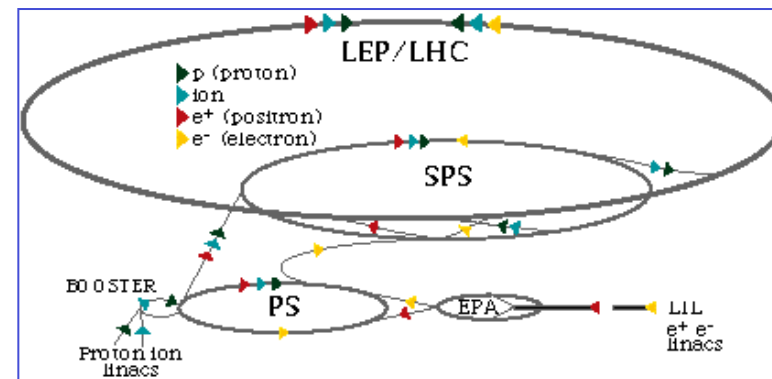
High energy Physics experiments
at Large Hadron Collider (LHC),
CERN, Geneva

p-p collision $L \sim 10^{34} \text{ cm}^{-2} \text{ s}^{-1}$

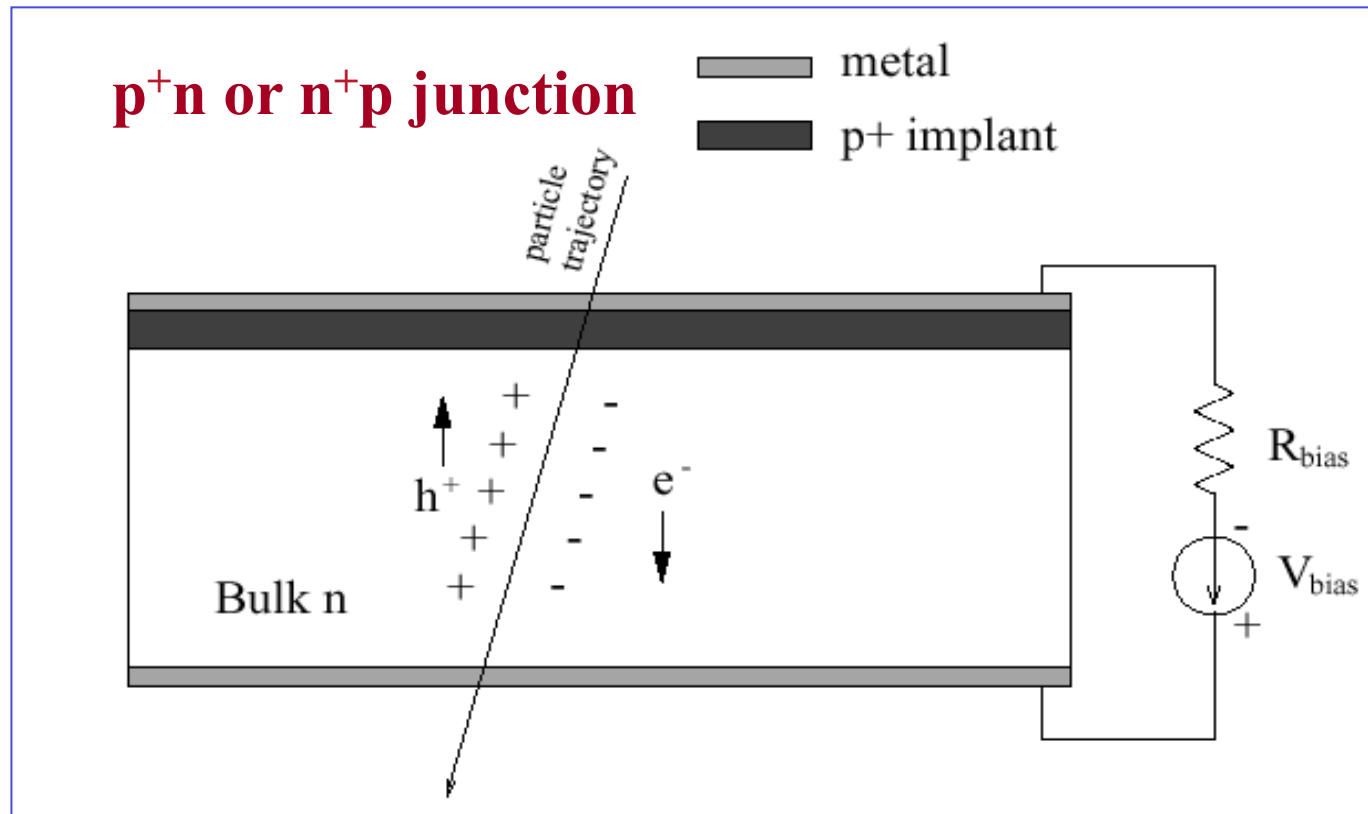
$E_{\text{cm}} = 14 \text{ TeV}$

Increase of luminosity of LHC up
to $10^{35} \text{ cm}^{-2} \text{ s}^{-1}$ discussed since
2002.

Main constraint is the survival of
the Si detector tracker to the
exceptionally high fluences of fast
hadrons.



Working principle of a semiconductor detector



Ohmic contact

Insulating $\rho > 10^{10} \Omega \text{cm}$

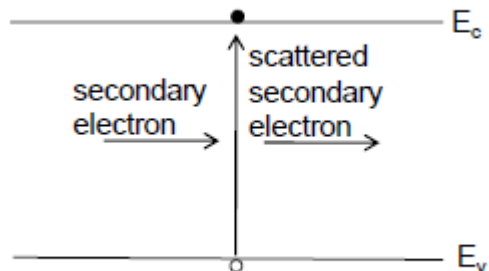
Ohmic contact

Schottky contact

n / p semiconductor

Ohmic contact

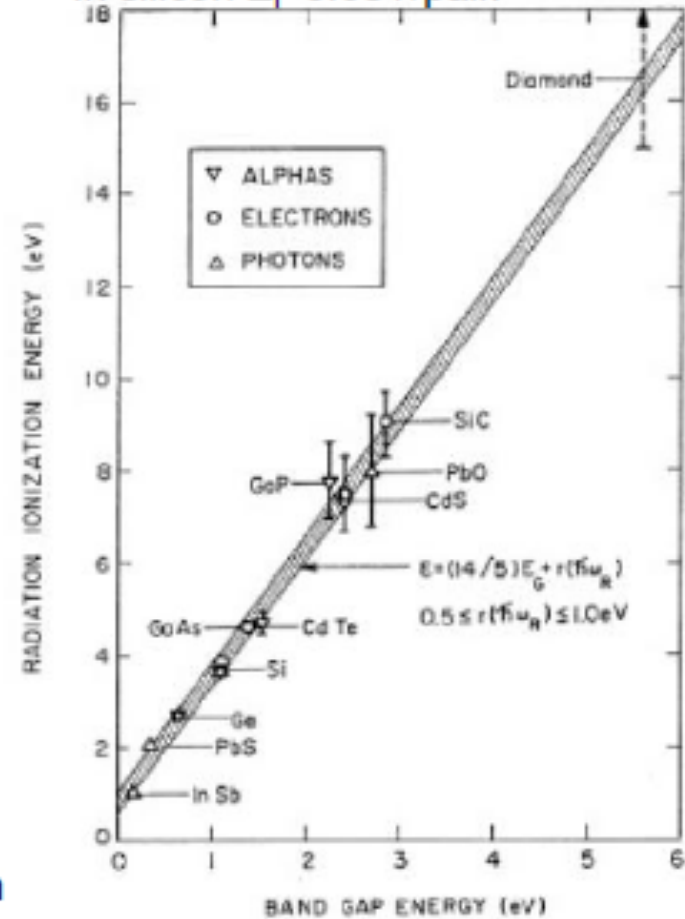
Selection of semiconductor gap



region

E_i/E_{gap} constant (at fixed T) for many semiconductors under general conditions.

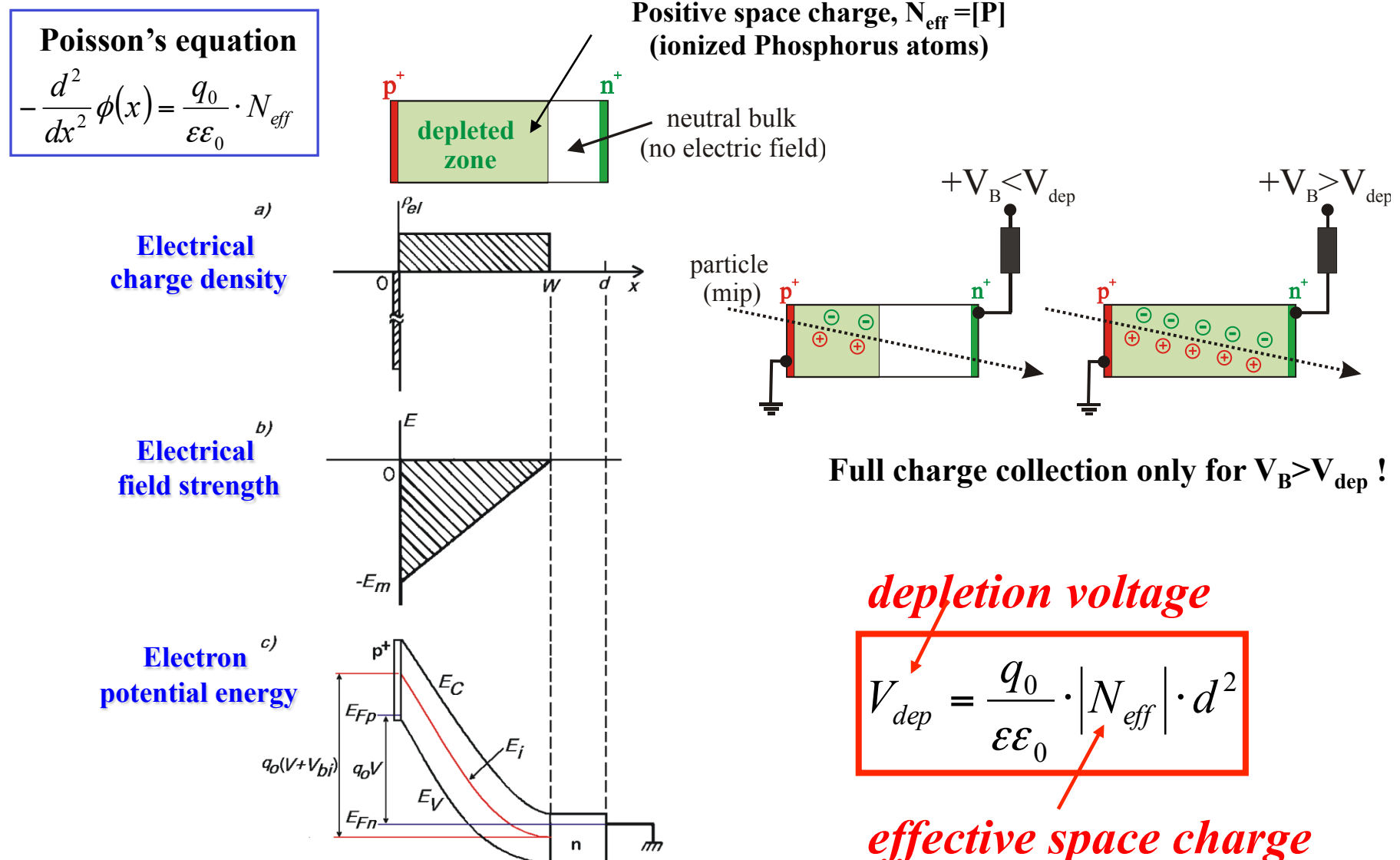
In silicon $E_i \approx 3.6 \text{ eV/pair}$.



Semiconductor used for detector applications

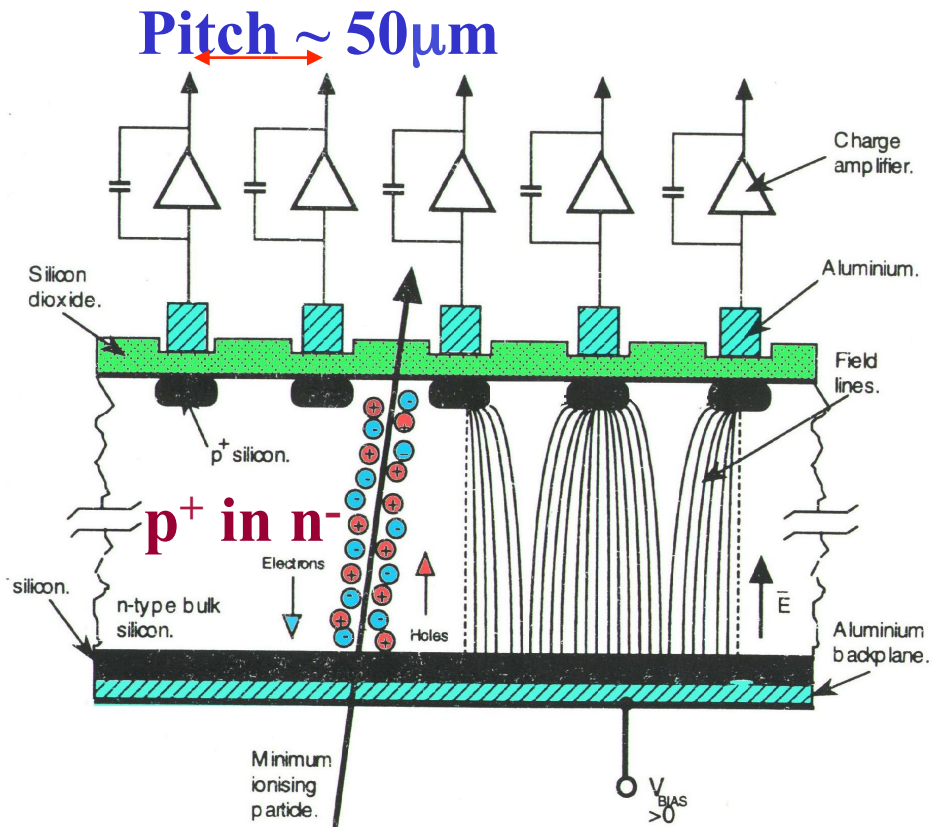
Property	Si	Diamond	Diamond	4H SiC
Material	MCz, FZ, epi	Polycrystal	single crystal	epitaxial
E _g [eV]	1.12	5.5	5.5	3.3
E _{breakdown} [V/cm]	3·10 ⁵	10 ⁷	10 ⁷	2.2·10 ⁶
μ _e [cm ² /Vs]	1450	1800	>1800	800
μ _h [cm ² /Vs]	450	1200	>1200	115
v _{sat} [cm/s]	0.8·10 ⁷	2.2·10 ⁷	2.2·10 ⁷	2·10 ⁷
Z	14	6	6	14/6
ε _r	11.9	5.7	5.7	9.7
e-h energy [eV]	3.6	13	13	7.6
Density [g/cm3]	2.33	3.515	3.515	3.22
Displacem. [eV]	13-20	43	43	25
e-h/μm for mips	~80	36	36	55
Max ccd [μm]	>500	300	800	55
Max wafer φ	6"	6"	~1.4cm	2"
Commercial	yes	H.Kagan talk	H.Kagan talk	limited
CERN R&Ds	RD50, RD39	RD42	RD42	RD50

Reminder: Reverse biased abrupt p⁺-n junction



Physics of Micro-strip Silicon Detectors

- Highly segmented silicon detectors have been used in Particle Physics experiments for nearly 30 years. They are the favourite choice for Tracker and Vertex detectors (high resolution, speed, low mass, relatively low cost, and now important, **radiation hard**)
- The principle application has been to detect the passage of ionising radiation with high **spatial** resolution and good efficiency.
- Segmentation → position
- Depletion depth → efficiency
- ~ $80e/h$ pairs/ μm produced by passage of minimum ionising particle ‘mip’



Resolution $\sim 5\mu m$

Relevant parameters of a detector

Leakage Current

$$J_{inversa} = \frac{1}{2} q \frac{n_i}{\tau_0} W \alpha \sqrt{V_{rev}}$$

Capacitance

$$C = \frac{\epsilon \cdot Area}{d}$$

Active region thickness

$$d = \sqrt{\frac{2\epsilon}{qN_{eff}}} V_{rev}$$

Effective space charge in depleted region

$$N_{eff} = \frac{2 \cdot \epsilon \cdot (V_{dep} + V_{bi})}{q \cdot W^2}$$

Physical parameters and detector requirements

- High Signal / Sensitivity
- Low Noise
- High spatial resolution
- High speed
- High stability



- ● Low energy for e-h generation → small gap
- ● Low leakage current → high gap
- ● Low full depletion voltage: high resistivity
- ● High mobility
- ● Radiation Hardness

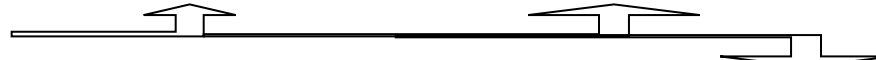
Radiation Damage RoadMap for Semiconductor Devices

Microscopic Damage

- Radiation induced defects

Traps

Recombination centres



Extended defects or clusters

- Carrier removal and increase of resistivity



Midgap Fermi level pinning

Macroscopic Damage

- Increase of the leakage current
- Change in N_{eff} and space charge sign - underdepletion
- Decrease of minority carrier lifetime and diffusion length



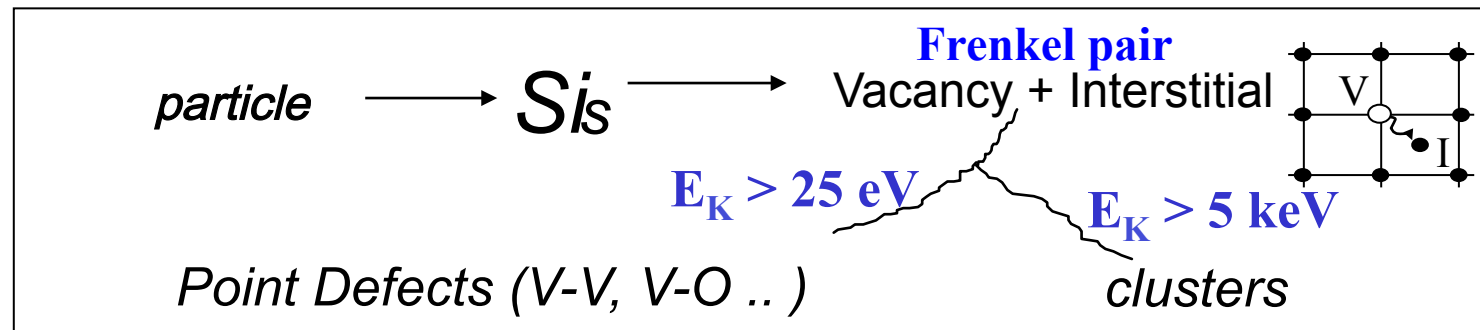
Decrease of the charge collection, sensitivity and energy conversion efficiency

Mara Bruzzi, Danno da radiazione in semiconduttori

Scuola Nazionale rivelatori ed elettronica per fisica delle alte energie , astrofisica 12 Aprile 2011,
Legnaro, Italy

Microscopic Radiation Damage

Mara Bruzzi, Danno da radiazione in semiconduttori
Scuola Nazionale rivelatori ed elettronica per fisica delle alte energie , astrofisica 12 Aprile 2011,
Legnaro, Italy



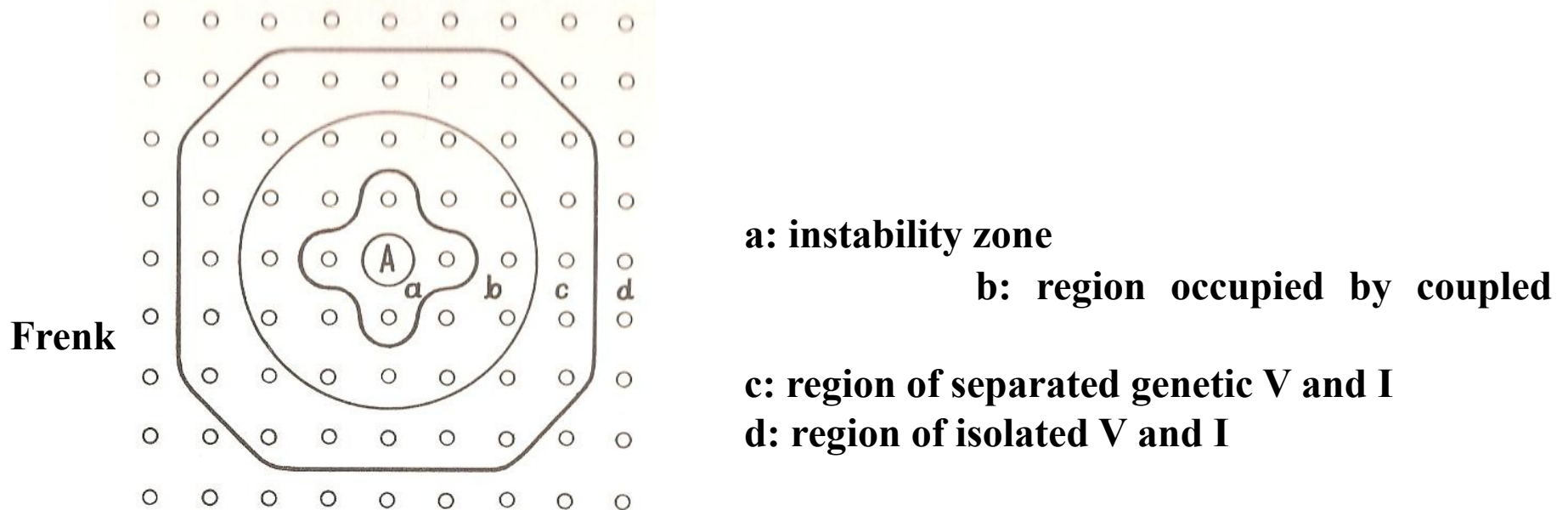
Simulation of Microscopic Damage

- ✓ Generation of hadronic interactions
- ✓ Transport of the produced heavy recoils
- ✓ Migration of V and I to form stable defects



Character of the Frenkel Pair

Character of Frenkel pair depend on relative distance of V and I:
if this is not too large ranges the atomic environment deformation of V and I overlap and their coupling is considerable (coupled Frenkel pair). If PKA departed from its site of several lattice constants separated V and I are created: position of energy levels diffusion coefficients may be appreciably different from those of coupled pair.



While the dimensions of the instability zones in metals are relatively large, the situation in semiconductor is contrary in most cases, the interstitial and vacancy being in neighboring cells, instability zone is restricted to one elementary cell.

Non Ionizing Energy Loss (NIEL) and Threshold Energy E_d

Proportionality between $N_t = \text{defect concentration}$ and $\Phi = \text{particle flux}$ assumed proportional through atomic concentration N_0 and a proportionality coefficient $\sigma(E)$ depending on the energy E of the incoming particle :

$$N_t = \sigma(E) N_0 \phi$$

$\sigma(E) = \text{defect formation cross section}$. Cross section can be evaluated e.g. for electrons as:

$$\sigma(E) = \pi \sigma_0 \left(\frac{E_M}{E_d} - 1 \right) \quad E_M = \frac{4mE}{M} \quad \sigma_0 = \left(\frac{Ze^2}{2E} \right)^2$$

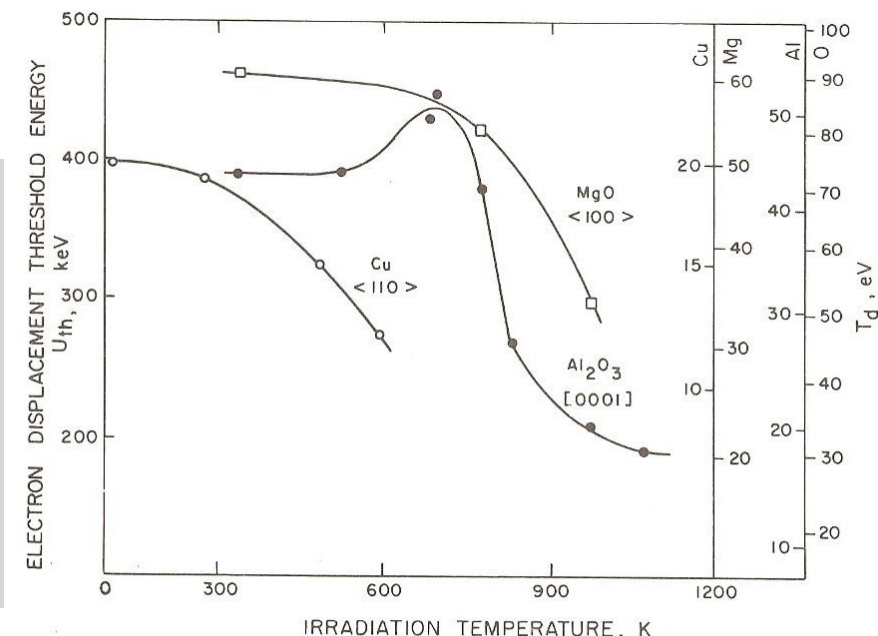
With Z, M atomic number and mass of a crystal atom and m electron mass, E_M maximum energy transferred. Thus, $\sigma(E)$ tends to zero when E_M is lower than the value E_d , energy required to separate the Frenkel pair.



Displacement energies E_d depend on :

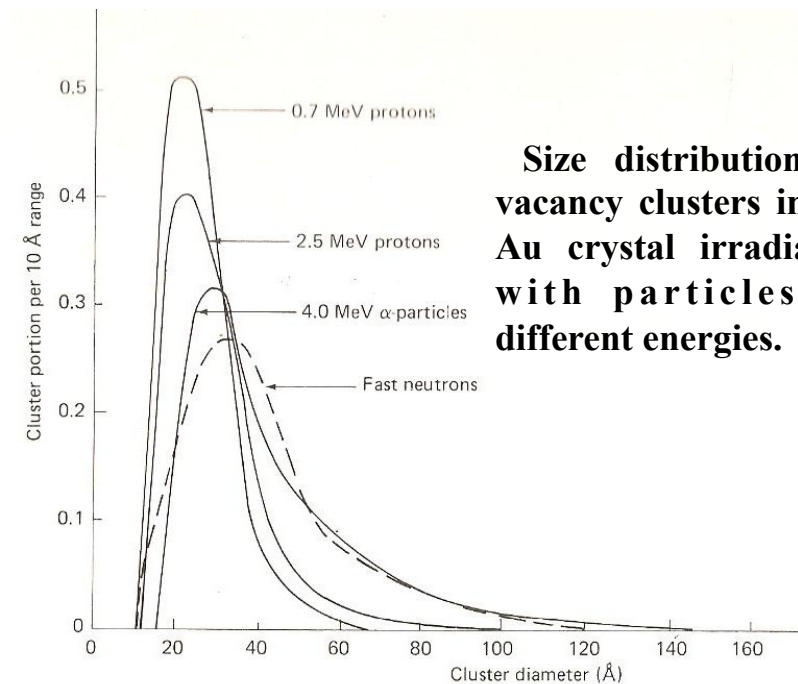
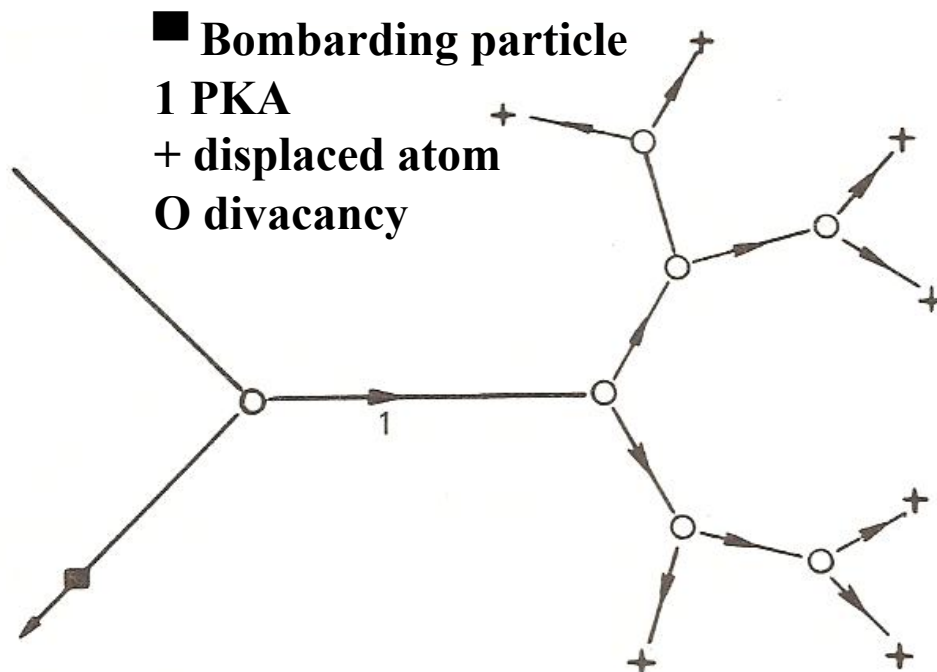
- (i) Bond strength
- (ii) Space available for accommodating an interstitial atom in the structure (may involve electrostatic repulsion for charged interstitials)
- (iii) Form of interstitial
- (iv) Temperature of irradiation

Material	T^d (eV)	Material	T^d (eV)
C (graphite)	28–31	SiC	45–90
C (diamond)	80	MgO	64(Mg) 60(O)
Si	11–22	Al_2O_3	18(Al) 76(O)
Ge	12–30	MgAl_2O_4	56(O)
GaAs	9(Ga) 9(As)	ZnO	40(Zn) 57(O)
ZnS	10(Zn) 15(S)	UO_2	40(U) 20(O)
CdS	7(Cd) 9(S)	BeO	76(O)



Cascades and cluster formation

Depending on its initial energy and crystallographic direction the process of collision and displacements initiated by the PKA can involve secondary knock-on atoms in a cascade, giving rise to separate Frenkel pairs and defective clusters composed of several vacancies and interstitials.



Vacancy amount and distribution depends on particle kind and energy

^{60}Co -gammas

- Compton Electrons
- with max. $E_{\gamma} \approx 1 \text{ MeV}$
- (no cluster production)

Electrons

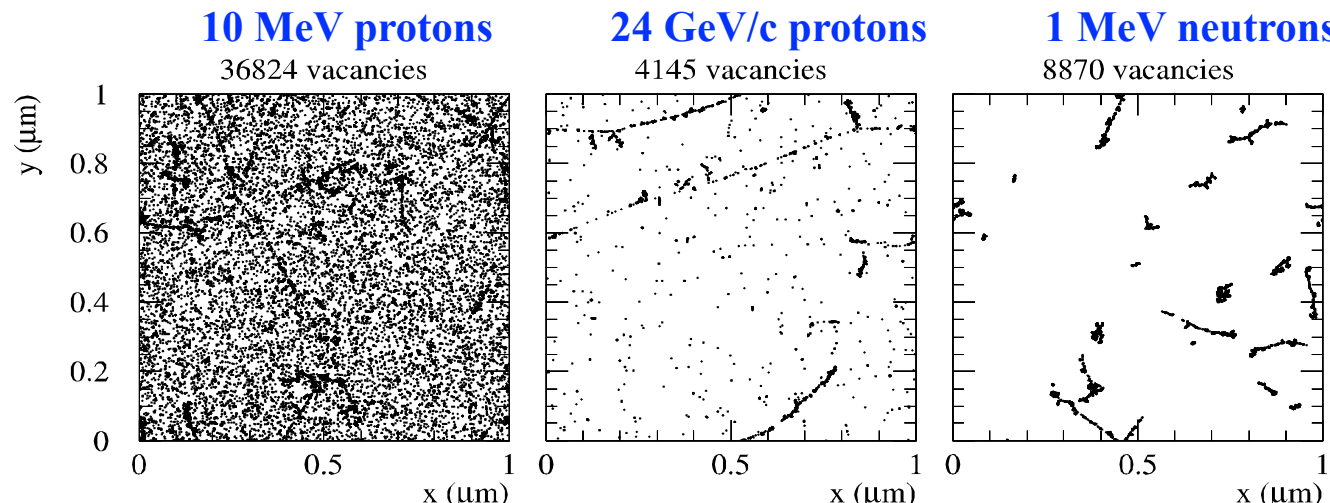
- $-E_e > 255 \text{ keV}$ for displacement
- $-E_e > 8 \text{ MeV}$ for cluster

Neutrons (elastic scattering)

- $-E_n > 185 \text{ eV}$ for displacement
- $-E_n > 35 \text{ keV}$ for cluster

Only point defects \longleftrightarrow point defects & clusters \longleftrightarrow Mainly clusters

Initial distribution of vacancies in $(1\mu\text{m})^3$ after 10^{14} particles/cm²



[Mika Huhtinen NIMA 491(2002) 194]



Mara Bruzzi, Danno da radiazione in semiconduttori
Scuola Nazionale rivelatori ed elettronica per fisica delle alte energie , astrofisica 12 Aprile 2011,
Legnaro, Italy



How to normalize radiation damage from different particles?

- **NIEL - Non Ionizing Energy Loss scaling using hardness factor κ**

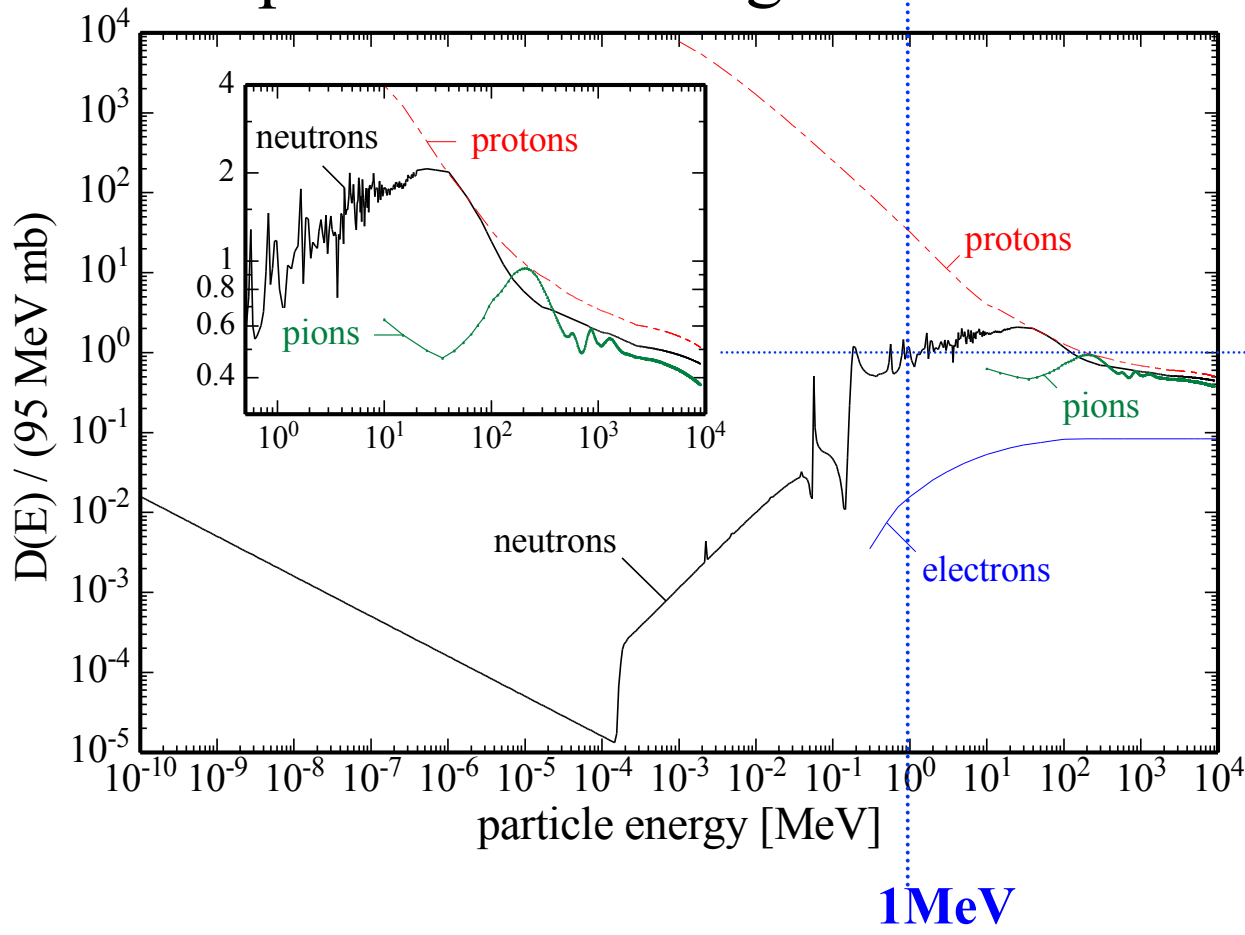
$$K = \frac{1}{D(1\text{MeV neutrons})} \cdot \frac{\int D(E) \phi(E) dE}{\int \phi(E) dE}$$

of a radiation field (or monoenergetic particle) with respect to 1 MeV neutrons

- **E** energy of particle
- **D(E)** displacement damage cross section for a certain particle at energy E
 $D(1\text{MeV neutrons})=95 \text{ MeV}\cdot\text{mb}$
- **$\phi(E)$** energy spectrum of radiation field
-

The integrals are evaluated for the interval $[E_{\text{MIN}}, E_{\text{MAX}}]$, being E_{MIN} and E_{MAX} the minimum and maximum cut-off energy values, respectively, and covering all particle types present in the radiation field

NIEL – Non Ionizing Energy Loss Displacement damage functions



1 **1 MeV
neutron
equivalent
damage**

- Hypothesis: Damage parameters scale with the NIE
 - Be careful, does not hold for all particles & damage parameters (see later)

Secondary defect formation in silicon

- Primary defect generation

I, I_2 higher order I

$\Rightarrow I$ - CLUSTER

$V, V_2,$ higher order V

$\Rightarrow V$ - CLUSTER

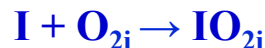
- Secondary defect generation

Dopants : P, B

Main impurities in silicon: Carbon C_s

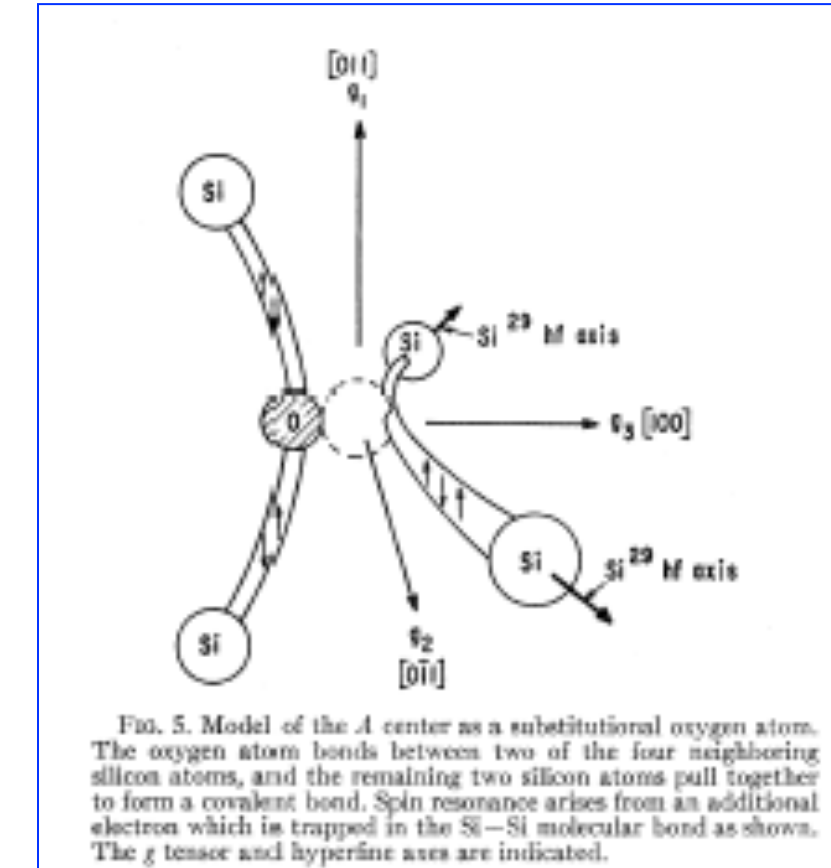
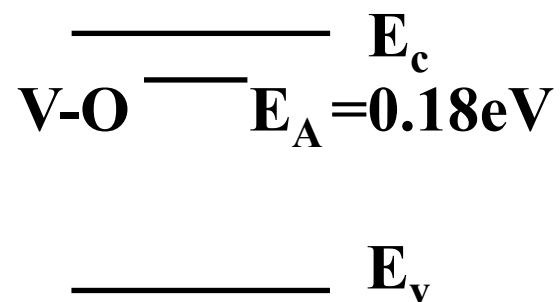
Oxygen O_i

Oxygen dimer: O_{2i}



Si Point-defects : The A centre

oxygen-doped silicon dominant centers of vacancy capture may be isolated interstitials O_i and trapping results in the formation of the V-O centre, so-called A centre

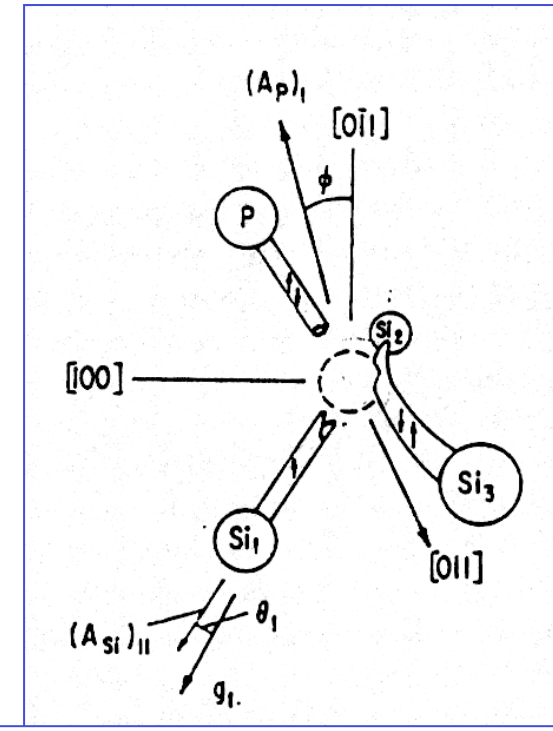
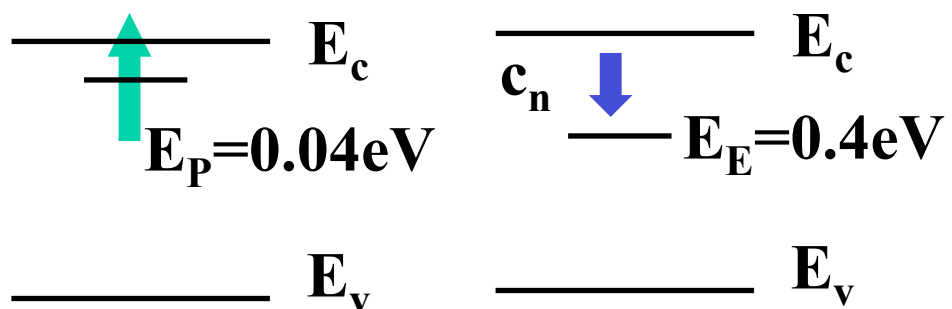


V-O defect (A centre)

Watkins, Corbett: Phys.Rev.,121,4, (1961),1001

Si Point-defects: The E centre

In Phosphorous doped Si vacancy is also trapped by P to create the P-V defect, the so-called E centre. This changes the doping of the crystal, removing the doping atom P and creating an acceptor-like energy level at $E_t = 0.42\text{eV}$ → carrier removal → doped semiconductors become almost intrinsic after heavy irradiation

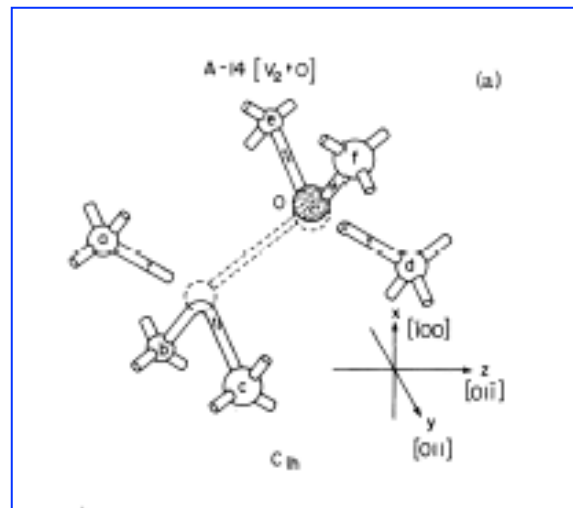


Phosphorous-Vacancy
P-V (E centre)

Corbett, Watkins et al, PRB, 60s

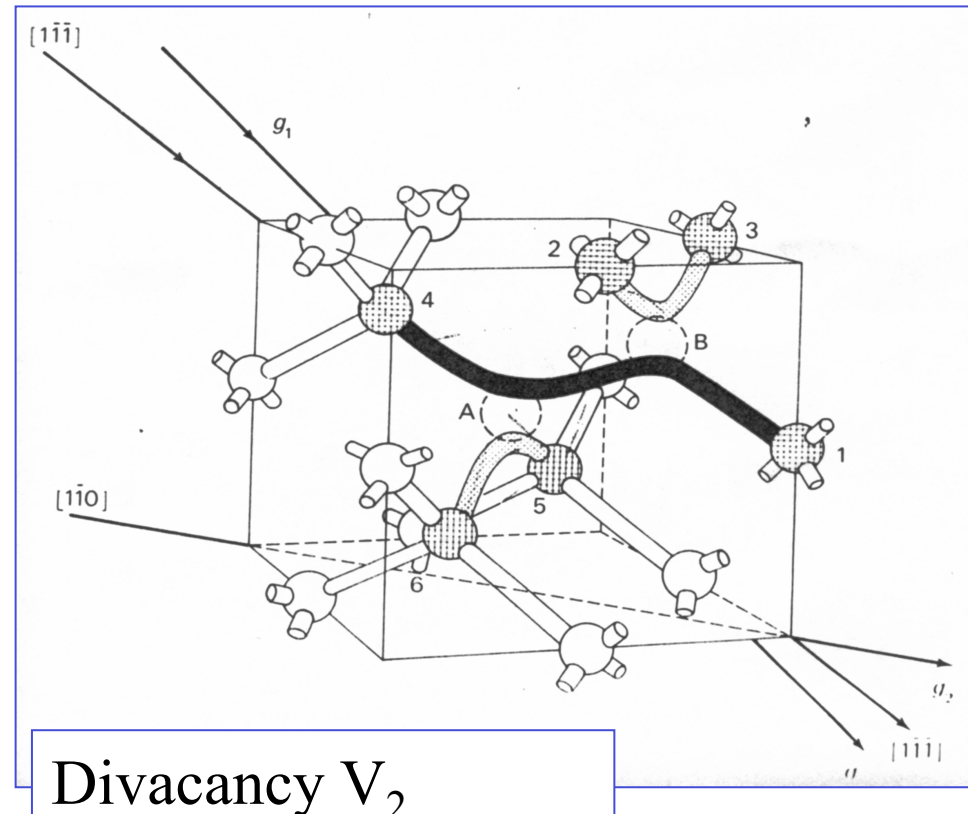
Si Point-defects involving more than one vacancy

Point-defects can involve more than one vacancy, creating deep levels in the Si gap: V_2 , V_2O , V_3O etc..



V_2O defect

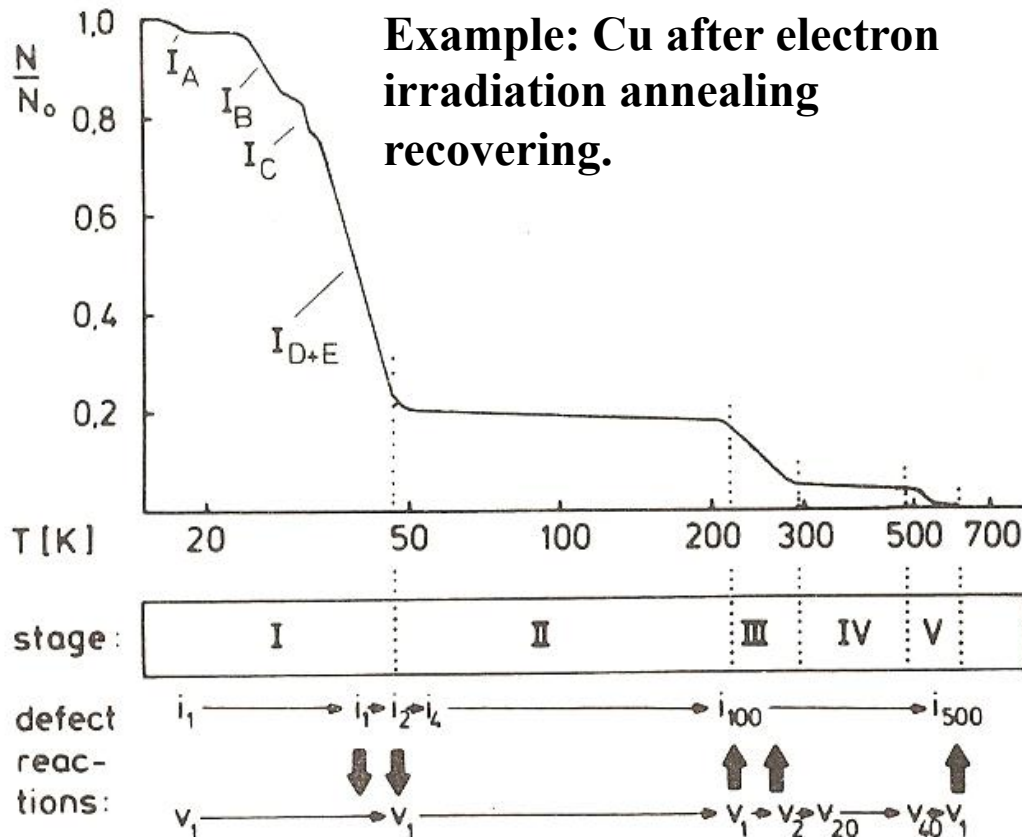
Lee, Corbett: Phys.Rev.B,13,6, (1976),2653



Divacancy V_2

Annealing

Defect configuration can significantly change by heating up the irradiated sample or storing at T higher than that of irradiation.



I₁, V₁ single vacancy, interstitial
I₂, V₂ di-interstitials ,divacancies...

I_A –I_E collapse of close to separated Frenkel pairs

II: formation of clusters as small interstitial loops

III: vacancies migrate and annihilate at interstitial clusters & vacancy agglomerate in vacancy clusters

IV: vacancy clusters grow in size

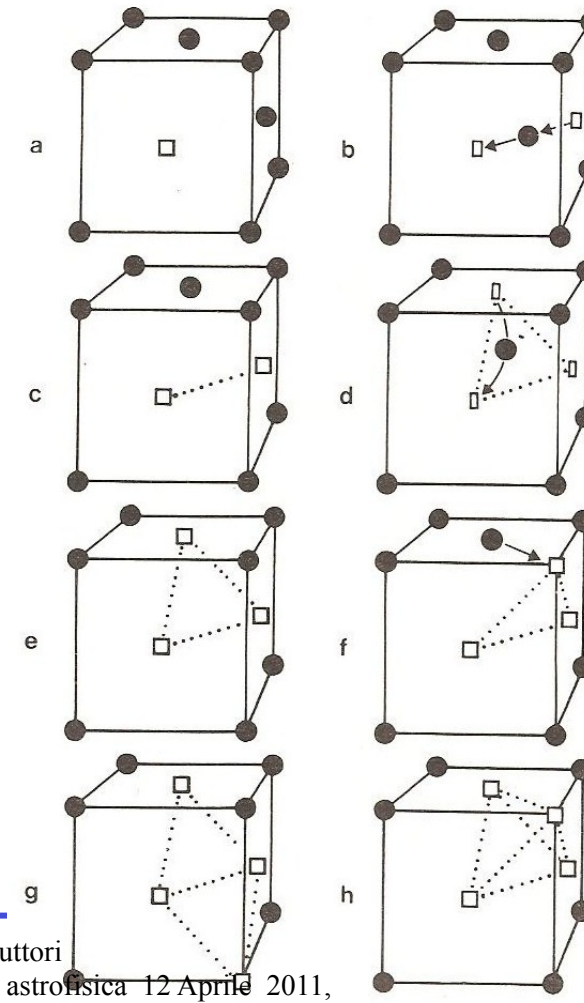
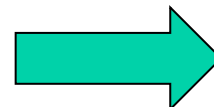
V: vacancy clusters dissociate thermally and annihilate at interstitial loops: **radiation damage is removed**

Diffusion and migration

Diffusion coefficients of isolated vacancies and interstitials are usually non negligible in the temperature ranges of interest. This leads to their migration to annihilation reactions or formation of quasimolecules .

vacancies in the fcc lattice and migration by jumping of one of the neighboring atoms to the vacancy site

- (a) Single vacancy in an fcc lattice
- (b) Vacancy migration saddle point
- (c) Divacancy
- (d) Divacancy migration saddle point
- (e) Trivacancy
- (f) Trivacancy reorientation
- (g) (h) tetravacancies



Electrical activity of energy levels related to defects



Mara Bruzzi, Danno da radiazione in semiconduttori
Scuola Nazionale rivelatori ed elettronica per fisica delle alte energie , astrofisica 12 Aprile 2011,
Legnaro, Italy



Capture coefficients

Defects are usually characterised by energy levels within the forbidden gap interacting with both conduction and valence bands, through capture and emission of electron or hole.

N_t = total concentration of energy levels;

n = concentration of free electrons,

$\langle v_n \rangle$ = rms electron thermal velocity;

σ_n = electron capture cross section;

n_t = concentration of occupied levels,

p = concentration of free holes;

$\langle v_p \rangle$ = rms hole thermal velocity

σ_p = hole capture cross section;

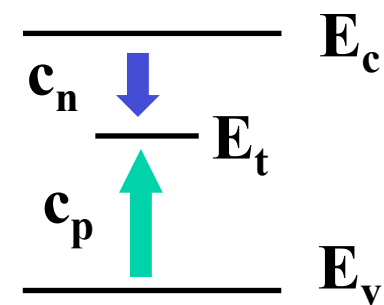
If a trap is exposed to a flux of free electrons per unit area: $n\langle v \rangle$, then number of electrons captured by the unoccupied states in interval Δt is:

$\Delta n_t = \sigma_n \langle v_n \rangle n (N_t - n_t) \Delta t$ then capture rate is:

$$c_n = \frac{\Delta n / \Delta t}{N_t - n_t} = \sigma_n \langle v_n \rangle n$$

Similarly for holes:

$$c_p = \frac{\Delta p / \Delta t}{N_t - n_t} = \sigma_p \langle v_p \rangle p$$



Emission constants

Occupancy of the level is determined by the competition of emission and capture processes. Electrons are emitted and holes captured by energy levels occupied with electrons (n_t), while electrons are captured and holes emitted by unoccupied energy levels ($N_t - n_t$). If $e_{n,p}$ = rate of emission for electrons and holes, rate of change of occupancy is:

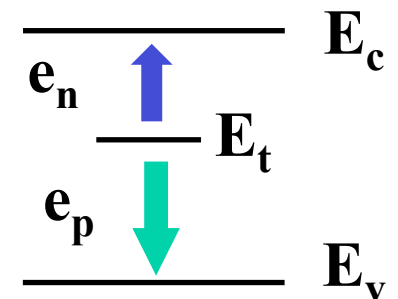
$$\frac{dn_t}{dt} = (c_n + e_p)(N_t - n_t) - (e_n + c_p)n_t$$

In thermal equilibrium emission and capture process must balance i.e. the rates of capture and emission must be equal both for electrons and holes:

$$e_n n_t = c_n (N_t - n_t)$$
$$e_p (N_t - n_t) = c_p n_t$$

Therefore the occupancy of traps is determined by:

$$\frac{n_t}{N_t} = \frac{c_n}{c_n + e_n} = \frac{e_p}{c_p + e_p}$$



Thermal Equilibrium

In thermal equilibrium the occupancy of traps is defined by the Fermi-Dirac distribution. For a deep state with degeneracy g_0 when empty with electrons and g_1 when occupied, in a system with Fermi energy E_F , the occupancy is defined as:

$$\frac{n_t}{N_t} = \left[1 + \frac{g_0}{g_1} \exp\left(\frac{E_t - E_F}{KT}\right) \right]^{-1}$$

$$e_n = c_n \exp\left(\frac{E_t - E_F}{KT}\right)$$

Assuming $g_0/g_1 = 1$ we obtain:

$$e_p = c_p \exp\left(\frac{E_F - E_t}{KT}\right)$$

$$n = N_c \exp\left(\frac{E_F - E_C}{KT}\right)$$

$$e_n = \sigma_n \langle v_n \rangle N_c \exp\left(-\frac{E_C - E_t}{KT}\right)$$

Finally, as:

$$p = N_v \exp\left(\frac{E_V - E_F}{KT}\right)$$

we get:

$$e_p = \sigma_p \langle v_p \rangle N_v \exp\left(-\frac{E_t - E_V}{KT}\right)$$



Non-equilibrium : Shockley-Read-Hall statistics

Out of equilibrium excess carriers are generated, and we set $n=(n_0+\Delta n)$, $p=(p_0+\Delta p)$, with $\Delta n=\Delta p$, of course. In this conditions $np>n_i^2$ and there is a net flow of current through the bands. In particular, at steady state, it is subject to the condition $R_e=R_h=U$, where U is the recombination-generation rate. The result is:

$$U = \frac{np - n_i^2}{(n + n_1)\tau_h + (p + p_1)\tau_e}.$$

U determines the rate at which excess carriers recombines through the defect level:

$$\frac{dn}{dt} = \frac{dp}{dt} = -U.$$

The following short notation has been used:

$$\tau_{e/h} = \frac{1}{\sigma_{e/h} v_{e/h} N_t},$$

$$n_1 = n_i \exp\left(\frac{E_t - E_i}{kT}\right), p_1 = n_i \exp\left(\frac{E_i - E_t}{kT}\right).$$



Minority Carrier Lifetime

Some particular cases are identified depending on excess carrier concentration. We consider, as an example, high resistivity p-type silicon $p_0 \gg p_1, n_1$:

$$U \approx \frac{\Delta n \cdot p_0}{\Delta n(\tau_e + \tau_h) + p_0 \tau_e}$$

Low injection level. In this situation $p_0 \gg \Delta n$ (at least three orders of magnitude). The recombination-generation rate simplifies into:

$$U \approx \frac{\Delta n}{\tau_e}.$$

τ_e is the lifetime of electrons. Because electrons are in this material the minority carriers, this characteristic time is customarily called "minority carriers lifetime".

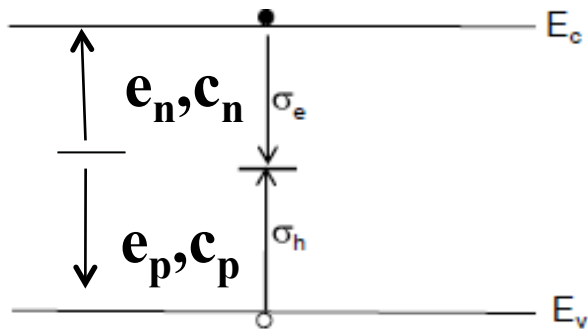
Diffusion length: $L_e = \sqrt{D_e \tau_e}$

$D_e = \mu_e K \cdot T / e$



Generation Recombination phenomenon via midgap levels

Indirect recombination via midgap levels dominant in Si...



.. a two-step process where both electron and hole are captured by the centre

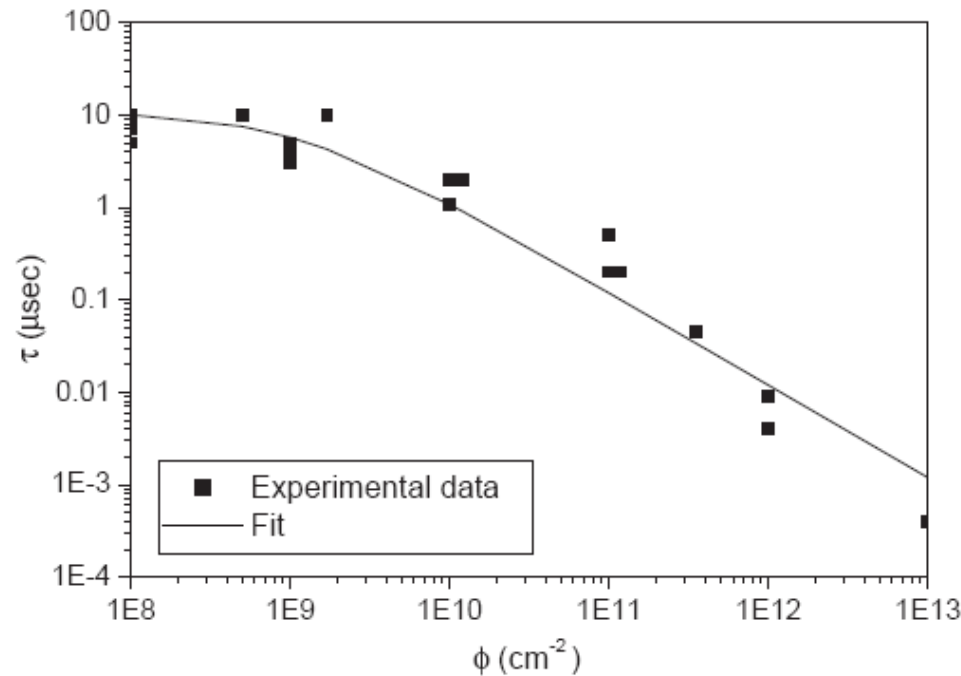
As N_t grows with irradiation τ decrease with the accumulated dose.

recombination leads to a decrease in sensitivity (photovoltaic mode) during device lifetime.

Further: Generation via midgaps leads to an increase of leakage current (reverse voltage applied) :

$$U \approx \frac{n_i}{\tau_e} \alpha T^2 \exp\left(-\frac{E_g}{KT}\right)$$

Deterioration of the minority carrier lifetime with irradiation



$$\frac{1}{\tau} = \frac{1}{\tau_0} + k_\tau \phi,$$

10MeV protons

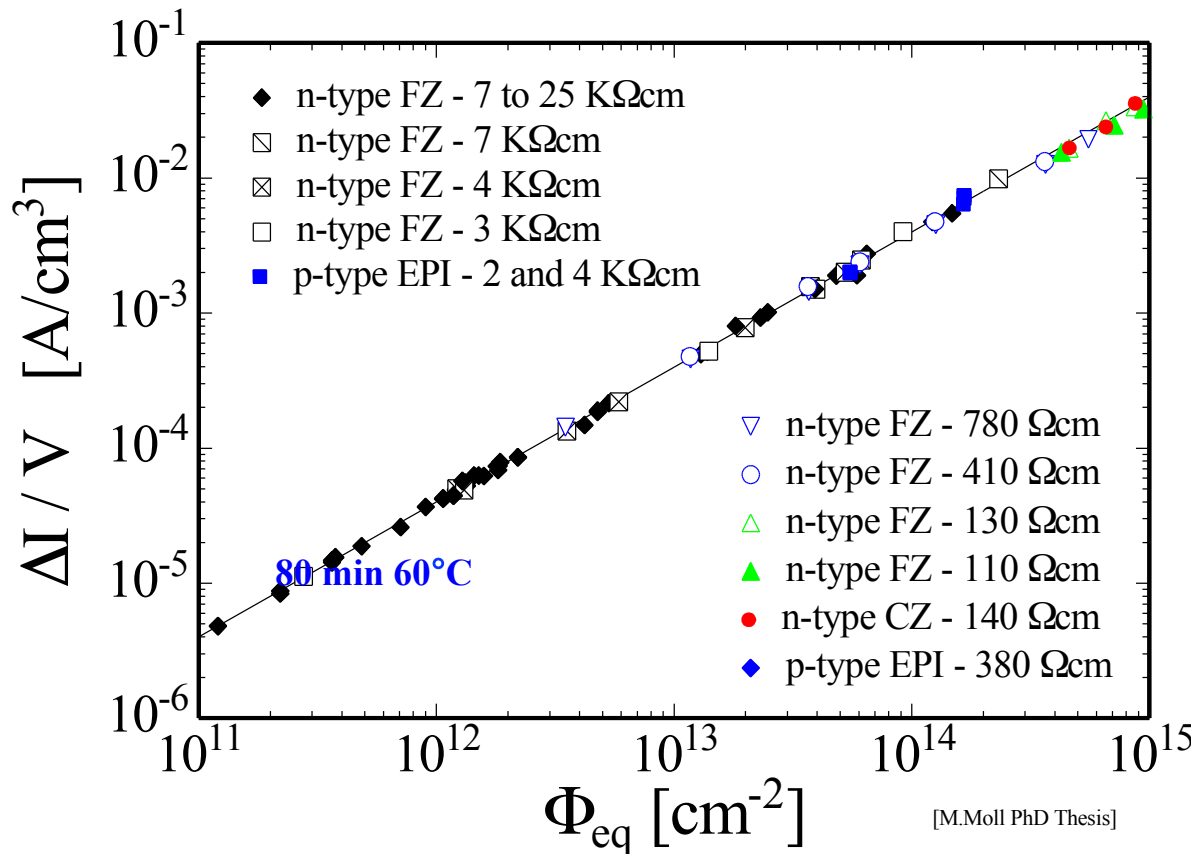
$$k_\tau = (1.52 \pm 0.05) \times 10^{-11} \mu\text{s}^{-1} \text{ cm}^2$$

$$L = \sqrt{D \cdot \tau}$$

$$k_L = (5.6 \pm 0.2) \times 10^{-7}$$

10 MeV protons produces a 3000 times larger equivalent damage compared to 1 MeV electrons

▪ Change of Leakage Current (as a function of hadron irradiation)



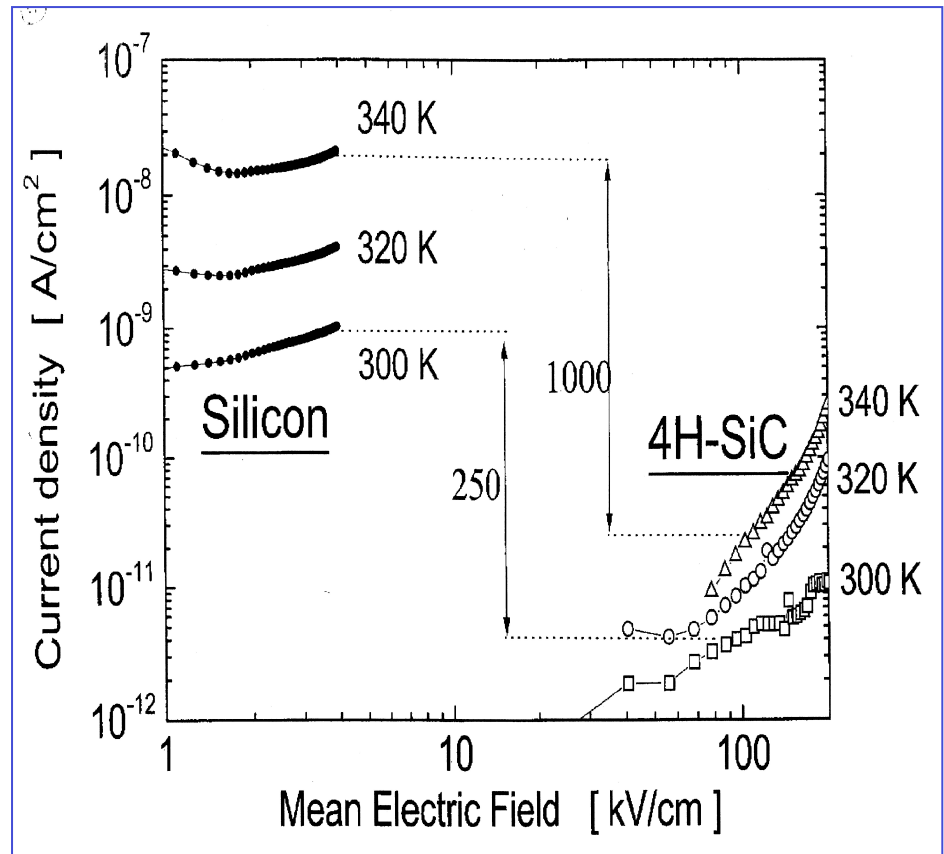
$$\alpha = \frac{\Delta I}{V \cdot \Phi_{eq}}$$

- **Damage parameter α**
Leakage current per unit volume and particle fluence

- **α is constant over several orders of fluence and independent of impurity concentration in Si**
⇒ can be used for fluence measurement

Leakage current depends on energy gap exponentially . High band gap materials are intrinsically radiation hard because even at high fluences of irradiation $<1\text{pA/cm}^2$

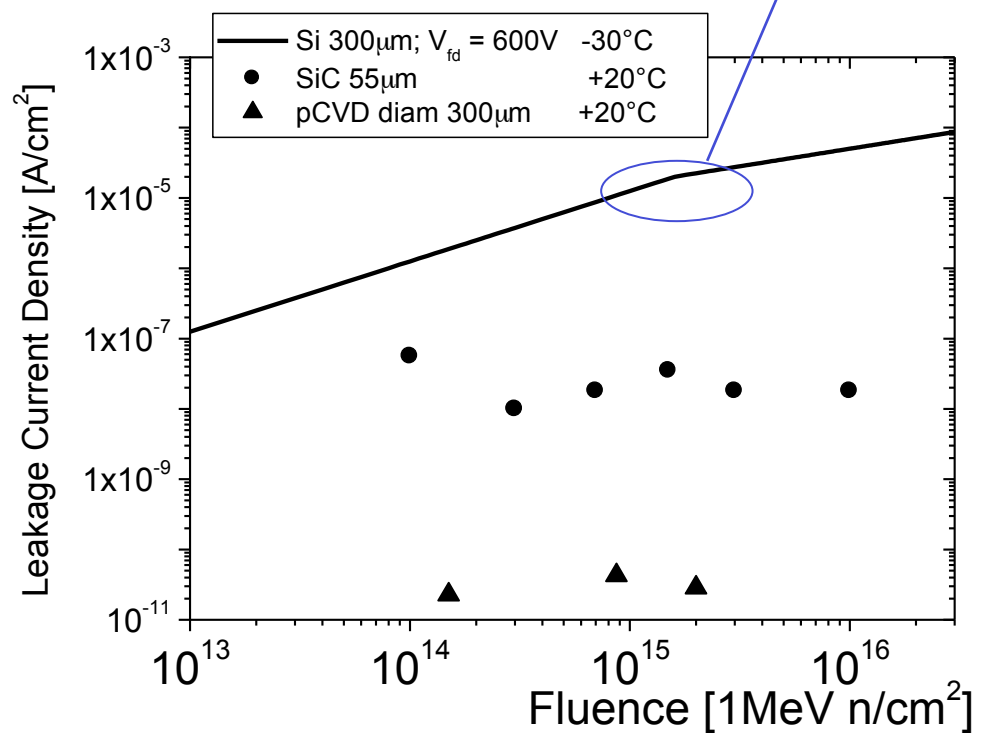
$$\text{Silicon: } J(\Phi) = \alpha \cdot \Phi \cdot d$$



$$T = -30^\circ\text{C}; V = 600\text{V}, W = 300\mu\text{m}$$

$$I(T) \propto T^2 \exp\left(-\frac{E_g}{KT}\right)$$

Partial depletion



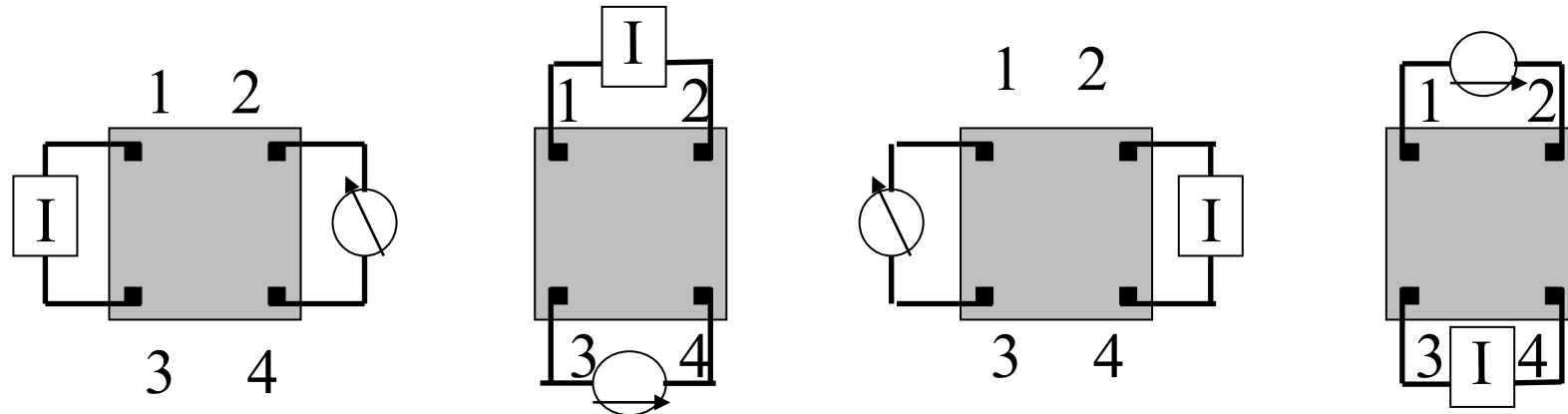
Microscopic Radiation Damage Analysis: Early methods



Mara Bruzzi, Danno da radiazione in semiconduttori
Scuola Nazionale rivelatori ed elettronica per fisica delle alte energie , astrofisica 12 Aprile 2011,
Legnaro, Italy



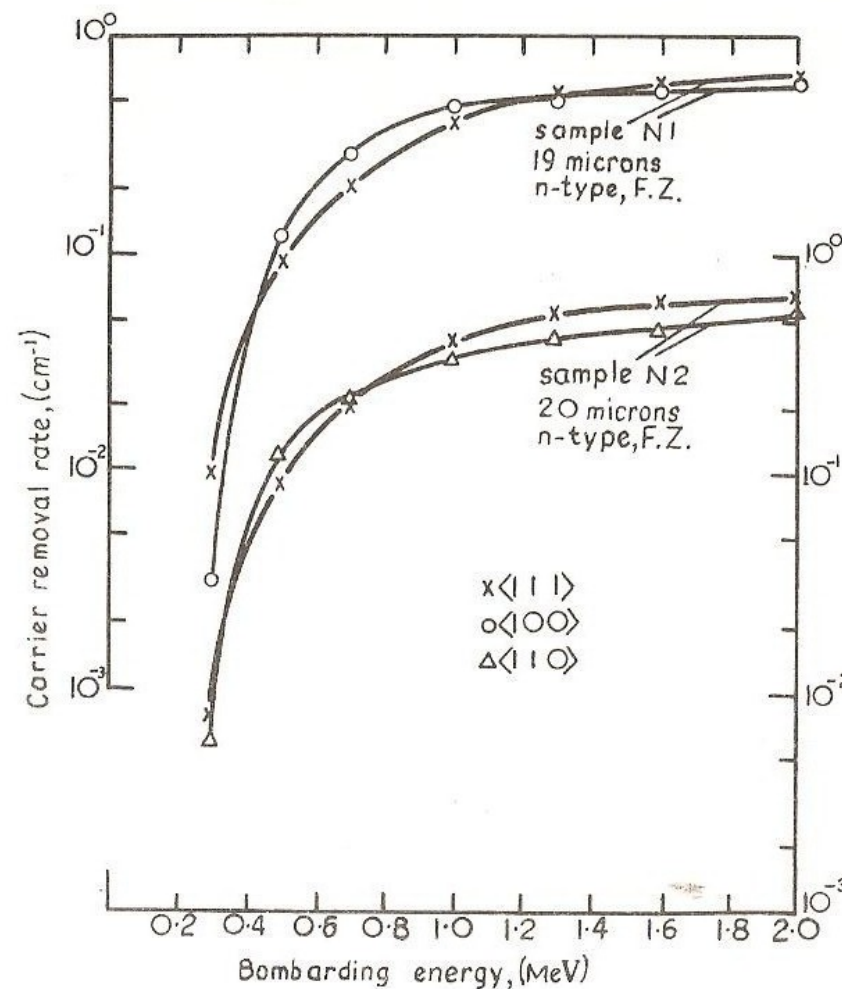
a. Electrical Resistivity Measurements



$$\rho = \frac{1}{q\mu_p(p + z \cdot n)}$$

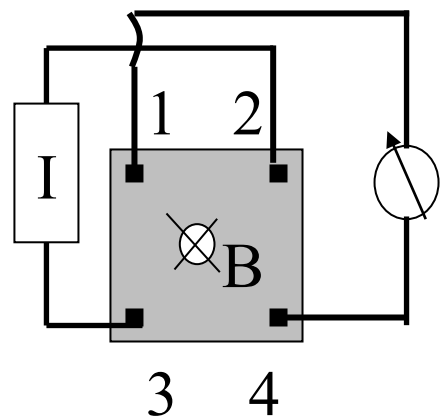
$$z = \mu_n/\mu_p$$

**Existence of a threshold energy E_d characteristic of the crystal
is evidenced e.g. by results on carrier removal rate after
electron irradiation**



b. Hall Coefficient Analysis

$$V_{\text{Hall}} = R_H J_x B_z h$$



$$R_H = r_H \cdot \frac{p - z^2 \cdot n}{q \cdot (p + z \cdot n)^2}$$

$$z = \mu_n / \mu_p$$

Evidence of the presence of defects by Hall Effect measured as a function of temperature

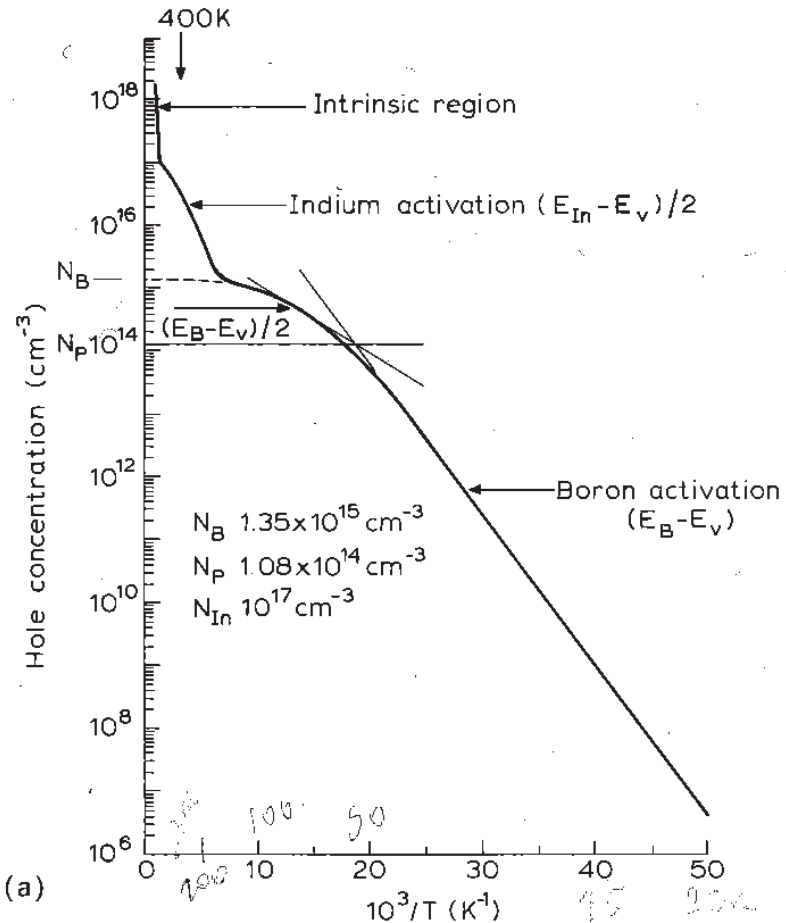
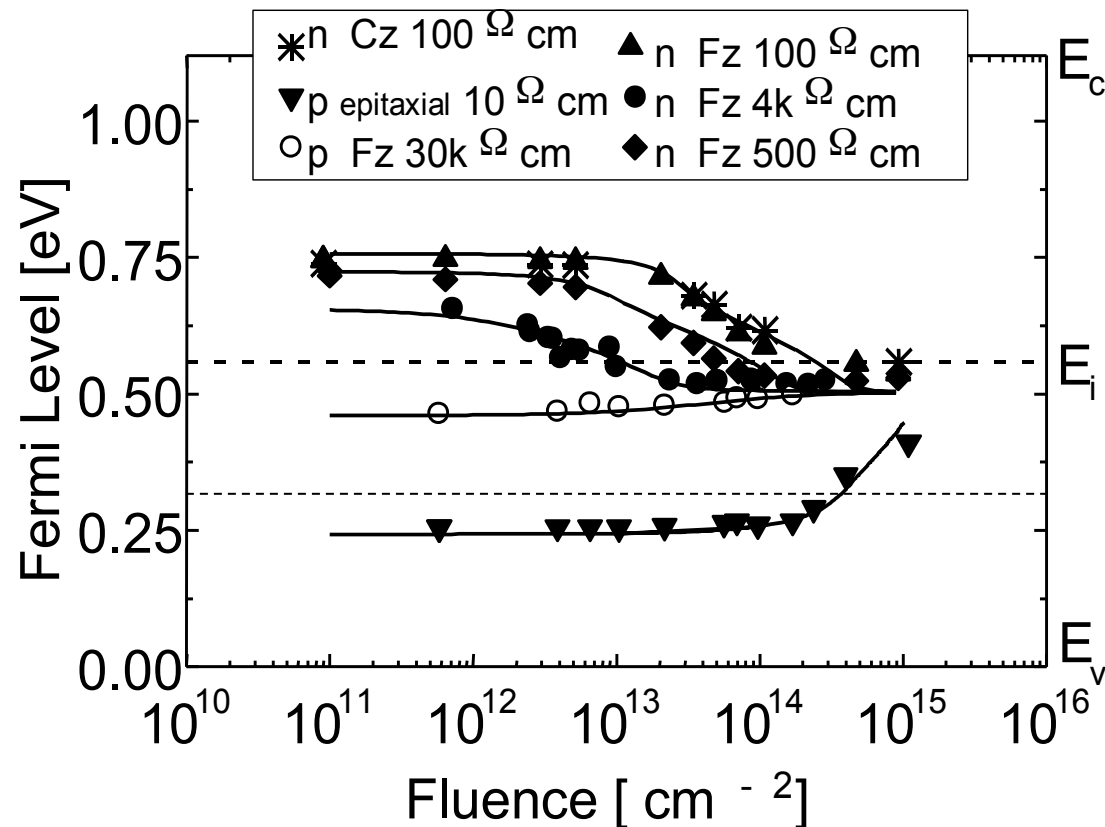


Fig. 3.27 Temperature dependence of the free hole density in In-doped Si as measured by the Hall effect (from Parker, 1982). In both cases the In concentration is 10^{17} cm^{-3} but in (a) the unwanted B impurity is under-compensated by P while in (b) it is over-compensated, resulting in widely different variation of hole density (note the different temperature scales).

Combining resistivity and Hall Coefficient results one can determine the Fermi level position in the forbidden gap

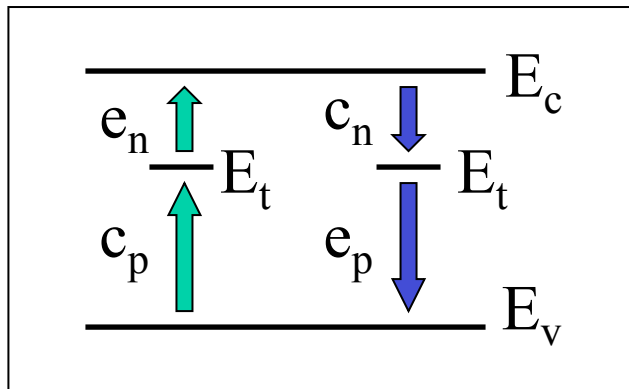


Irradiated Si (1MeV n-equivalent) showing pinning of the Fermi level at $E_v + 0.5$ eV

Defect Spectroscopy in semiconductors

- 1. Thermally Stimulated Currents TSC**
- 2. Deep Level Transient Spectroscopy DLTS**
- 3. Photo Induced Current Transient Spectroscopy PICTS**

Main trap parameters:



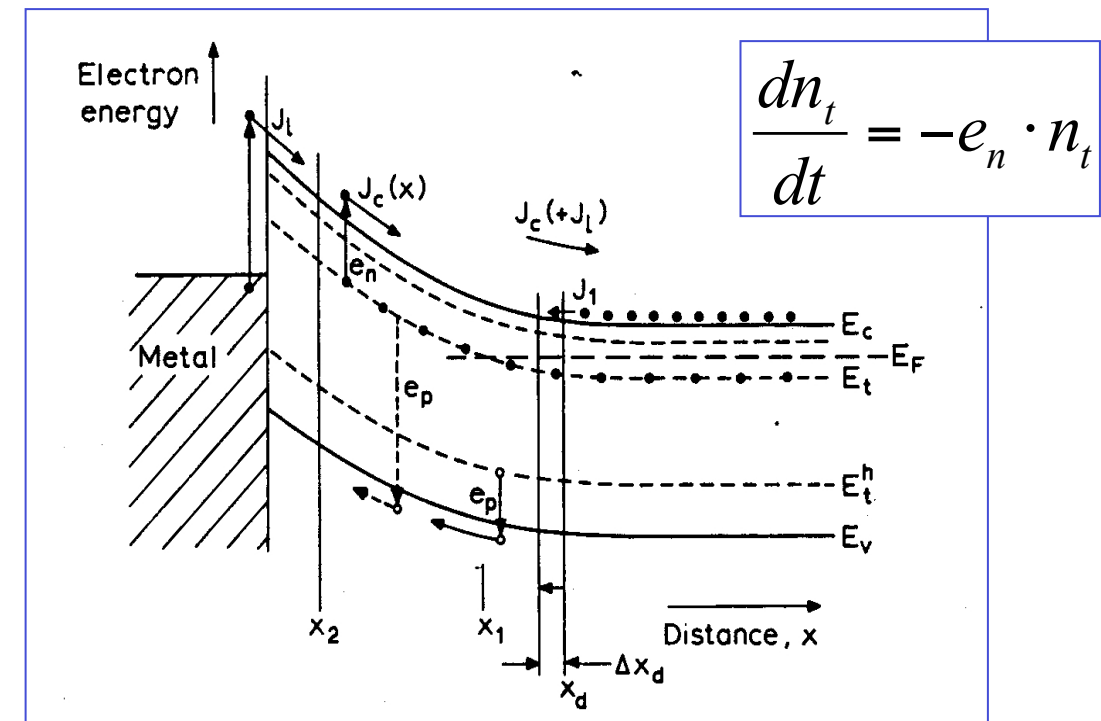
E_t, σ, N_t
 Concentration
 Cross section
 Activation energy

Emission coefficient:

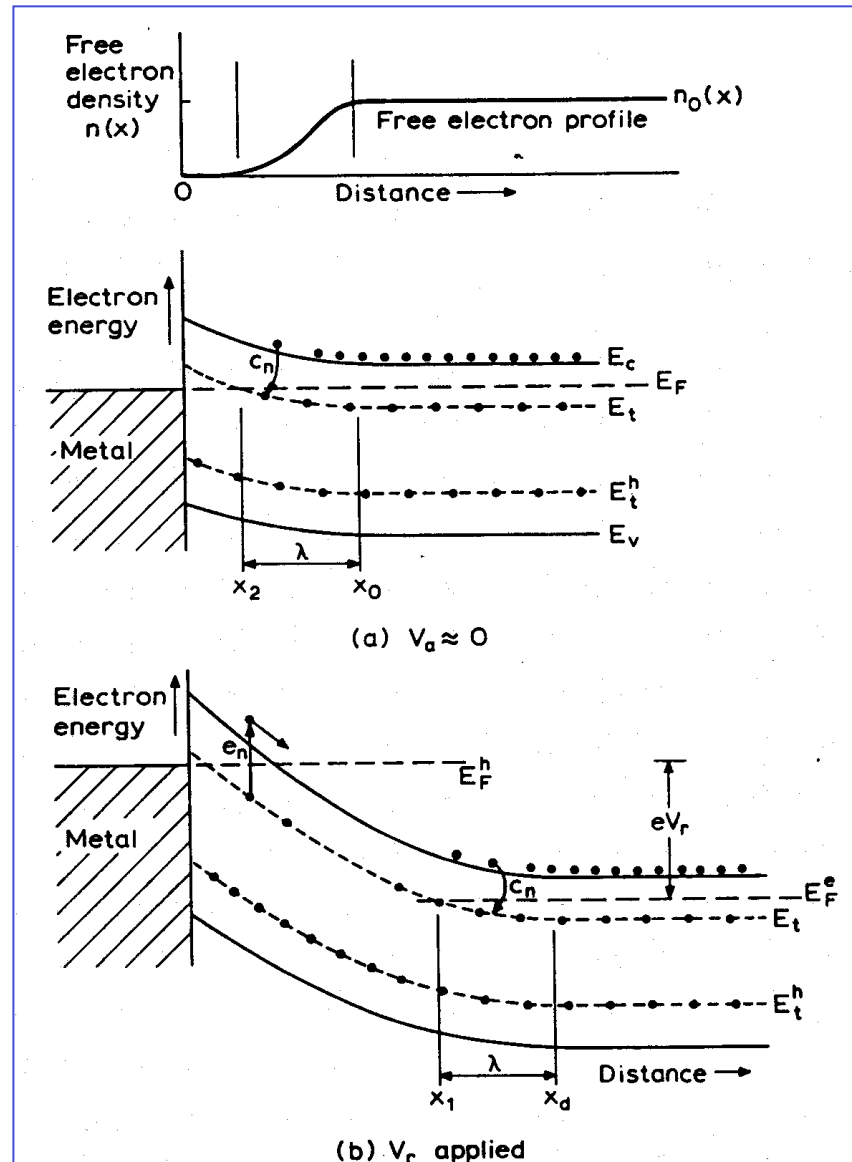
$$e_n = N_c \sigma n v_{th} \cdot e^{-\frac{E_c - E_t}{KT}}$$

Capture coefficient :

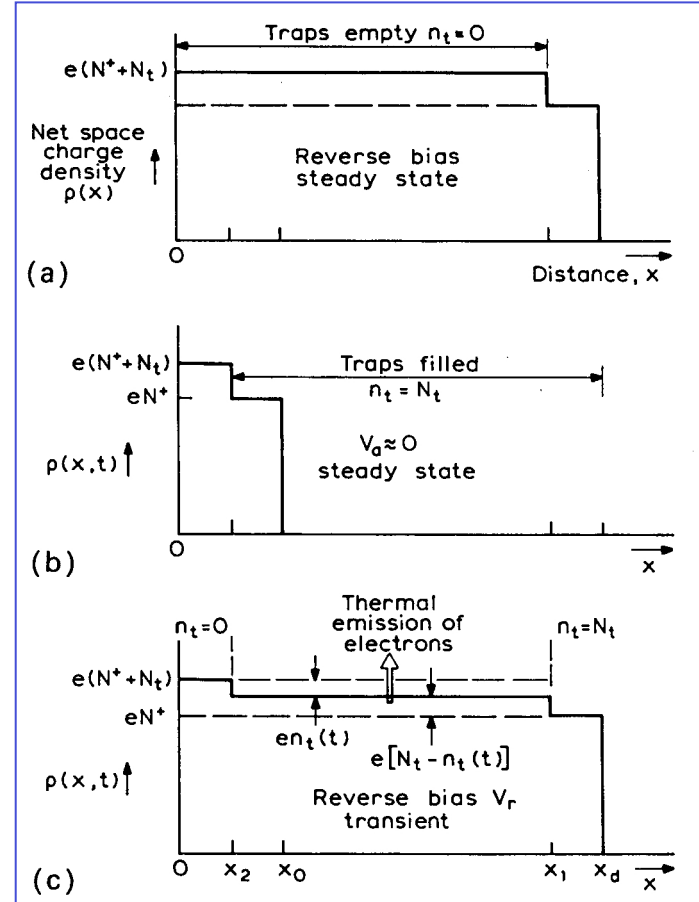
$$c_n = n \sigma n v_{th}$$



Space charge due to deep levels in depleted region

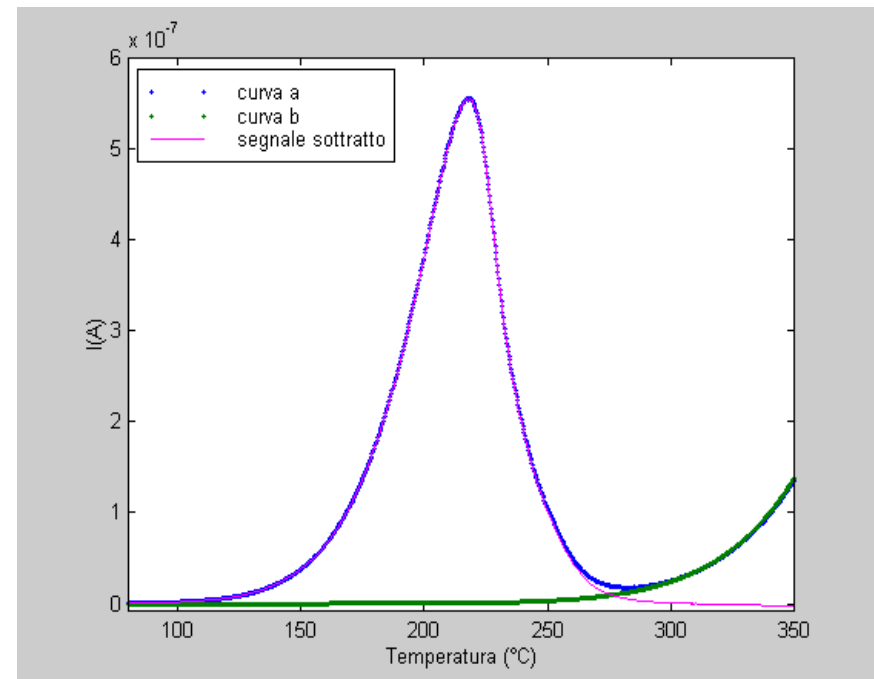
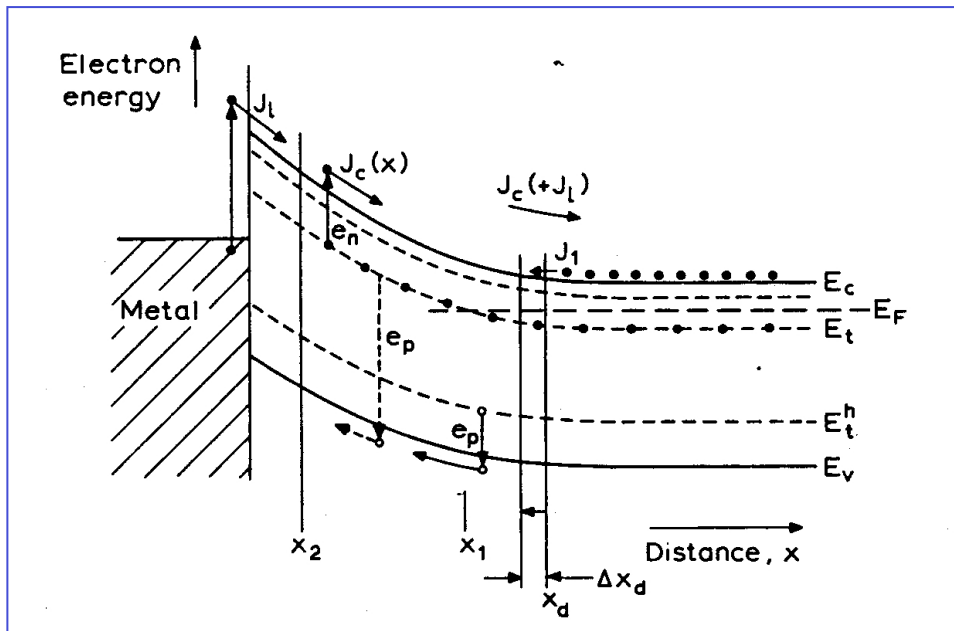


$$\frac{dn_t}{dt} = -e_n \cdot n_t$$



Thermally Stimulated Current TSC

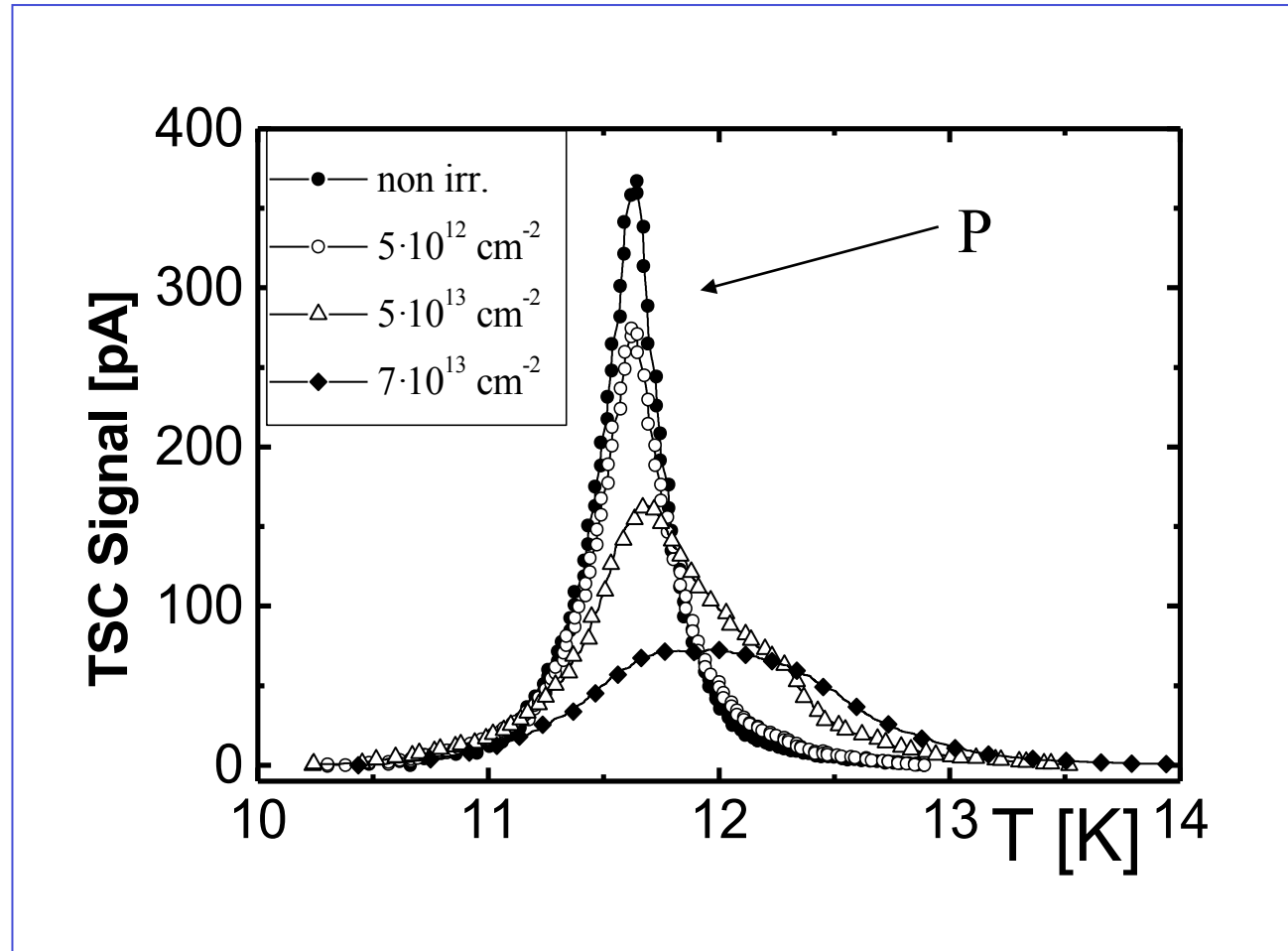
$$J_{TSC} = J_c + \frac{\partial D}{\partial t} = -\frac{1}{2} q W_d e_n n_t$$



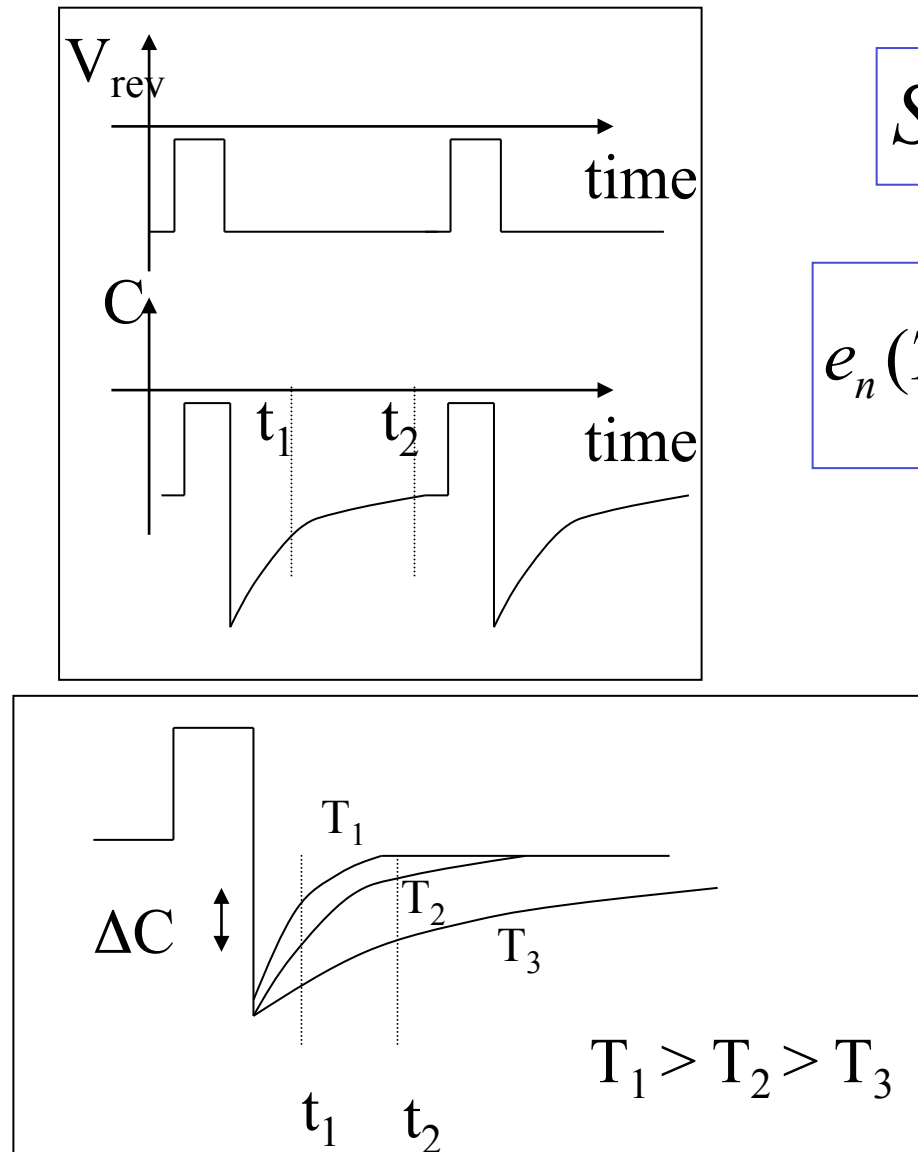
$$I_{TSC}(T) = -\frac{1}{2} q \cdot A \cdot N_t \cdot W \cdot e_n(T) \exp\left(-\frac{1}{b} \int_{T_i}^T e_n(T) dT\right)$$

Mara Bruzzi, Danno da radiazione in semiconduttori
 Scuola Nazionale rivelatori ed elettronica per fisica delle alte energie , astrofisica 12 Aprile 2011,
 Legnaro, Italy

Example: TSC at Low Temperature to evidence Shallow Donor Removal in n-type Si irradiated with neutrons

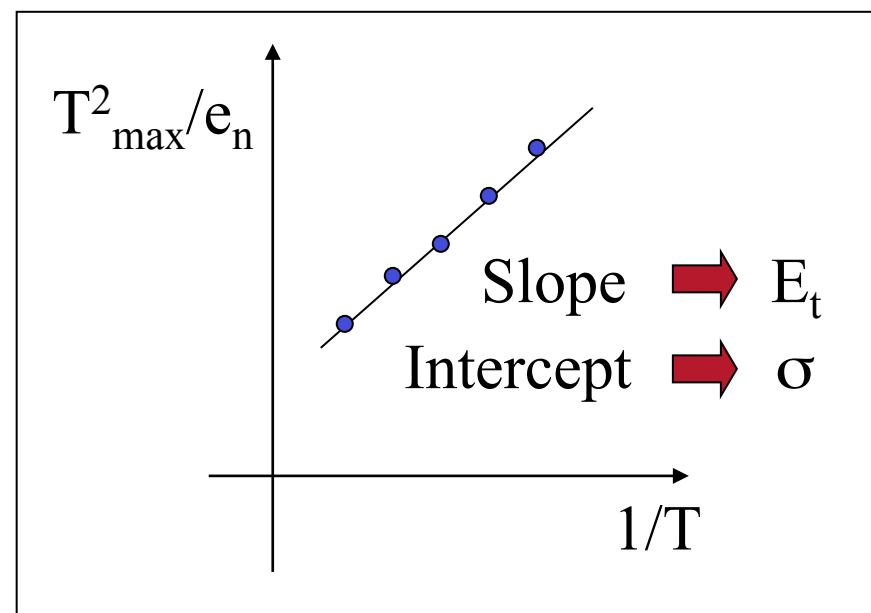


Deep Level Transient Spectroscopy DLTS

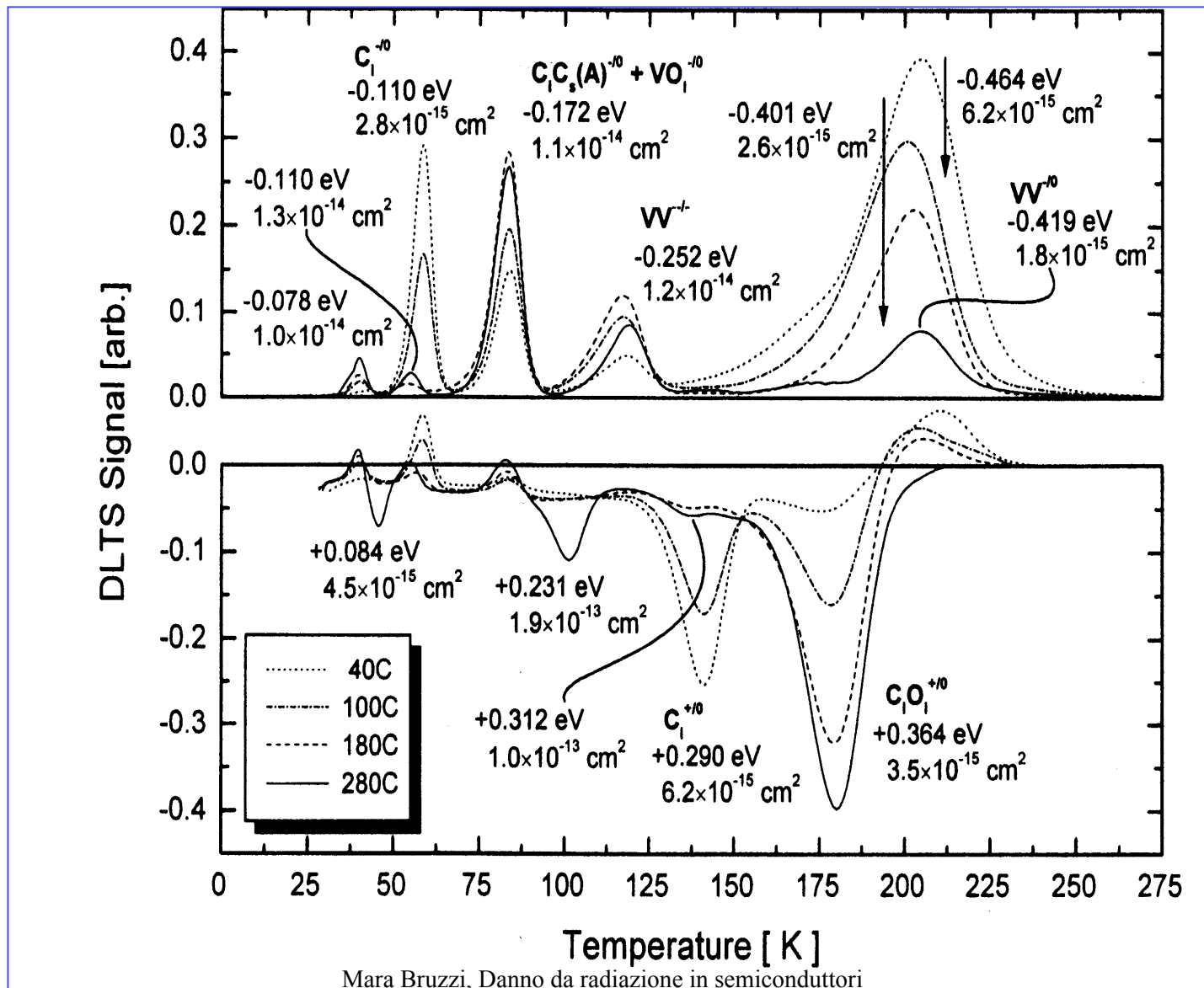


$$S = \Delta C_0 \left(e^{-e_n(T)t_1} - e^{-e_n(T)t_2} \right)$$

$$e_n(T_{\max}) = \frac{t_2 - t_1}{\ln(t_2/t_1)} \alpha T_{\max}^2 \cdot e^{-E_t/KT_{\max}}$$



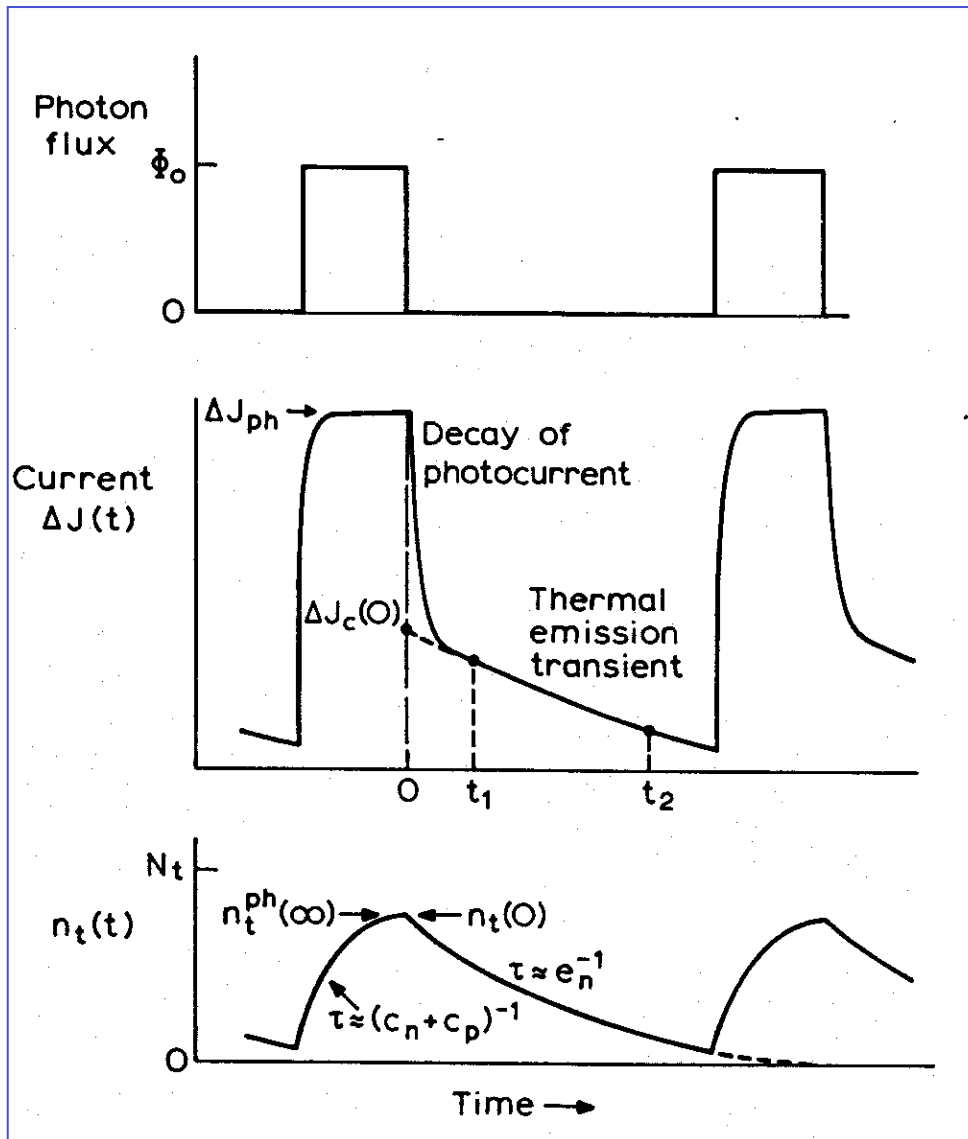
Example: DLTS - $f = 10^{11} \text{ cm}^{-2}$ 5.3MeV neutrons
 ROSE Coll. NIM A 466 (2001) 308-326



Mara Bruzzi, Danno da radiazione in semiconduttori

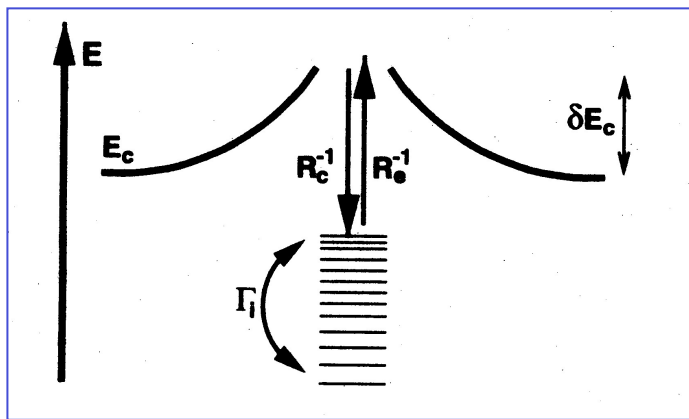
Scuola Nazionale rivelatori ed elettronica per fisica delle alte energie , astrofisica 12 Aprile 2011,
 Legnaro, Italy

Photo Induced Current Transient Spectroscopy PICTS



Similarly as DLTS, trap priming is performed by exposing to an optical excitation with $h\nu > E_g$ and current transient is measured

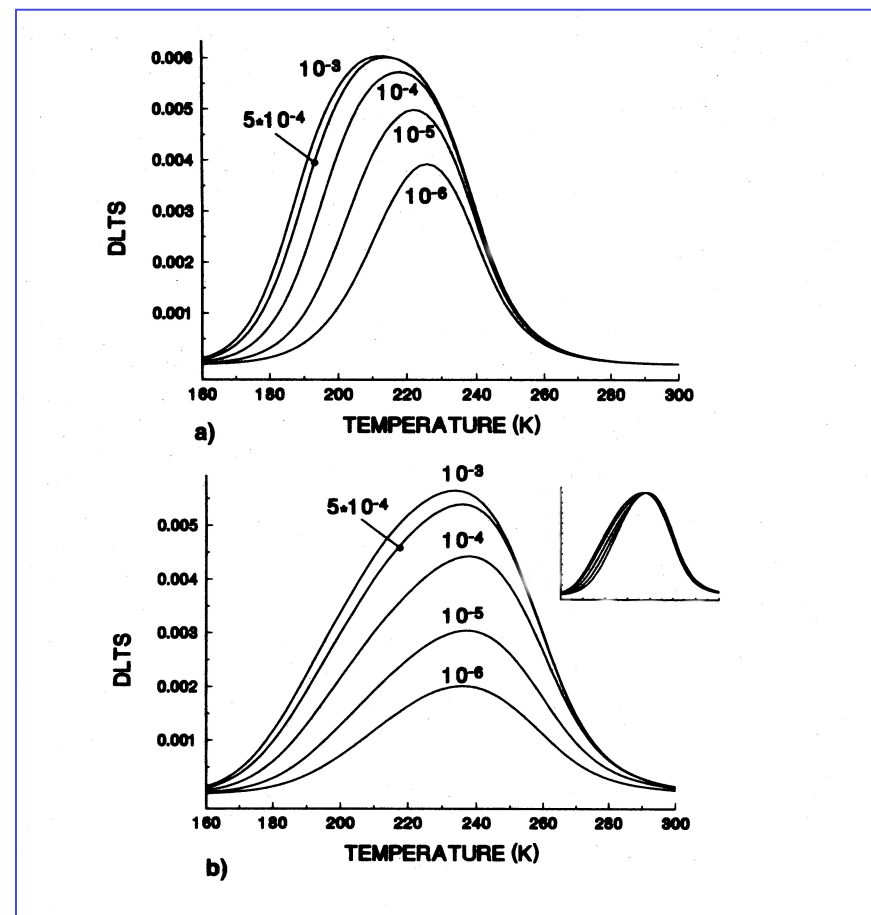
Clusters observed by DLTS



$$R_c(E, t) = \sigma_n v_{th} n [1 - f(E, t)] \exp\left[-\frac{\delta E_c}{kT}\right]$$

Main effect of clustering is a widening of the DLTS signal

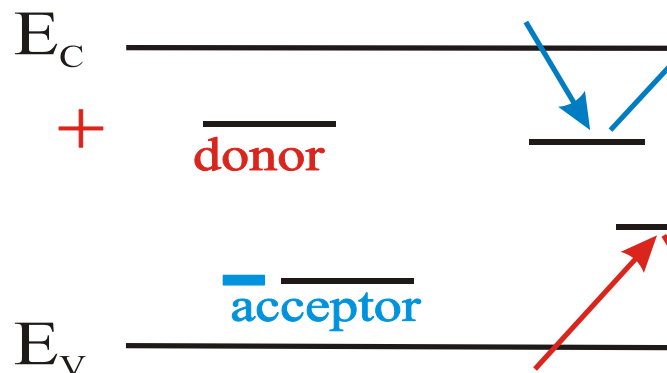
A potential barrier is usually screening the extended defect



Impact of Defects on Detector properties

Mara Bruzzi, Danno da radiazione in semiconduttori
Scuola Nazionale rivelatori ed elettronica per fisica delle alte energie , astrofisica 12 Aprile 2011,
Legnaro, Italy

Shockley-Read-Hall statistics (standard theory)

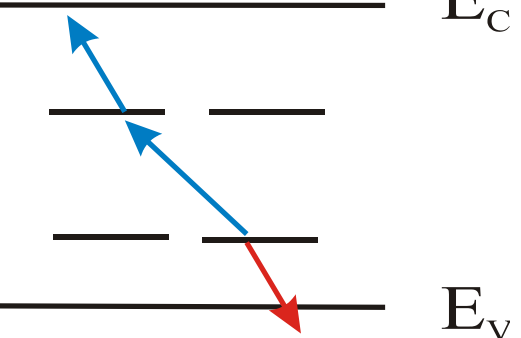


charged defects
 $\Rightarrow N_{\text{eff}}, V_{\text{dep}}$
e.g. donors in upper
and acceptors in
lower half of band
gap

Trapping (e and h)
 $\Rightarrow \text{CCE}$
shallow defects do not
contribute at room
temperature due to fast
detrapping

generation
 \Rightarrow leakage current
Levels close to
midgap
most effective

Inter-center charge transfer model (inside clusters only)



enhanced generation
 \Rightarrow leakage current
 \Rightarrow space charge

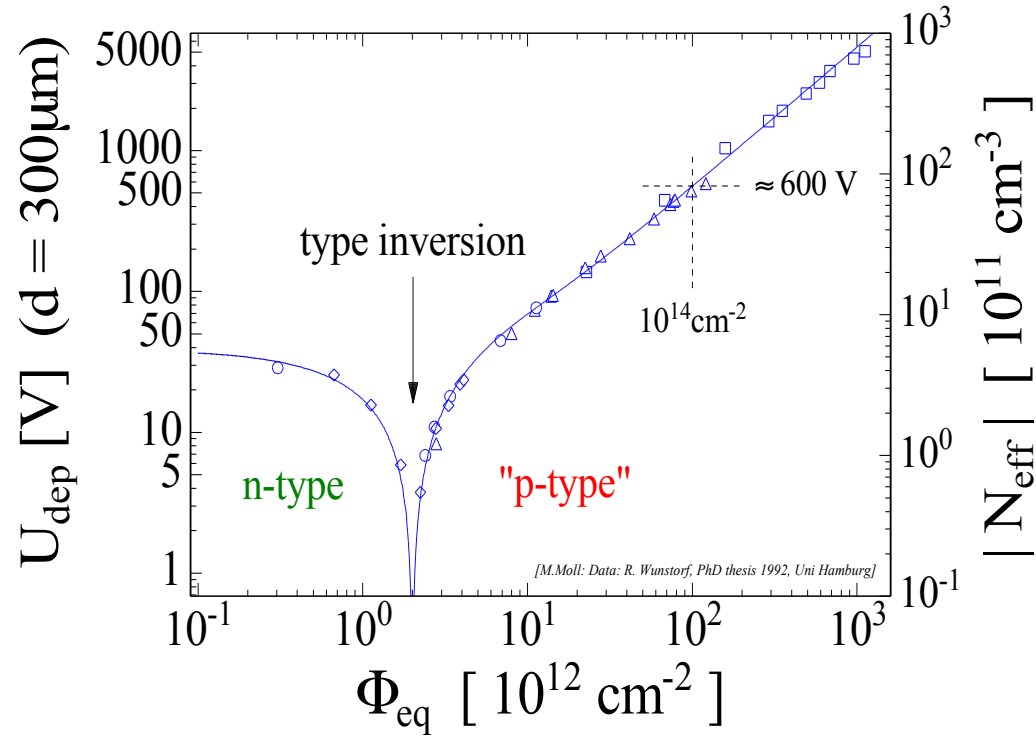
Impact on detector properties can be calculated if all defect parameters are known:

$\sigma_{n,p}$: cross sections

ΔE : ionization energy

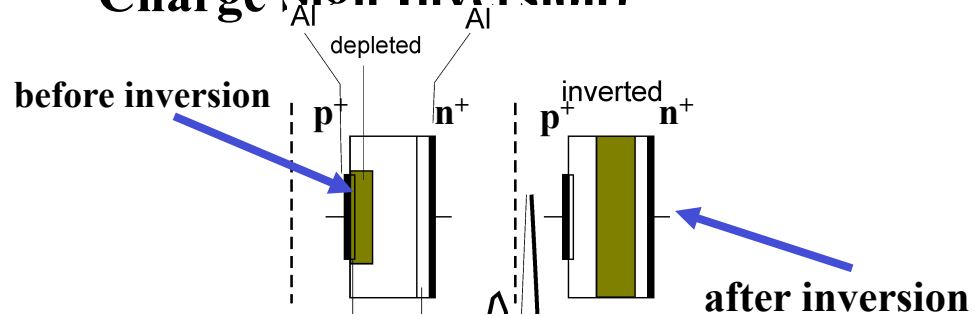
N_t : concentration

■ Change of Depletion Voltage V_{dep} (N_{eff})



- “**Type inversion**”: N_{eff} changes from positive to negative (Space

Charge Sign Inversion)

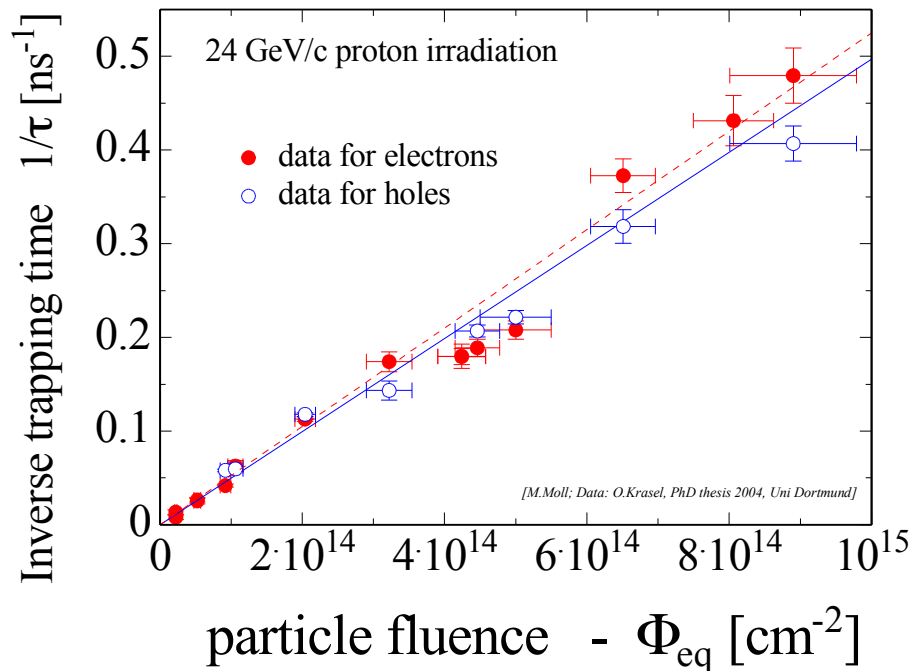


- Deterioration of Charge Collection Efficiency (CCE) by trapping

Trapping is characterized by an effective trapping time τ_{eff} for electrons and holes:

$$Q_{e,h}(t) = Q_{0e,h} \exp\left(-\frac{1}{\tau_{\text{eff } e,h}} \cdot t\right) \quad \text{where} \quad \frac{1}{\tau_{\text{eff } e,h}} \propto N_{\text{defects}}$$

Increase of inverse trapping time ($1/\tau$) with fluence



Expected signal from charge trapping

Effect of trapping on the Charge Collection Distance:

Expected collection distance at saturation velocity λ_{av} :

after $1 \times 10^{15} n_{eq} \text{ cm}^{-2}$: $240 \mu\text{m}$
expected charge $\sim 19 \text{ ke}$.

λ_{av} after $1 \times 10^{16} n_{eq} \text{ cm}^{-2}$: $25 \mu\text{m}$
expected charge $< 1.3 \text{ ke}$: quite inefficient detector!

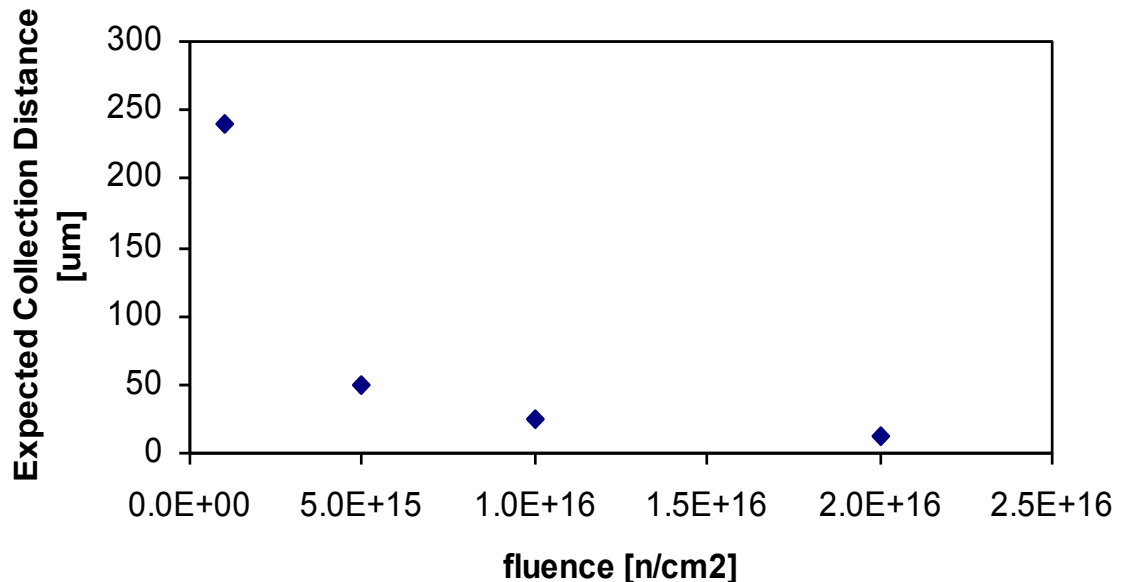
$$Q_{tc} \cong Q_0 \exp(-t_c/\tau_{tr}), \quad 1/\tau_{tr} = \beta \Phi.$$

$$v_{sat,e} \times \tau_{tr} = \lambda_{av}$$

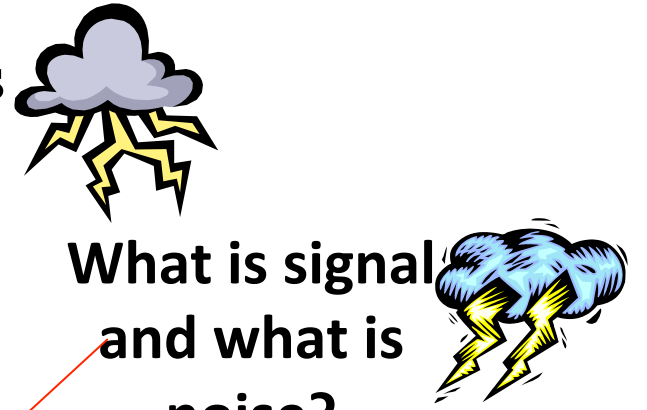
$$\beta_e = 4.2 \times 10^{-16} \text{ cm}^{-2}/\text{ns}$$

$$\beta_h = 6.1 \times 10^{-16} \text{ cm}^{-2}/\text{ns}$$

G. Kramberger et al.,
NIMA 476(2002),
645-651.



Signal to Noise ratio Example with diodes



- Landau distribution has a low energy tail
- becomes even lower by noise broadening

- Noise sources: (ENC = Equivalent Noise Charge)

- Capacitance

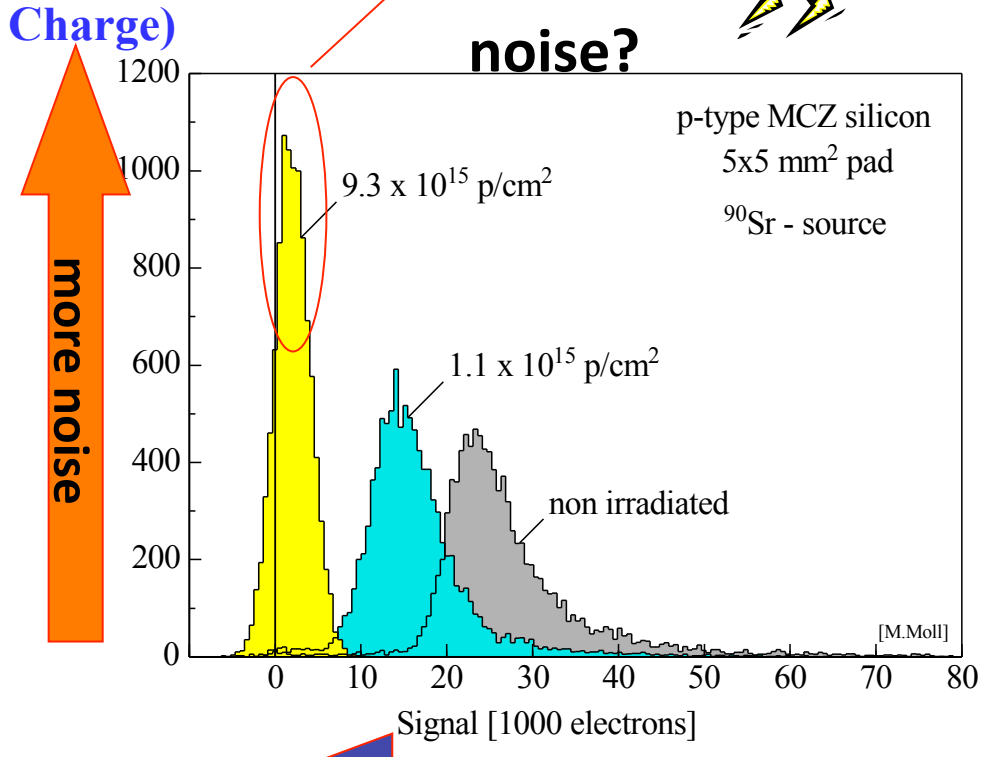
$$ENC \propto C_d$$

- Leakage Current

$$ENC \propto \sqrt{I}$$

- Thermal Noise
(bias resistor)

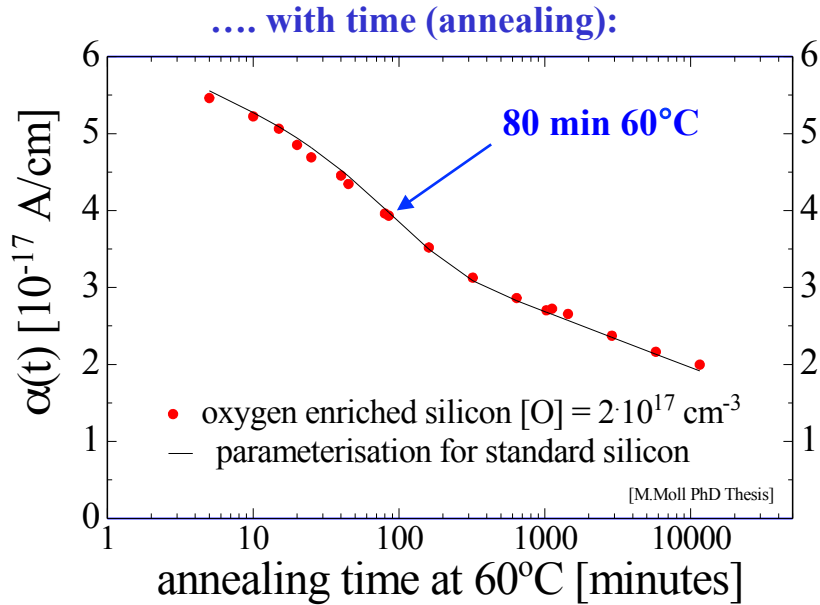
$$ENC \propto \sqrt{k_B T / R}$$



- Figure of Merit: Signal-to-Noise Ratio S/N. Radiation damage severely degrades the S/N.

Changes with time and temperature after irradiation (annealing)

■ Leakage Current and N_{eff} (after hadron irradiation)



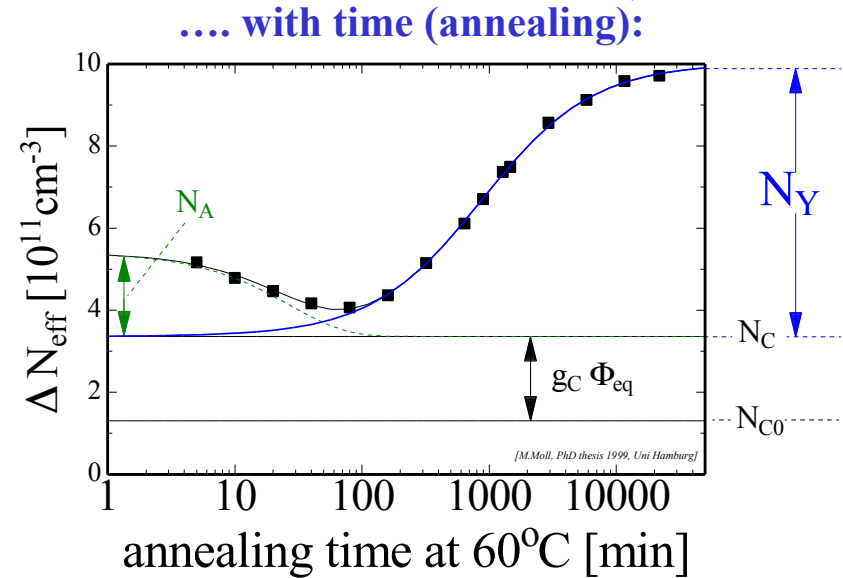
- Leakage current decreasing in time (depending on temperature)
- Strong temperature dependence

$$I \propto \exp\left(-\frac{E_g}{2k_B T}\right)$$

Consequence:

Cool detectors during operation!

Example: $I(-10^\circ\text{C}) \sim 1/16 I(20^\circ\text{C})$



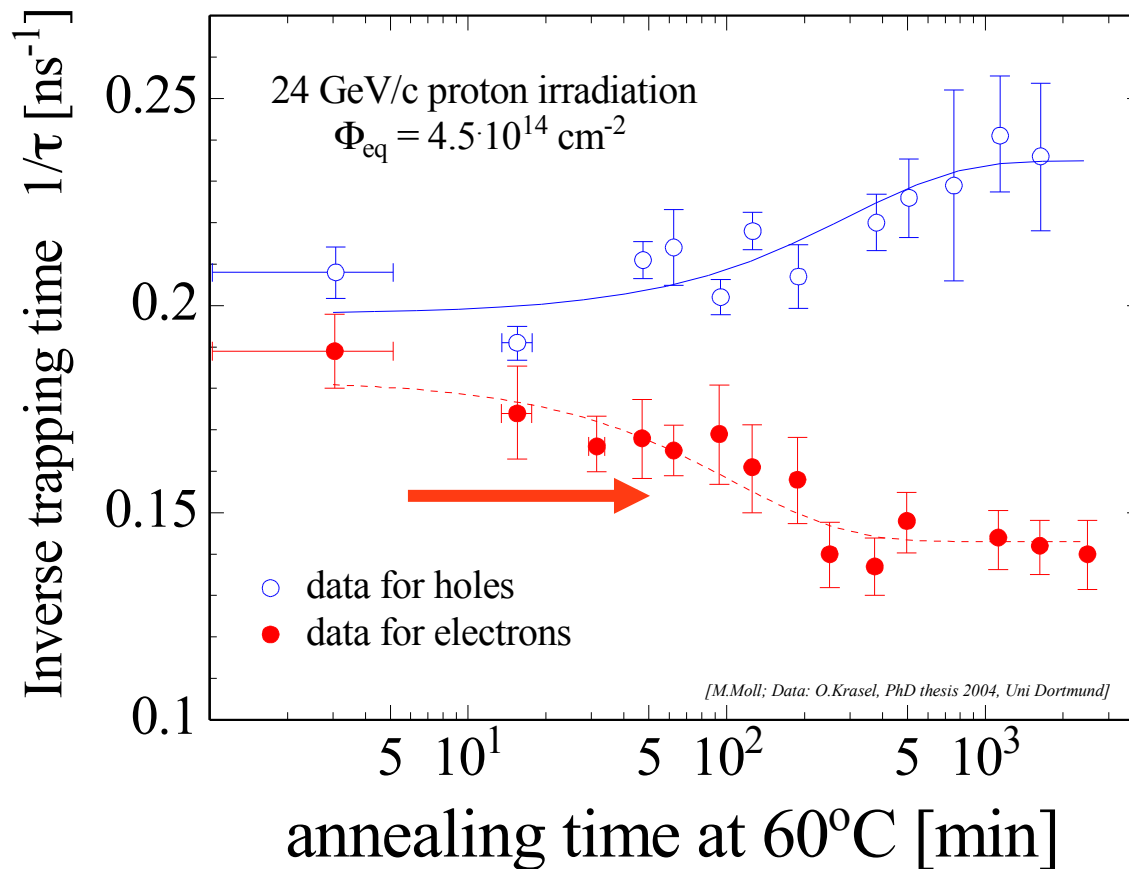
- Short term: “**Beneficial annealing**”
- Long term: “**Reverse annealing**”
- time constant depends on temperature:
 - ~ 500 years (-10°C)
 - ~ 500 days (20°C)
 - ~ 21 hours (60°C)
- Consequence: Detectors must be cooled even when the experiment is not running!

Mara Bruzzi, Danno da radiazione in semiconduttori

Scuola Nazionale rivelatori ed elettronica per fisica delle alte energie , astrofisica 12 Aprile 2011,
Legnaro, Italy

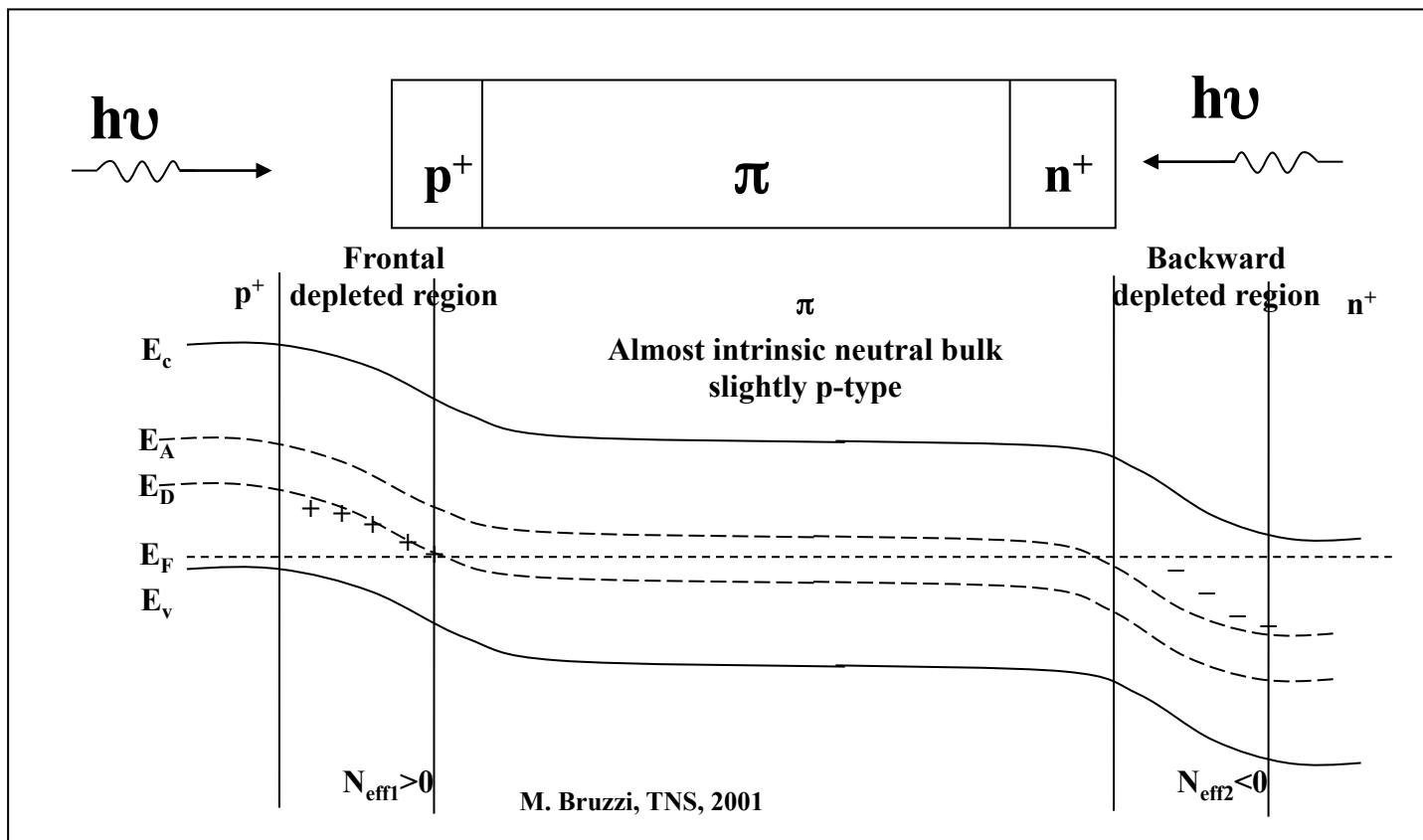
Change of inverse trapping time

Decrease of inverse trapping time ($1/\tau$) with annealing for electrons



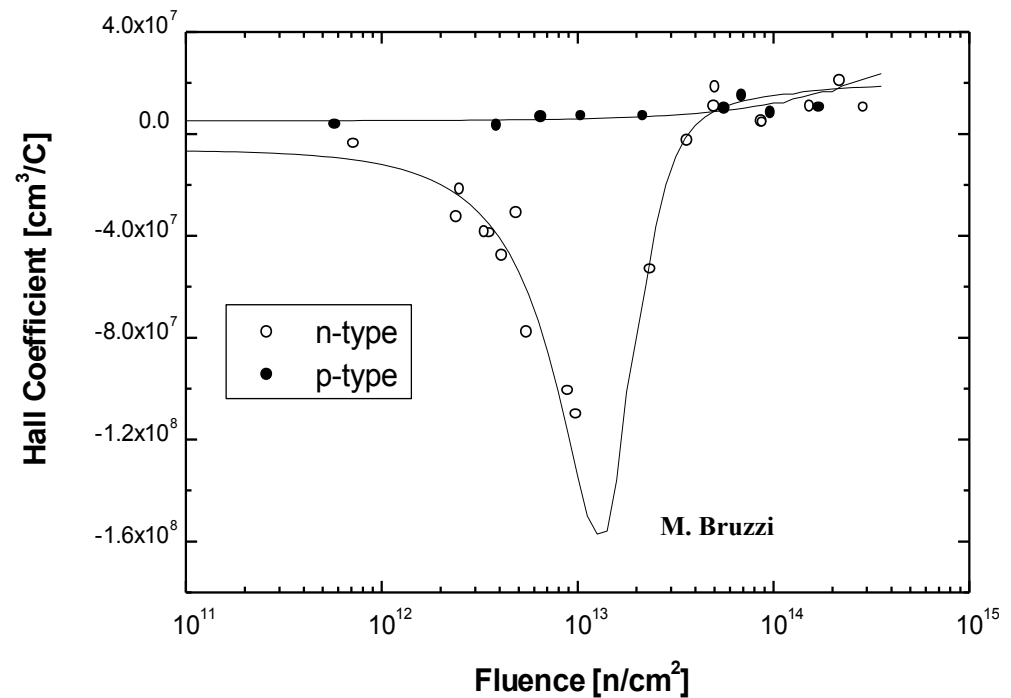
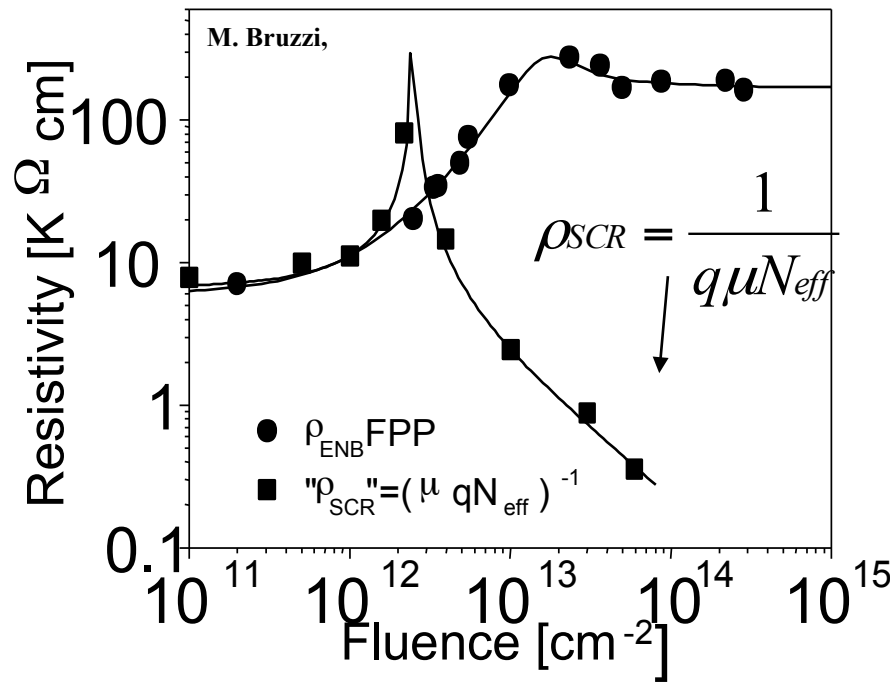
Appearance of a Double Junction at electrodes

Double level model: Acceptor in second half – Donor in first half of bandgap originate the double junction. Levels are neutral in bulk, ionised close to contacts .

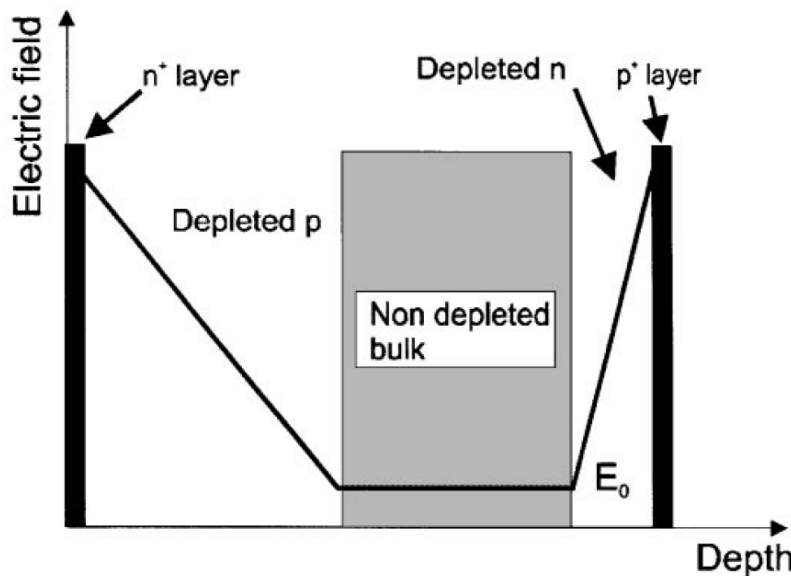


Radiation Damage of the Neutral bulk

Despite the high space charge at electrodes the neutral bulk in between the two junctions has almost intrinsic resistivity and slightly p-type conductivity due to removal of shallow dopants and deep defect formation

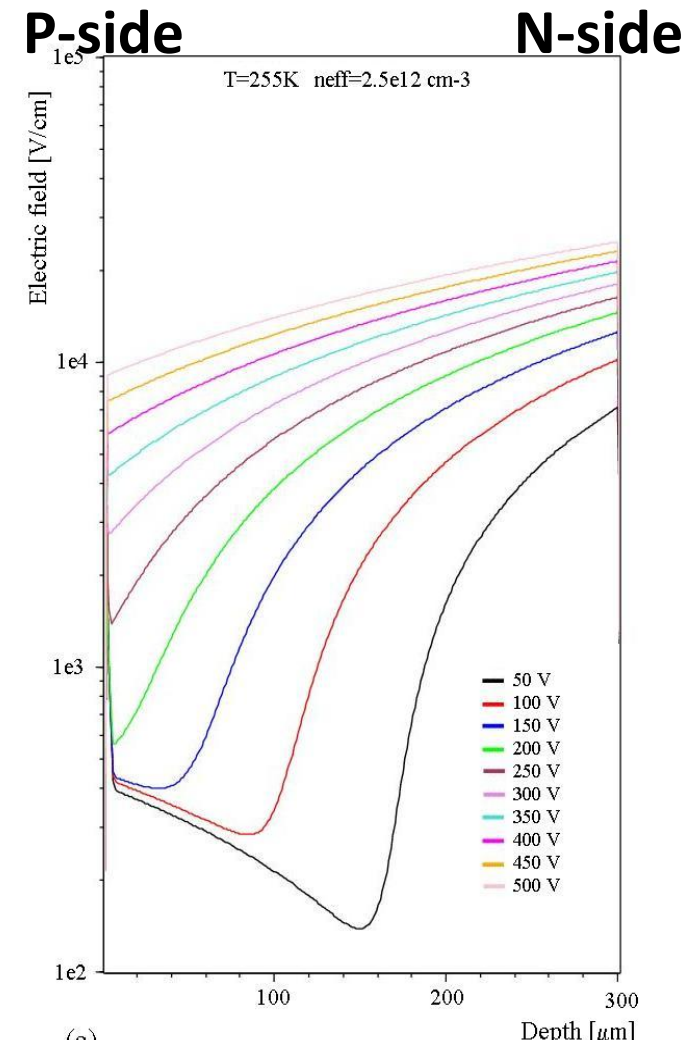


Double Junction



In reality, after irradiation electric fields show a double junction structure with a non-depleted bulk in the middle of the sensor below the full depletion voltage

See G. Casse, et. al., NIMA 426 (1999) 140-146 and G. Kramberger, et. al., NIMA 579 (2007) 762-765 for details



ISE-TCAD simulation after $6. 10^{14} \text{ p cm}^{-2}$

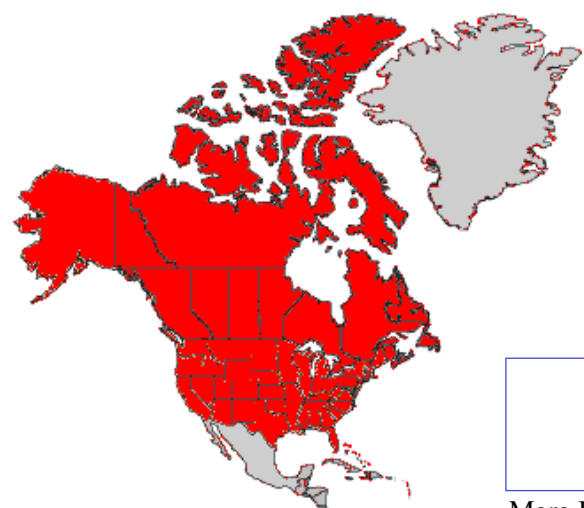
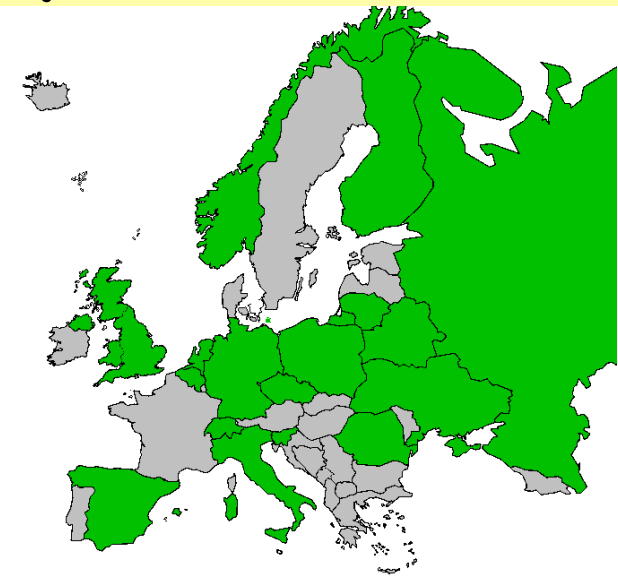
Material Engineering

Mara Bruzzi, Danno da radiazione in semiconduttori
Scuola Nazionale rivelatori ed elettronica per fisica delle alte energie , astrofisica 12 Aprile 2011,
Legnaro, Italy

RD50 - Development of Radiation Hard Semiconductor Devices for High Luminosity Colliders

38 European institutes

Belarus (Minsk), Belgium (Louvain), Czech Republic (Prague (3x)), Finland (Helsinki, Lappeenranta), Germany (Dortmund, Erfurt, Freiburg, Hamburg, Karlsruhe, Munich), Italy (Bari, Florence, Padova, Perugia, Pisa, Trento), Lithuania (Vilnius), Netherlands (NIKHEF), Norway (Oslo (2x)), Poland (Warsaw(2x)), Romania (Bucharest (2x)), Russia (Moscow, St.Petersburg), Slovenia (Ljubljana), Spain (Barcelona, Valencia), Switzerland (CERN, PSI), Ukraine (Kiev), United Kingdom (Glasgow, Lancaster, Liverpool)



8 North-American institutes

Canada (Montreal), USA (BNL, Fermilab, New Mexico, Purdue, Rochester, Santa Cruz, Syracuse)

1 Middle East institute

Israel (Tel Aviv)

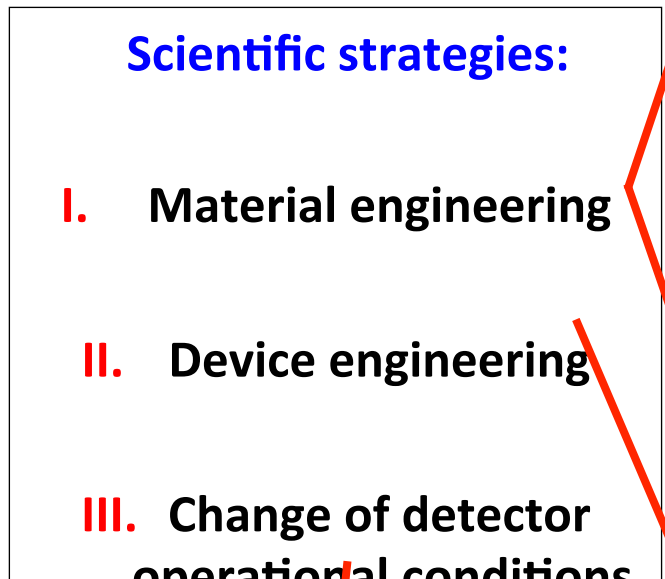
257 Members from 47 Institutes

Detailed member list: <http://cern.ch/rd50>

Mara Bruzzi, Danno da radiazione in semiconduttori

Scuola Nazionale rivelatori ed elettronica per fisica delle alte energie , astrofisica 12 Aprile 2011,
Legnaro, Italy

Approaches to develop radiation harder solid state tracking detectors



CERN-RD39
“Cryogenic Tracking Detectors”
operation at 100-200K
to reduce charge loss

- **Defect Engineering of Silicon**

Deliberate incorporation of impurities or defects into the silicon bulk to improve radiation tolerance of detectors

- **Needs:** Profound understanding of radiation damage
 - microscopic defects, macroscopic parameters
 - dependence on particle type and energy
 - defect formation kinetics and annealing
- **Examples:**
 - Oxygen rich Silicon (DOFZ, Cz, MCZ, EPI)
 - Oxygen dimer & hydrogen enriched Si
 - Pre-irradiated Si
 - Influence of processing technology

New Materials

- Silicon Carbide (SiC), Gallium Nitride (GaN)
- Diamond (CERN RD42 Collaboration)
- Amorphous silicon

Device Engineering (New Detector Designs)

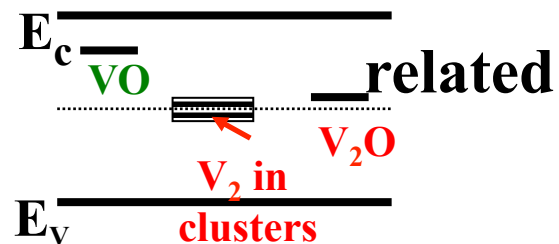
- p-type silicon detectors (n-in-p)
- thin detectors, epitaxial detectors
- 3D detectors and Semi 3D detectors, Stripixels
- Cost effective detectors
- Monolithic devices



Oxygen Enrichment for Radiation Hardening

RD48 (ROSE) and RD50 CERN Collaborations

Main Hypothesis: Oxygen beneficial as sink of vacancies
 $V-O_i$ complex concentration increase → reduction of mainly divacancy
deeper levels



Typical oxygen concentration in Si:

- FZ [O_i] 10^{15} cm^{-3}
- Diffusion oxygenated FZ : DOFZ [O_i] $10^{16}\text{-}10^{17} \text{ cm}^{-3}$
- Czochralski Si: [O_i] up to 10^{18} cm^{-3}

Note: as VO is a point defect the beneficial effect of oxygen is expected especially when cluster formation by irradiation is less important than point defect formation.

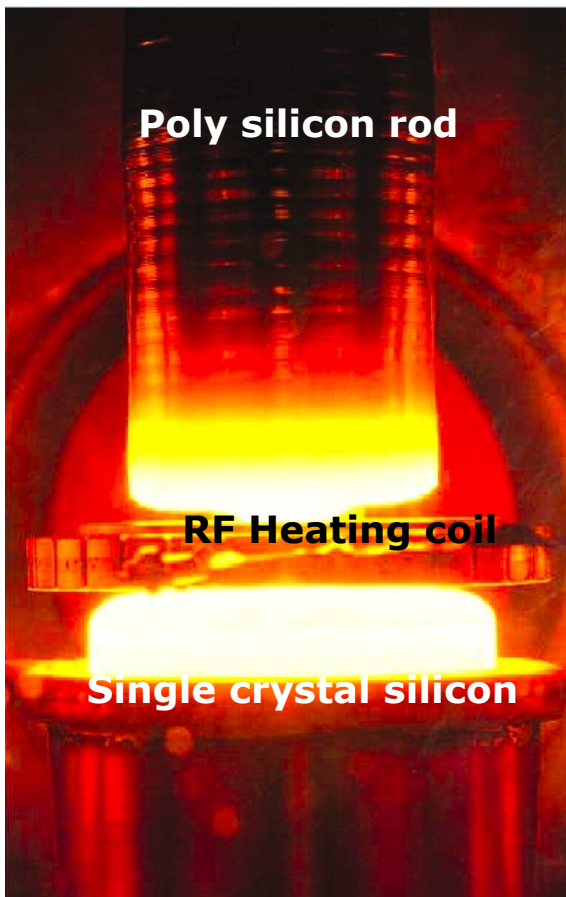
Mara Bruzzi, Danno da radiazione in semiconduttori

Scuola Nazionale rivelatori ed elettronica per fisica delle alte energie , astrofisica 12 Aprile 2011,
Legnaro, Italy

Material: Float Zone Silicon (FZ)

■ Float Zone process

Using a single Si crystal seed, melt the vertically oriented rod onto the seed using RF power and “pull” the monocrystalline ingot

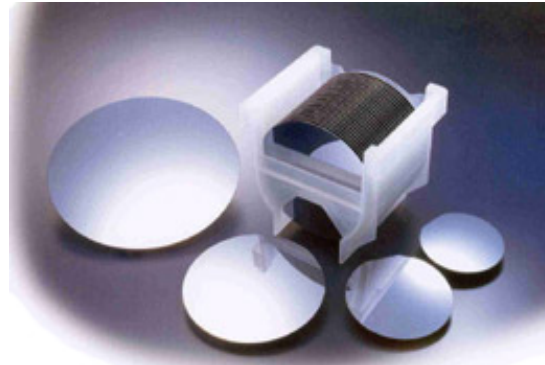


■ Mono-crystalline Ingot



■ Wafer production

- Slicing, lapping, etching, polishing



■ Highly pure crystal

- Low concentration of [O] and [C] 10^{15}cm^{-3}

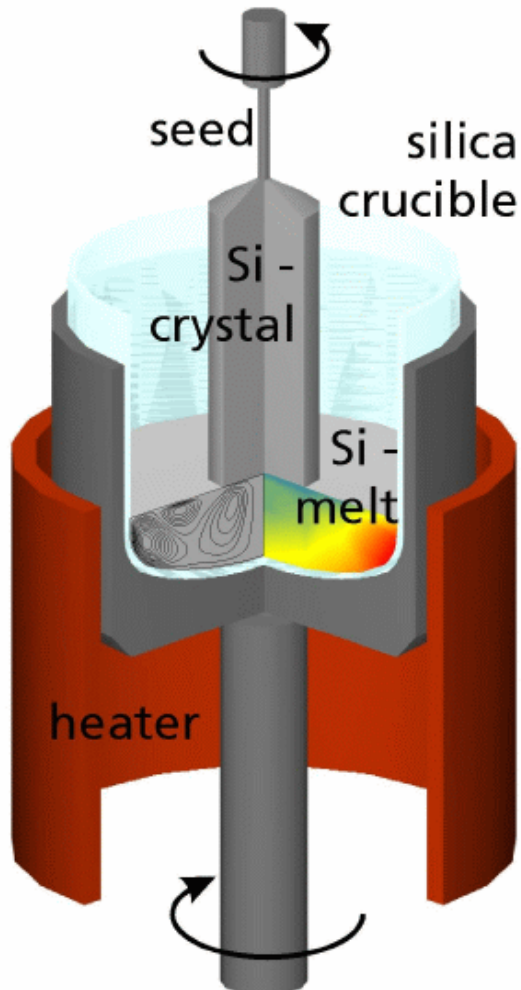
Mara Bruzzi, Danno da radiazione in semiconduttori

Scuola Nazionale rivelatori ed elettronica per fisica delle alte energie , astrofisica 12 Aprile 2011,
Legnaro, Italy

RD50: Defect Engineering of Si

Czochralski silicon (Cz) & Epitaxial silicon (EPI)

■ Czochralski silicon



- Pull Si-crystal from a Si-melt contained in a silica crucible while rotating.
- Silica crucible is dissolving oxygen into the melt \Rightarrow high concentration of O in CZ
- Material used by IC industry (cheap)
- Recent developments (~5 years) made CZ available in sufficiently high purity (resistivity) to allow for use as particle detector.

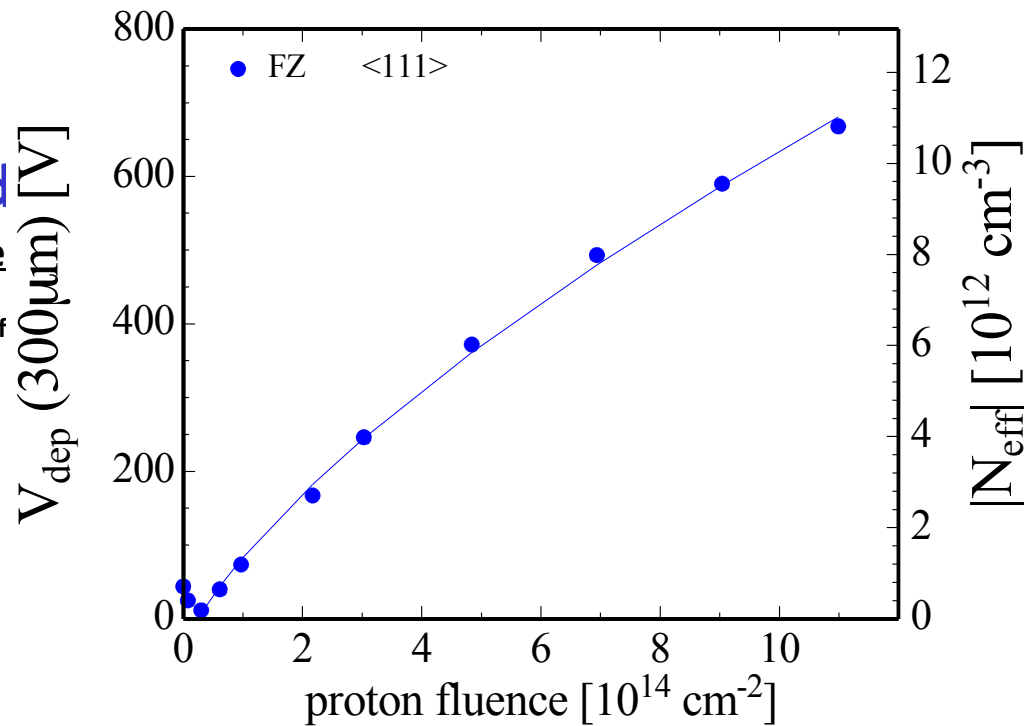
■ Epitaxial silicon

- Chemical-Vapor Deposition (CVD) of Silicon
- CZ silicon substrate used \Rightarrow in-diffusion of oxygen
 - growth rate about $1\mu\text{m}/\text{min}$
 - excellent homogeneity of resistivity
- up to $150\ \mu\text{m}$ thick layers produced (thicker is possible)
 - price depending on thickness of epi-layer but not extending $\sim 3 \times$ price of FZ wafer

Standard FZ, DOFZ, MCz and Cz silicon

24 GeV/c proton irradiation

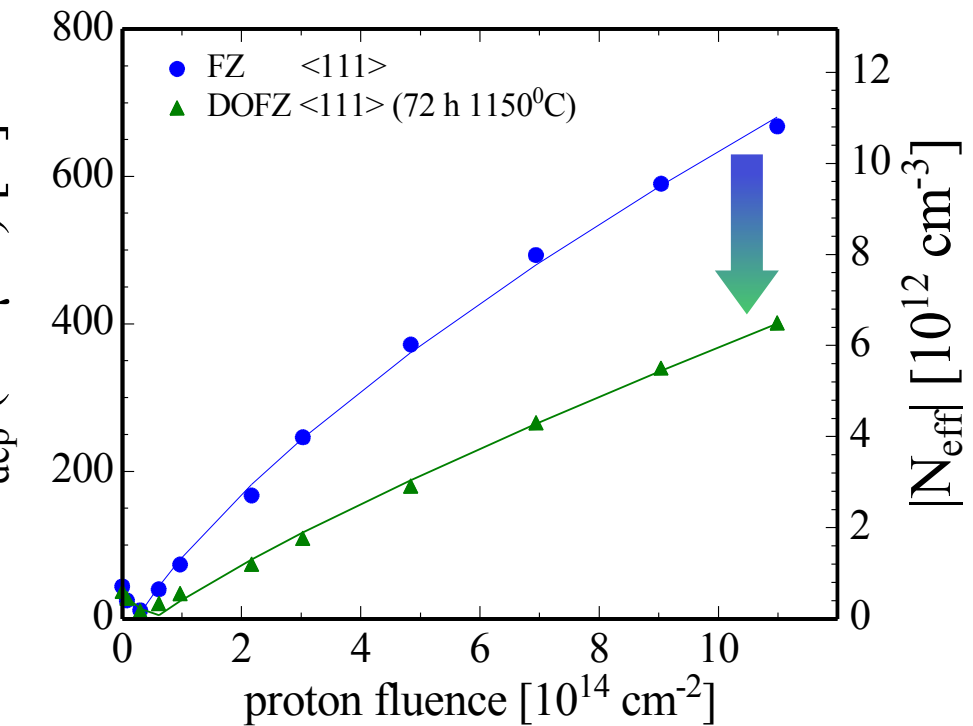
- Stand
- type inve
- strong N_{eff}



Standard FZ, DOFZ, MCz and Cz silicon

24 GeV/c proton irradiation

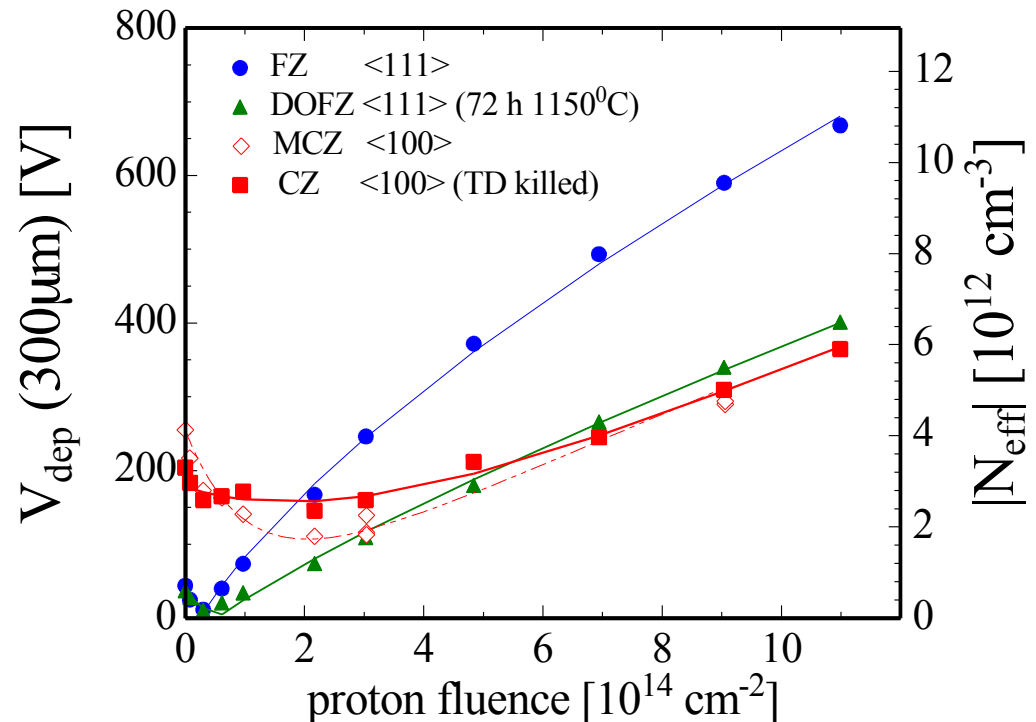
- Stand
- type inve
- strong N_{ef}
- Oxygen
- type inve
- reduced N_e



Standard FZ, DOFZ, MCz and Cz silicon

24 GeV/c proton irradiation

- Standard FZ silicon
 - type inversion at $\sim 2 \times 10^{13} \text{ p/cm}^2$
 - strong N_{eff} increase at high fluence
- Oxygenated FZ (DOFZ)
 - type inversion at $\sim 2 \times 10^{13} \text{ p/cm}^2$
 - reduced N_{eff} increase at high fluence
- CZ silicon and MCZ silicon
 - “no type inversion” in the overall fluence range

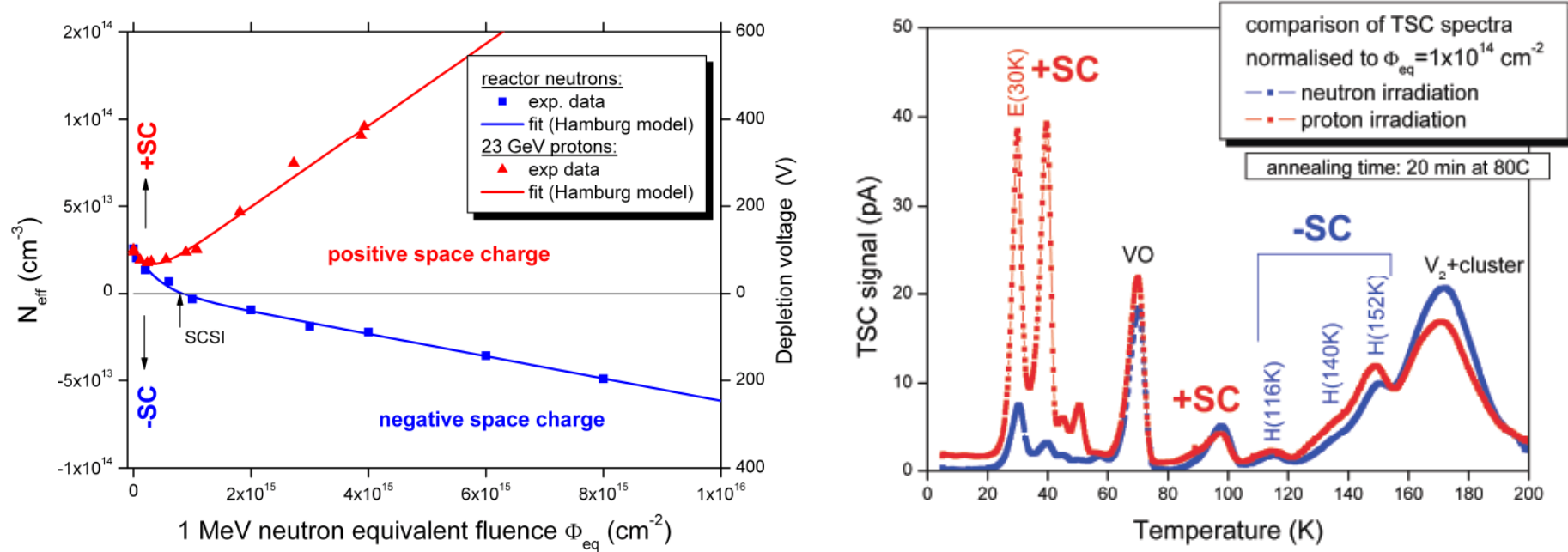


(for experts: there is no “real” type inversion, a more clear understanding of the observed effects is obtained by investigating directly the internal electric field; look for: TCT, MCZ, double junction)

- Common to all materials (after hadron irradiation, not after γ irradiation):
 - reverse current increase
 - increase of trapping (electrons and holes) within $\sim 20\%$

From microscopic to macroscopic: N_{eff} changes explained with TSC

Epi-Si irradiated with 23 GeV protons and reactor neutrons



[Pintilie, Lindstroem, Junkes, Fretwurst, NIM A 611 (2009) 52–68]

- **SCSI “Type Inversion” after neutrons but not after protons**
- **donor generation enhanced after proton irradiation**

Summary – defects with strong impact on the device properties at operating temperature

Point defects

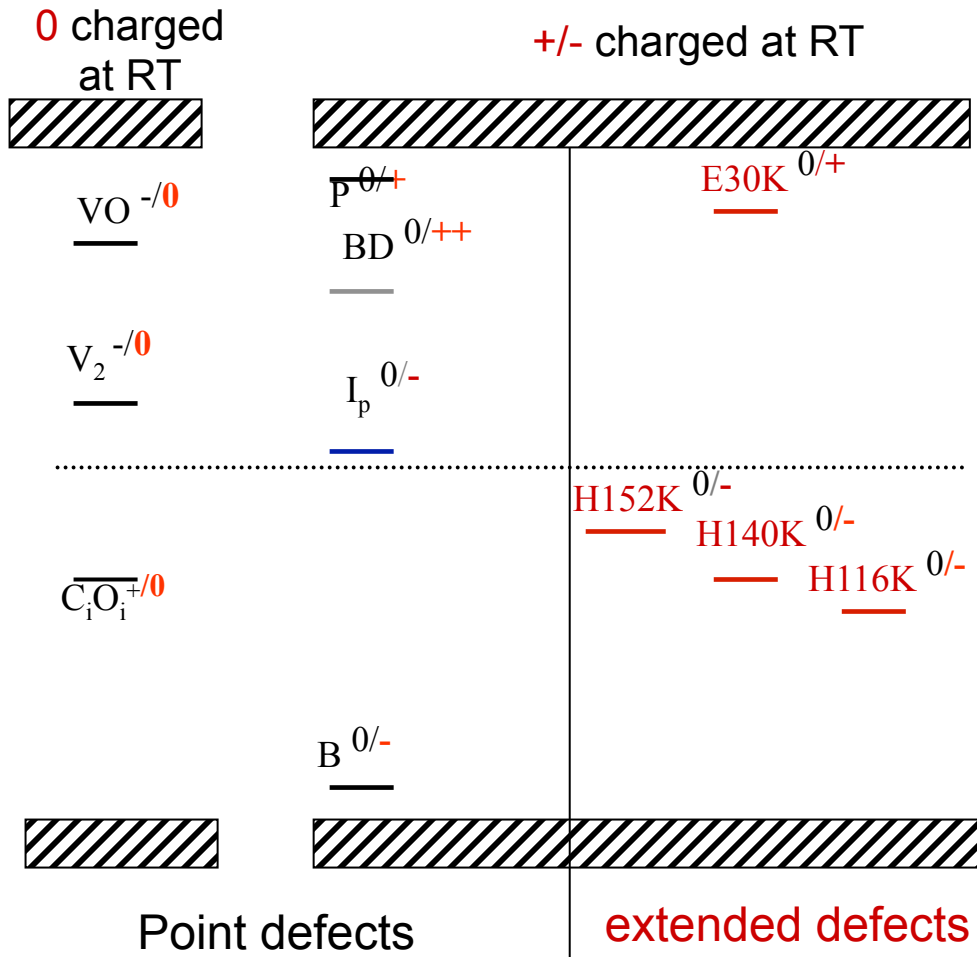
- $E_i^{BD} = E_c - 0.225 \text{ eV}$
- $\sigma_n^{BD} = 2.3 \cdot 10^{-14} \text{ cm}^2$

$$E_i^I = E_c - 0.545 \text{ eV}$$

- $\sigma_n^I = 2.3 \cdot 10^{-14} \text{ cm}^2$
- $\sigma_{op}^I = 2.3 \cdot 10^{-14} \text{ cm}^2$

Cluster related centers

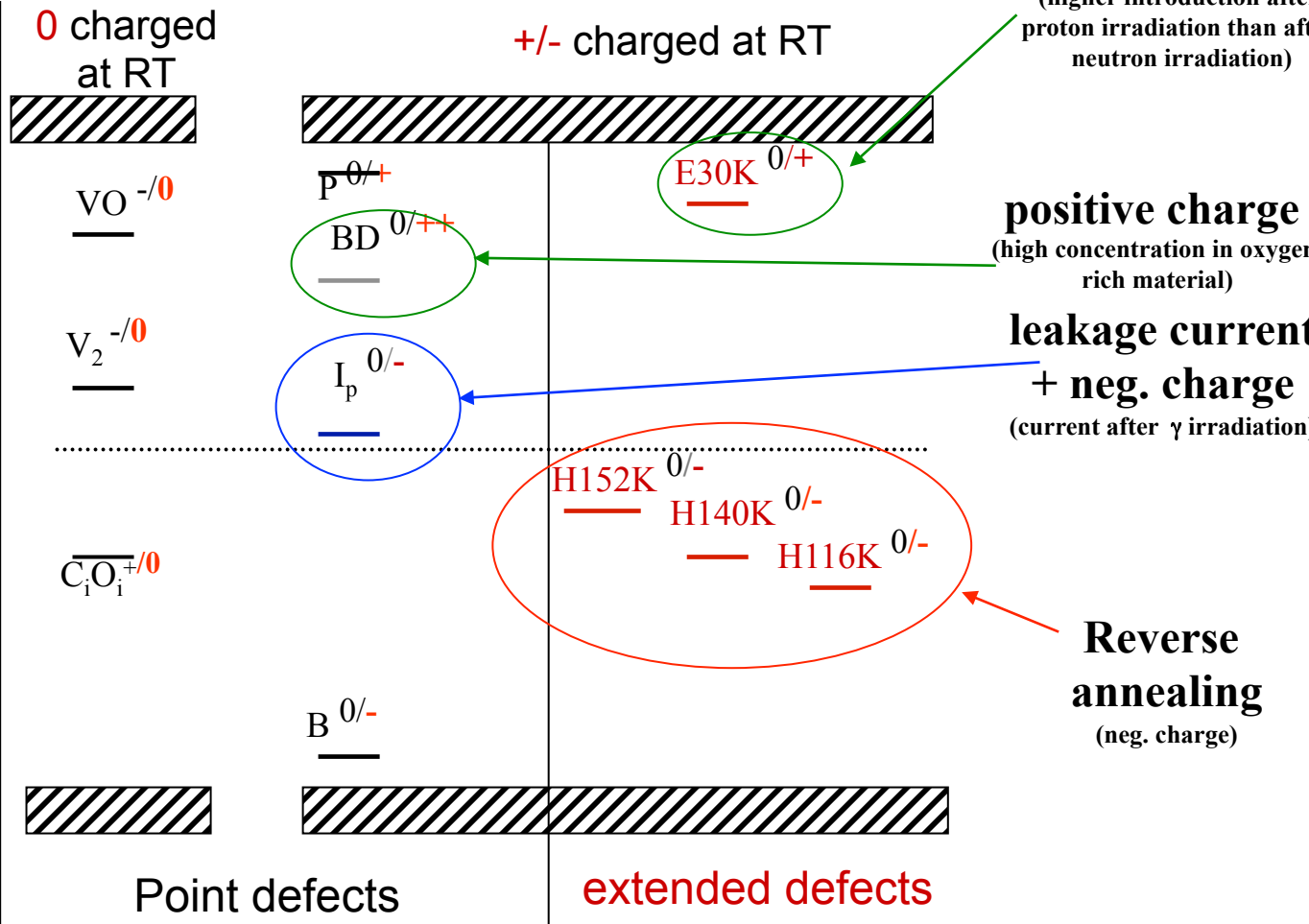
- $E_i^{116K} = E_v + 0.33 \text{ eV}$
- $\sigma_p^{116K} = 4 \cdot 10^{-14} \text{ cm}^2$
- $E_i^{140K} = E_v + 0.36 \text{ eV}$
- $\sigma_p^{140K} = 2.5 \cdot 10^{-15} \text{ cm}^2$
- $E_i^{152K} = E_v + 0.42 \text{ eV}$
- $\sigma_p^{152K} = 2.3 \cdot 10^{-14} \text{ cm}^2$
- $E_i^{30K} = E_c - 0.1 \text{ eV}$
- $\sigma_n^{30K} = 2.3 \cdot 10^{-14} \text{ cm}^2$



I.Pintilie, NSS, 21 October 2008, Dresden

device properties at operating temperature

<u>Point defects</u>
• $E_i^{BD} = E_c - 0.225 \text{ eV}$
• $\sigma_n^I = 2.3 \cdot 10^{-14} \text{ cm}^2$
• $\sigma_p^I = 2.3 \cdot 10^{-14} \text{ cm}^2$
Cluster related centers
• $E_i^{116K} = E_v + 0.33 \text{ eV}$
• $\sigma_p^{116K} = 4 \cdot 10^{-14} \text{ cm}^2$
• $E_i^{140K} = E_v + 0.36 \text{ eV}$
• $\sigma_p^{140K} = 2.5 \cdot 10^{-15} \text{ cm}^2$
• $E_i^{140K} = E_v + 0.36 \text{ eV}$
• $\sigma_p^{140K} = 2.5 \cdot 10^{-15} \text{ cm}^2$
• $E_i^{152K} = E_v + 0.42 \text{ eV}$
• $\sigma_p^{152K} = 2.3 \cdot 10^{-14} \text{ cm}^2$
• $E_i^{30K} = E_c - 0.1 \text{ eV}$
• $\sigma_n^{30K} = 2.3 \cdot 10^{-14} \text{ cm}^2$

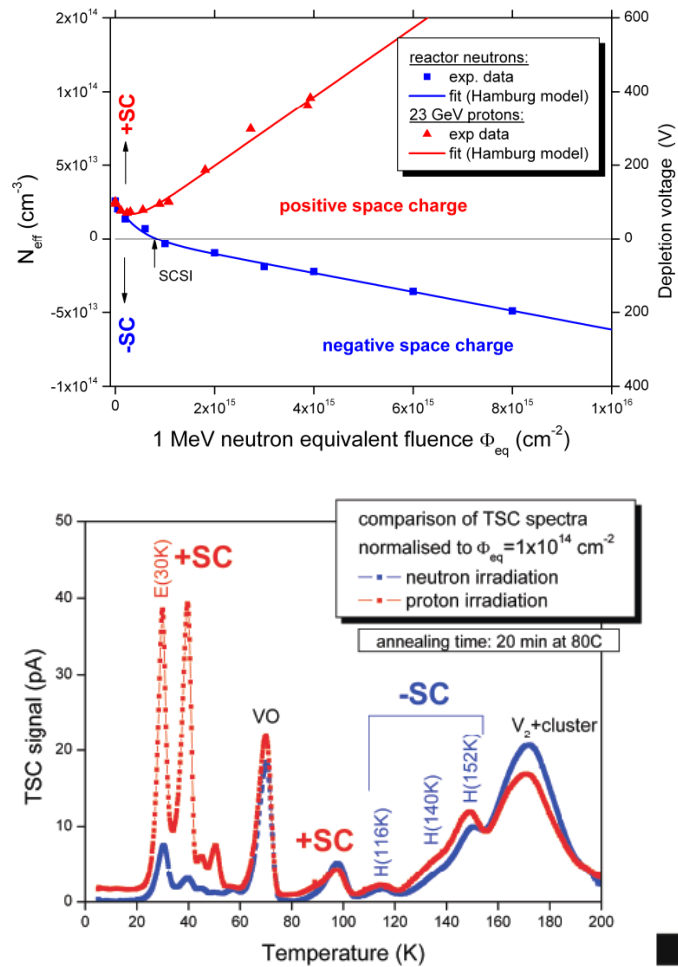


I.Pintilie, NSS, 21 October 2008, Dresden

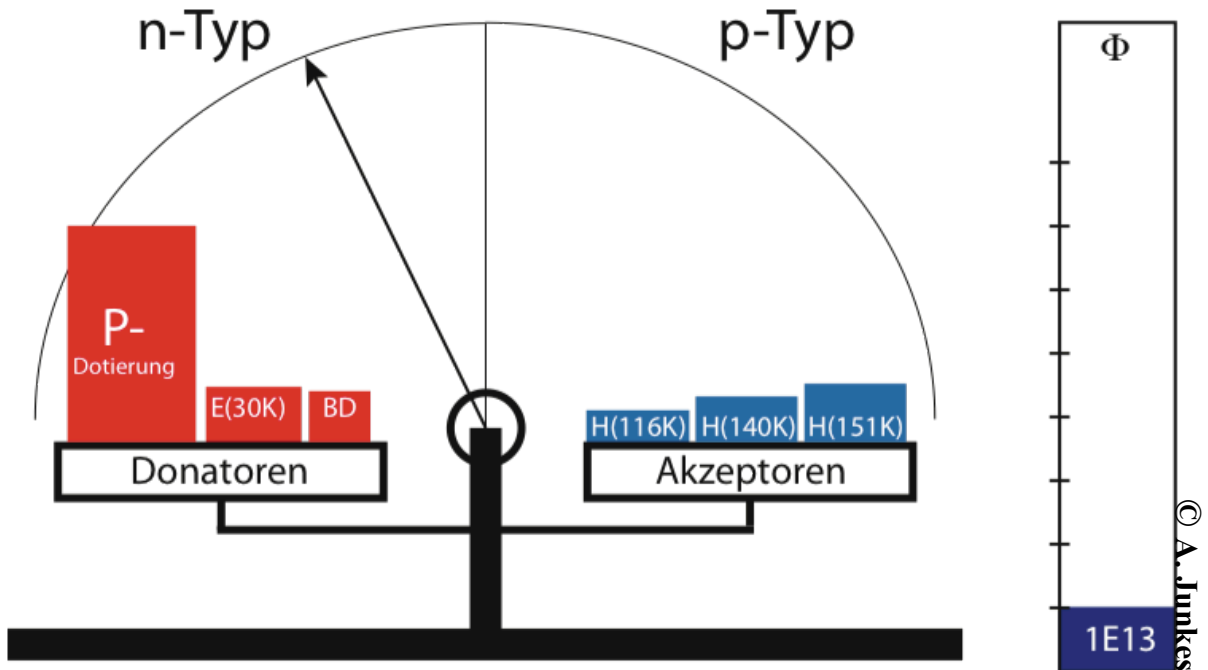
Mara Bruzzi, Danno da radiazione in semiconduttori

Scuola Nazionale rivelatori ed elettronica per fisica delle alte energie , astrofisica 12 Aprile 2011,
Legnaro, Italy

N_{eff} : Neutron irradiation

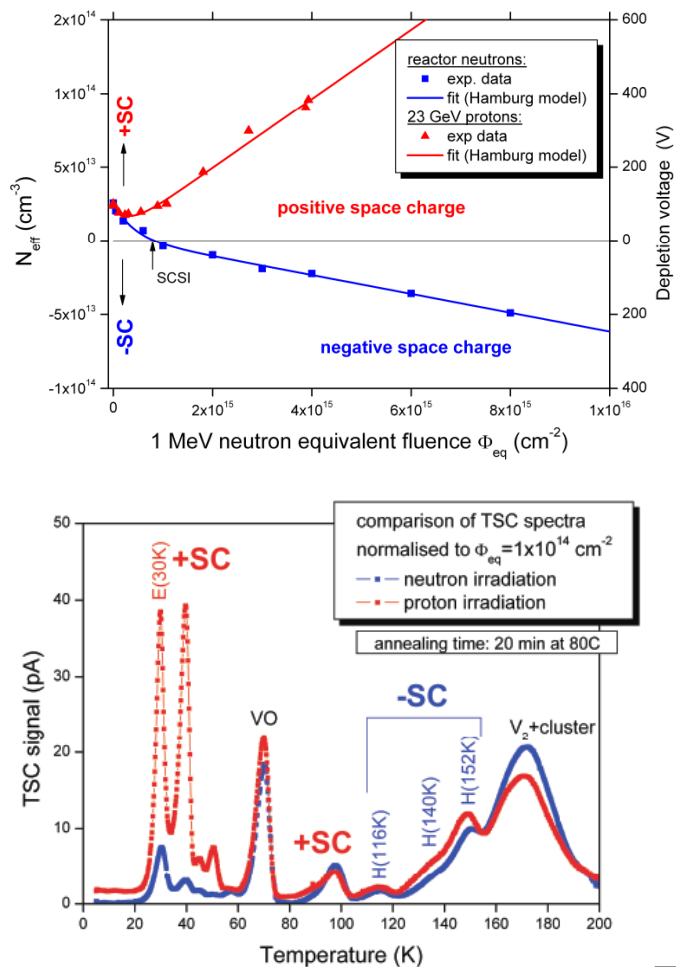


Epitaxial silicon (*EPI-DO, 72 μm, 170 Ωcm, diodes*) irradiated with reactor neutrons

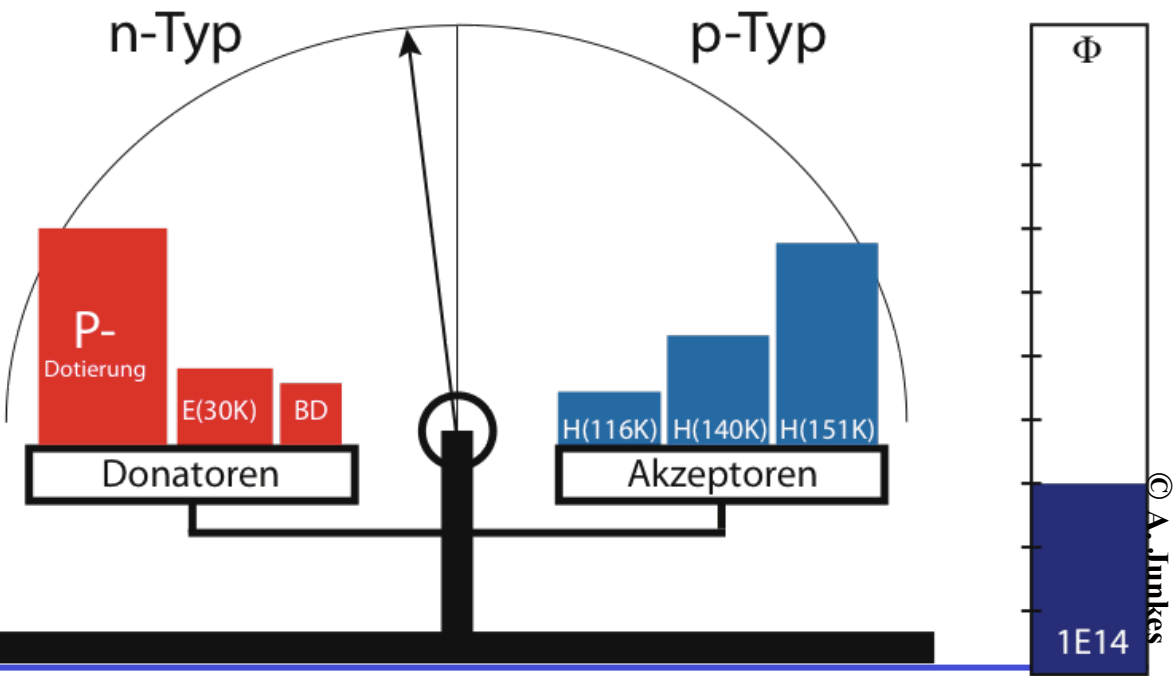


By A. Junkes, presented by U. Parzefal on behalf of the RD50 Collaboration, RESMDD10 , Oct. 2010, Florence

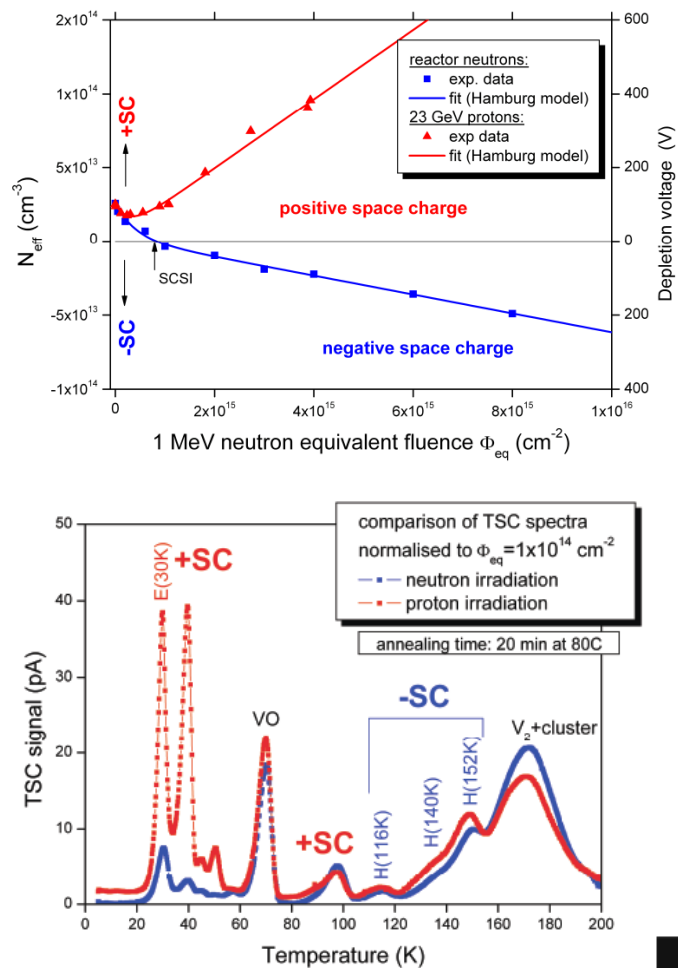
N_{eff} : Neutron irradiation



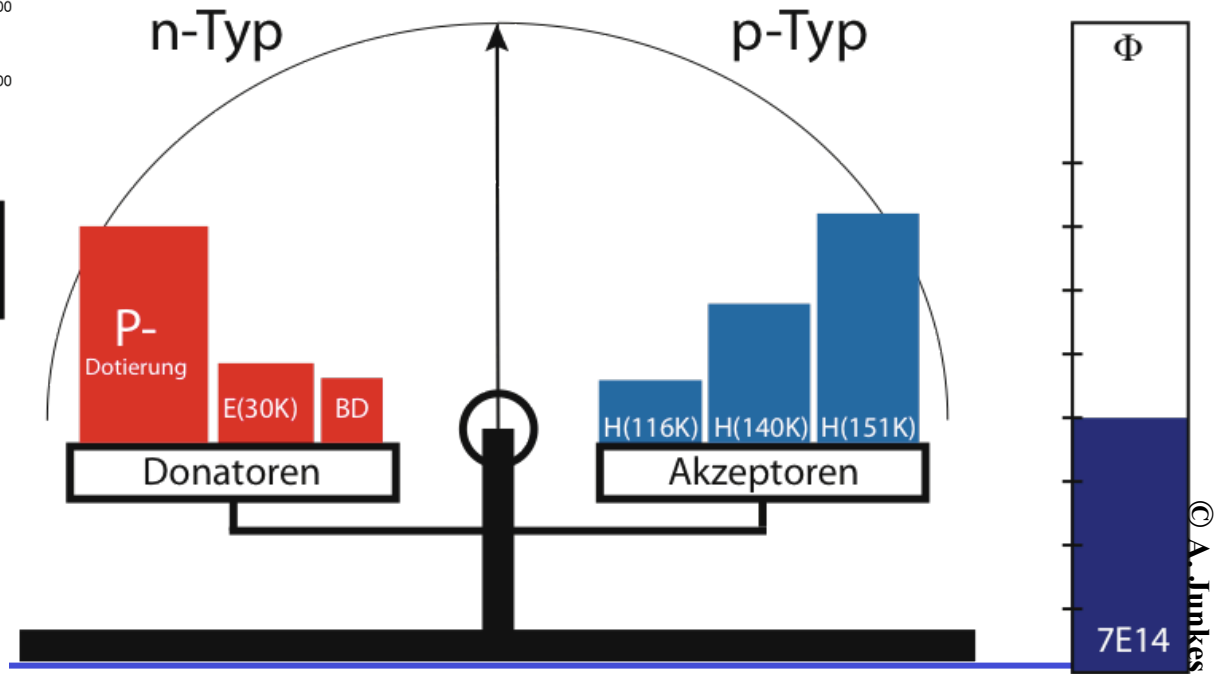
Epitaxial silicon (*EPI-DO, 72 μm, 170 Ωcm, diodes*) irradiated with reactor neutrons



N_{eff} : Neutron irradiation



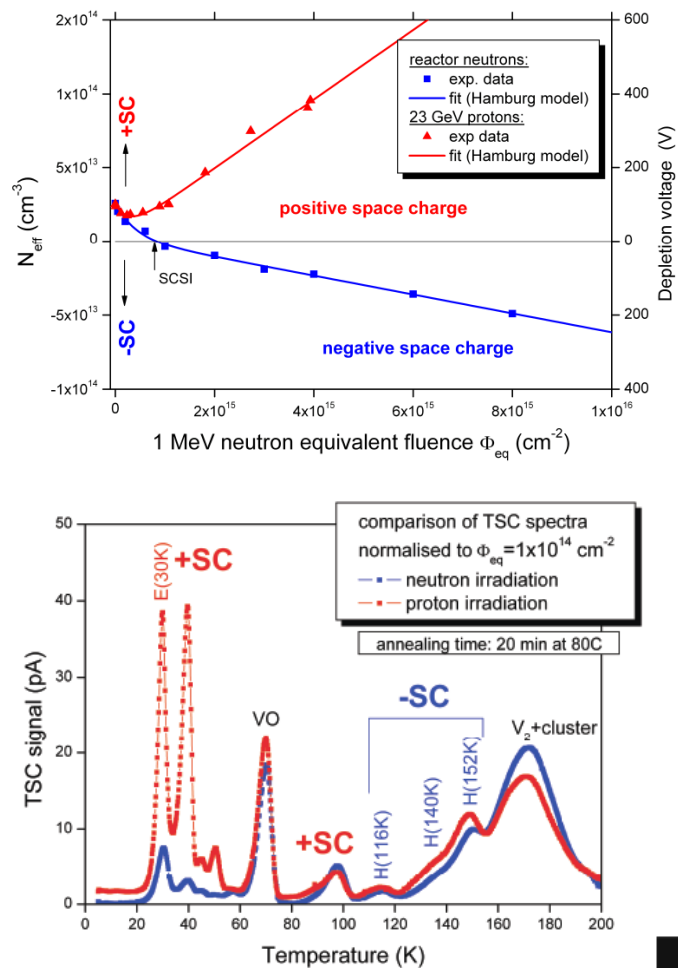
Epitaxial silicon (*EPI-DO, 72 μm, 170 Ωcm, diodes*) irradiated with reactor neutrons



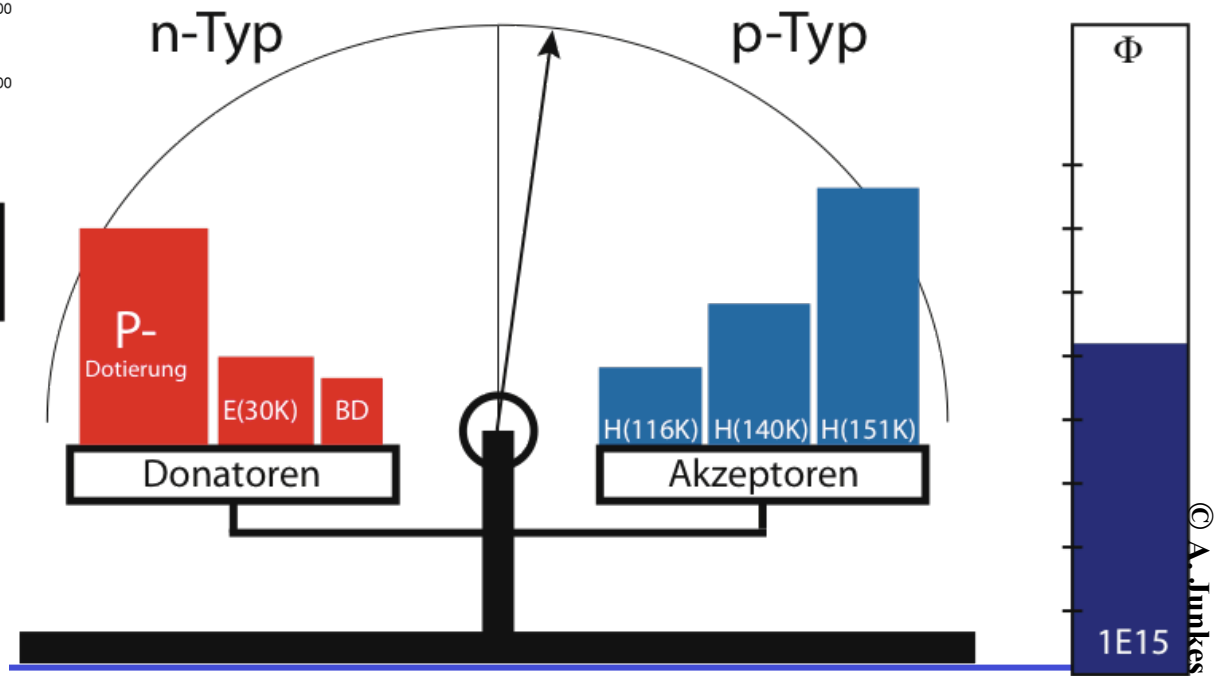
Mara Bruzzi, Danno da radiazione in semiconduttori
Scuola Nazionale Rivelatori ed elettronica per fisica delle alte energie, astrophysica 12 Aprile 2011,
Legnaro, Italy



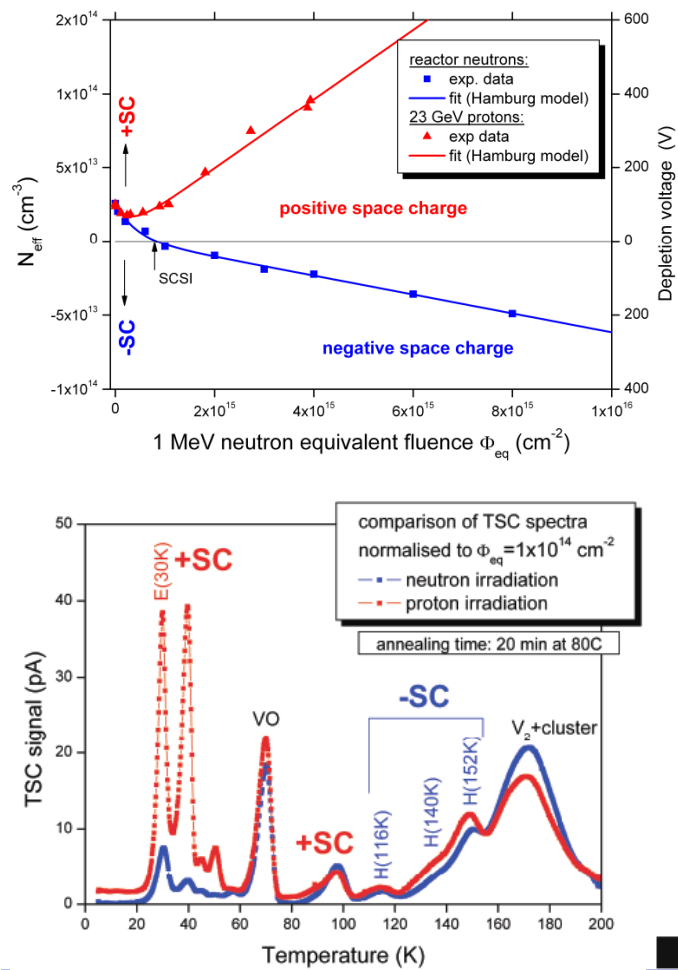
N_{eff} : Neutron irradiation



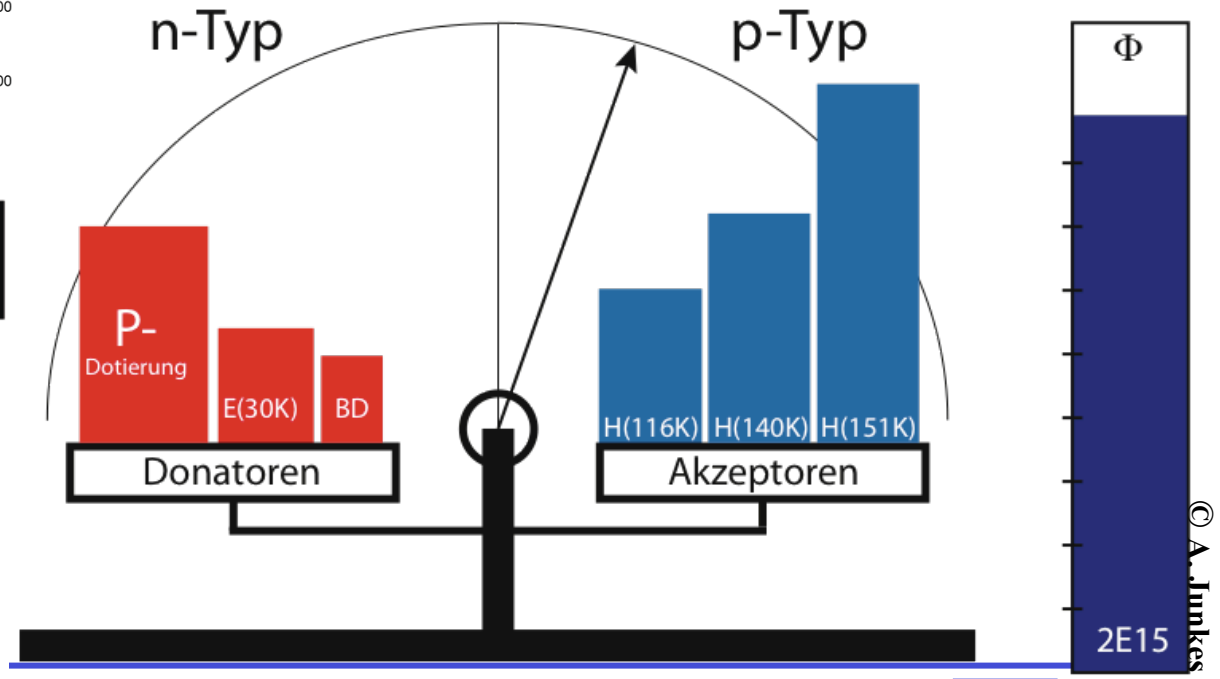
Epitaxial silicon (*EPI-DO, 72 μm, 170 Ωcm, diodes*) irradiated with reactor neutrons



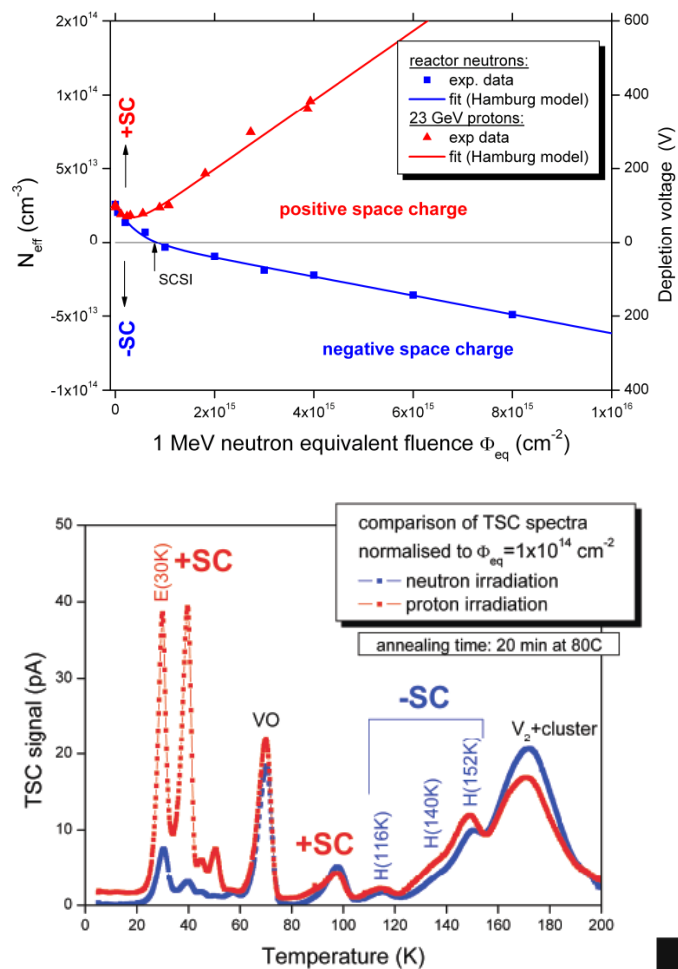
N_{eff} : Neutron irradiation



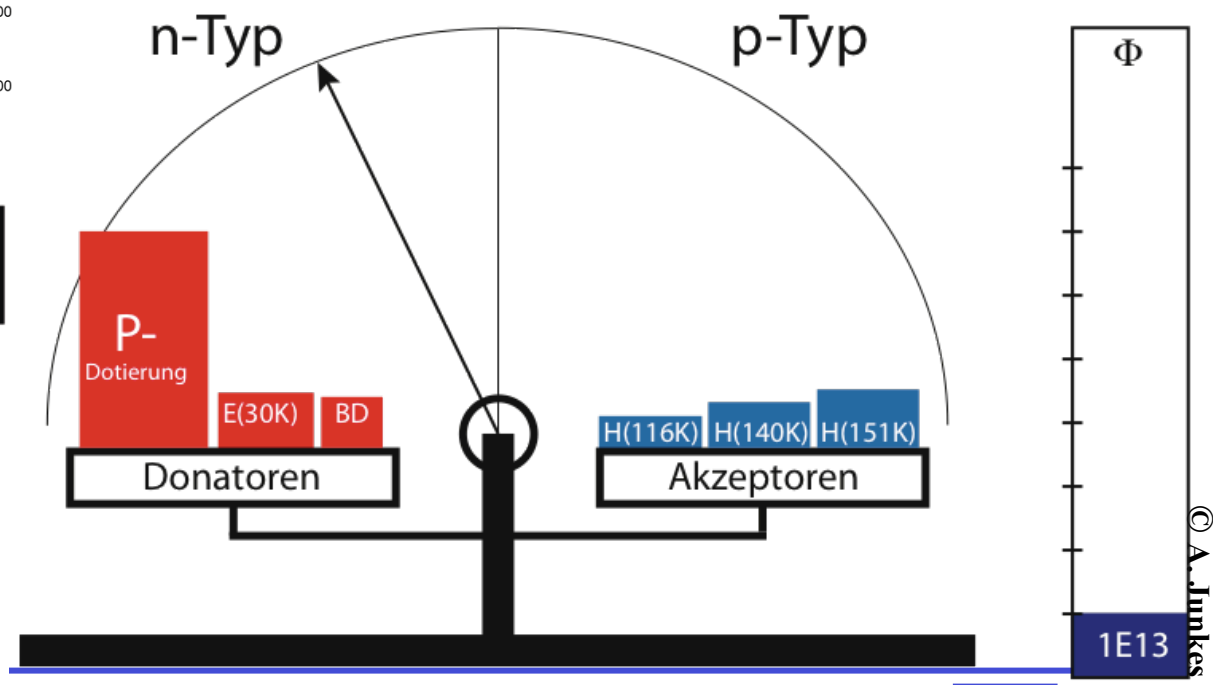
Epitaxial silicon (*EPI-DO, 72 μm, 170 Ωcm, diodes*) irradiated with reactor neutrons



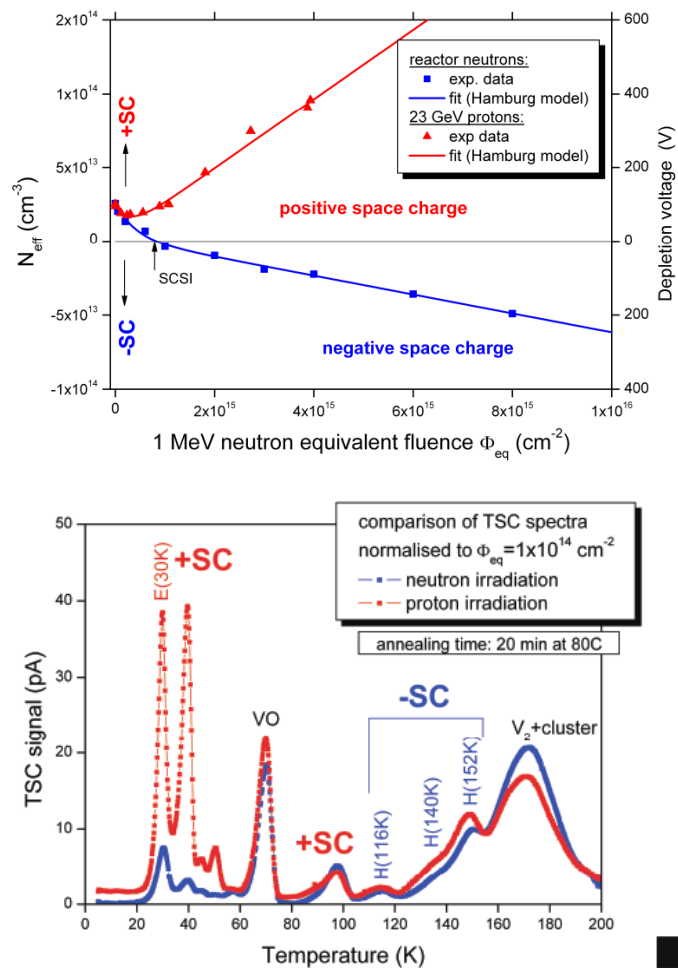
N_{eff} : Proton irradiation



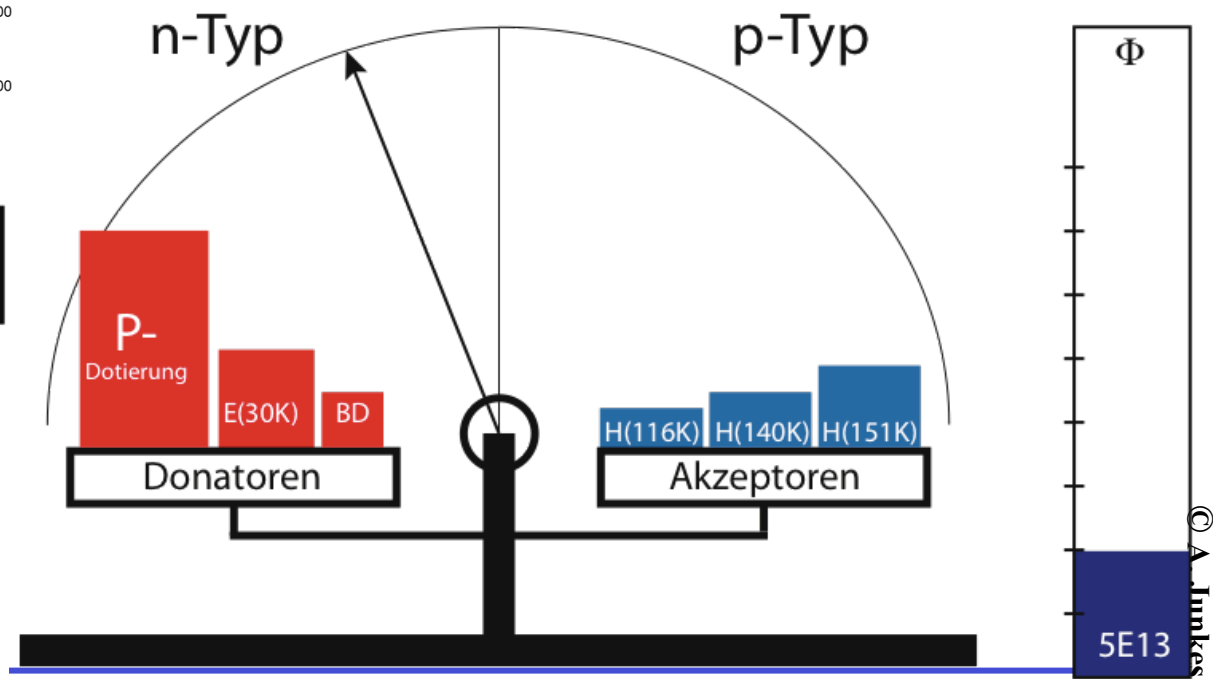
Epitaxial silicon (*EPI-DO, 72 μm, 170 Ωcm, diodes*) irradiated with 23 GeV Protons



N_{eff} : Proton irradiation



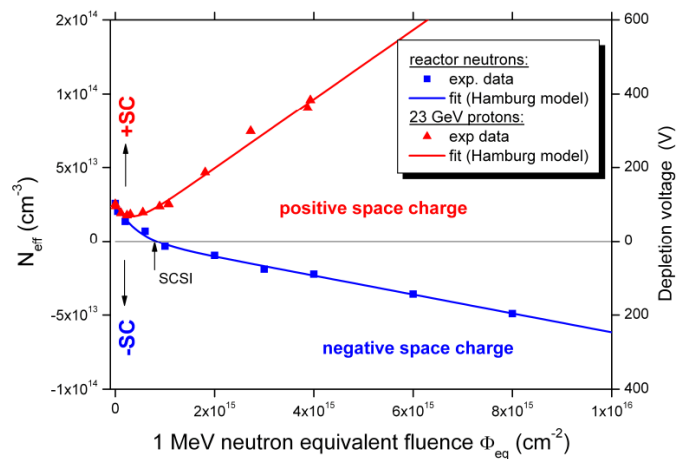
Epitaxial silicon (*EPI-DO, 72 μm, 170 Ωcm, diodes*) irradiated with 23 GeV Protons



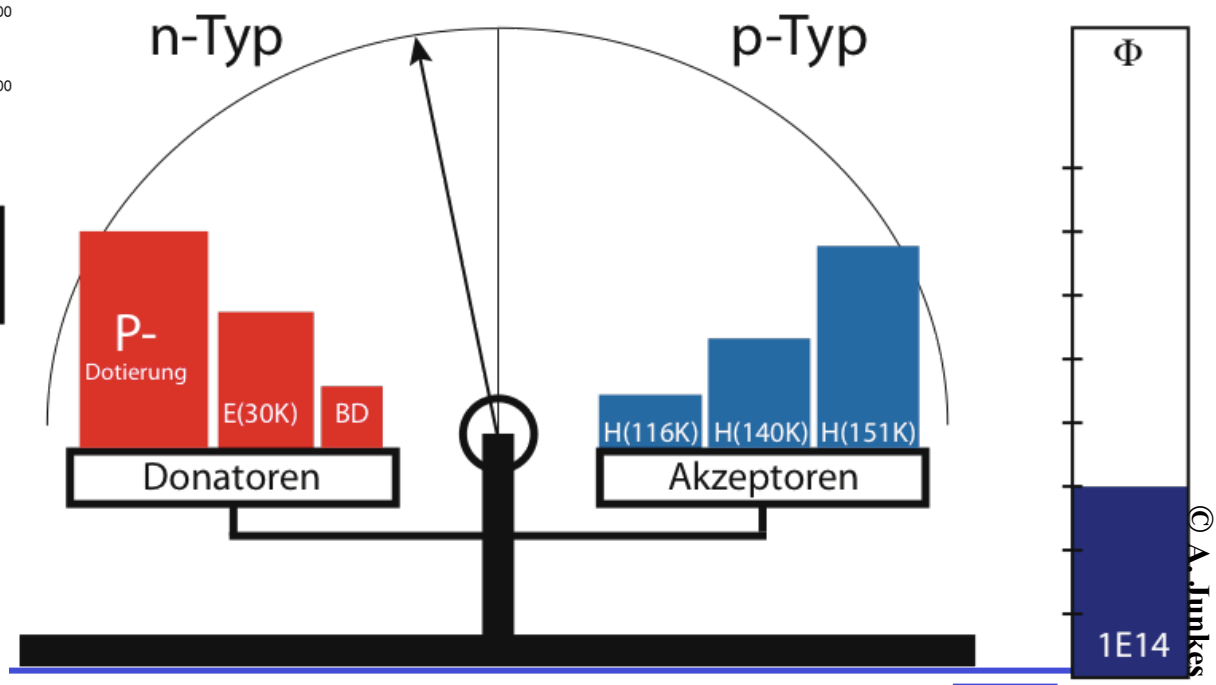
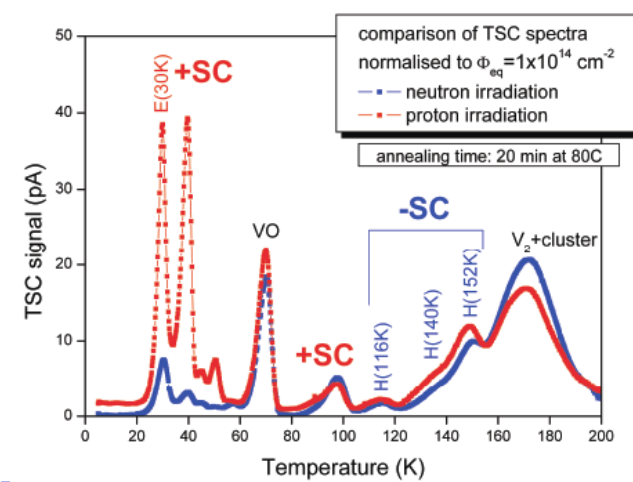
Junkes, presented by U. Parzefal on behalf of the RD50 Collaboration, RESMDD10 , Oct. 2010, Florence



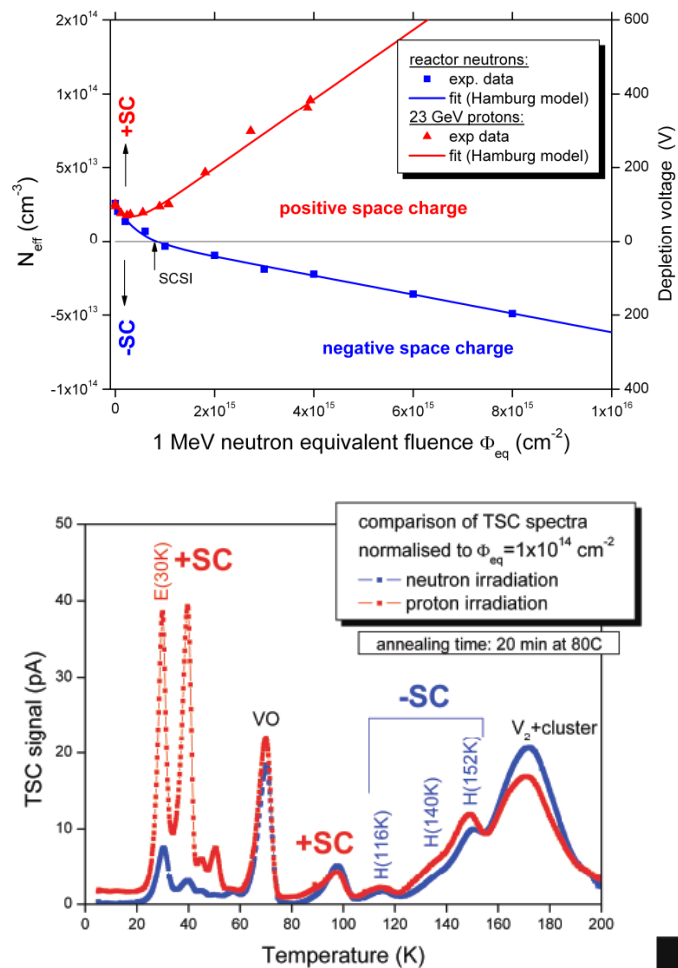
N_{eff} : Proton irradiation



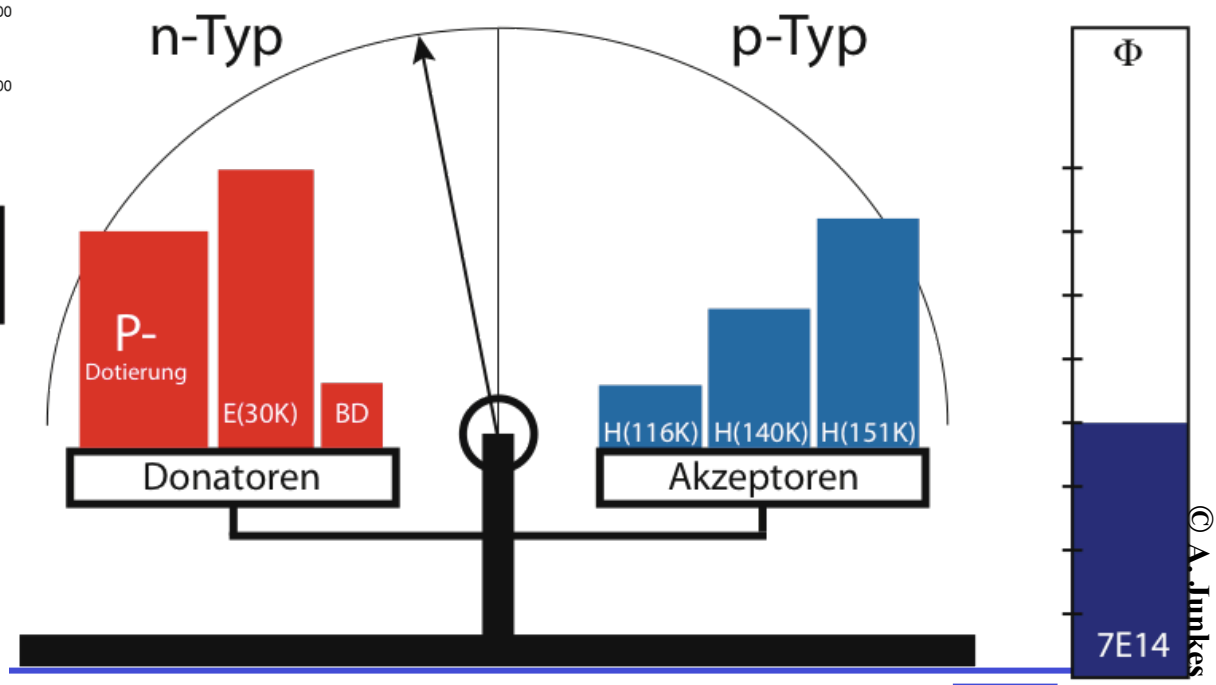
Epitaxial silicon (*EPI-DO, 72 μm, 170 Ωcm, diodes*) irradiated with 23 GeV Protons



N_{eff} : Proton irradiation



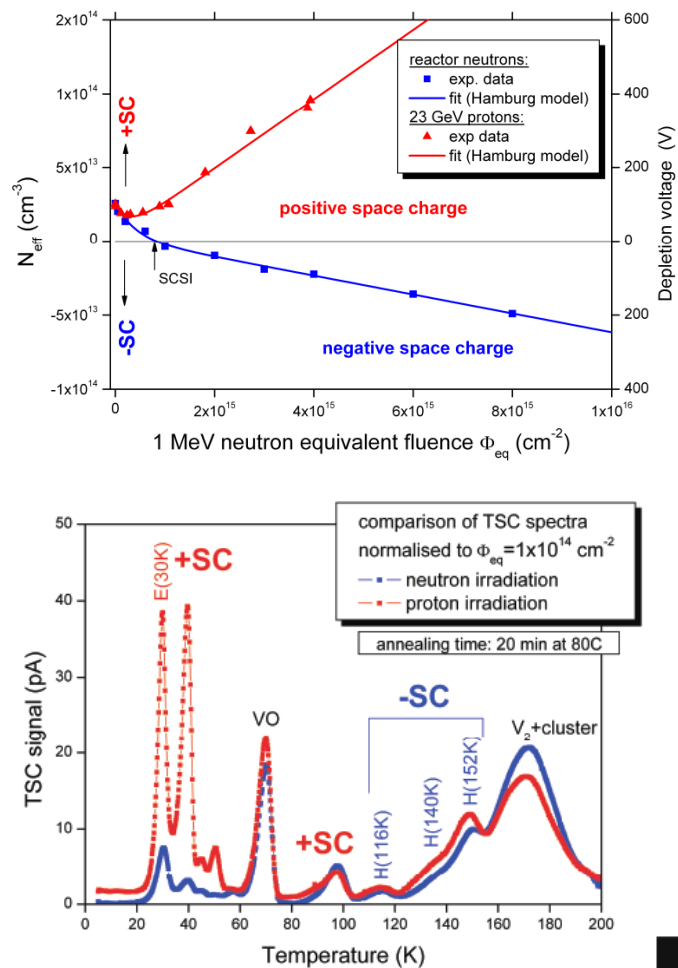
Epitaxial silicon (*EPI-DO, 72 μm, 170 Ωcm, diodes*) irradiated with 23 GeV Protons



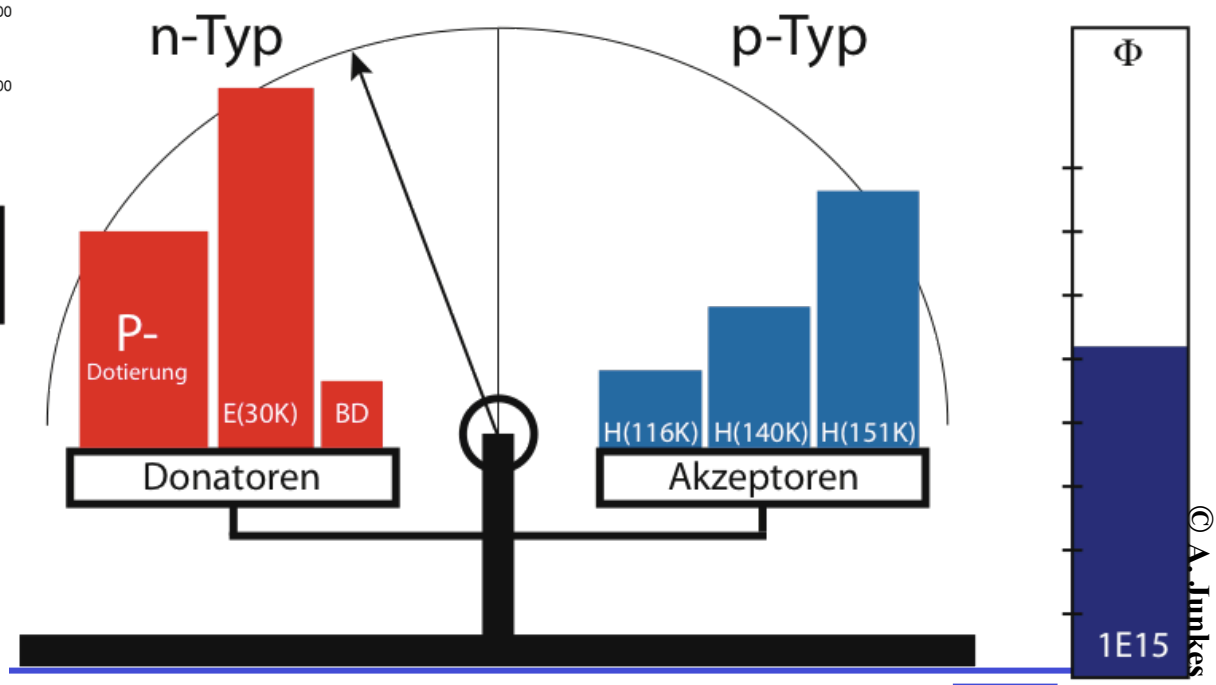
Junkes, presented by U. Parzefal on behalf of the RD50 Collaboration, RESMDD10 , Oct. 2010, Florence



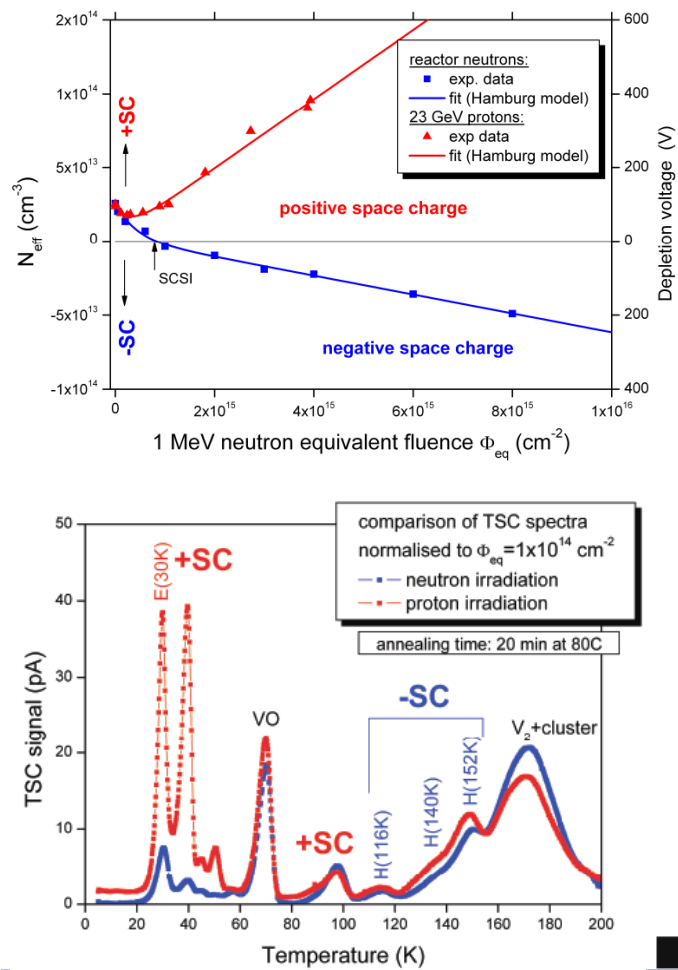
N_{eff} : Proton irradiation



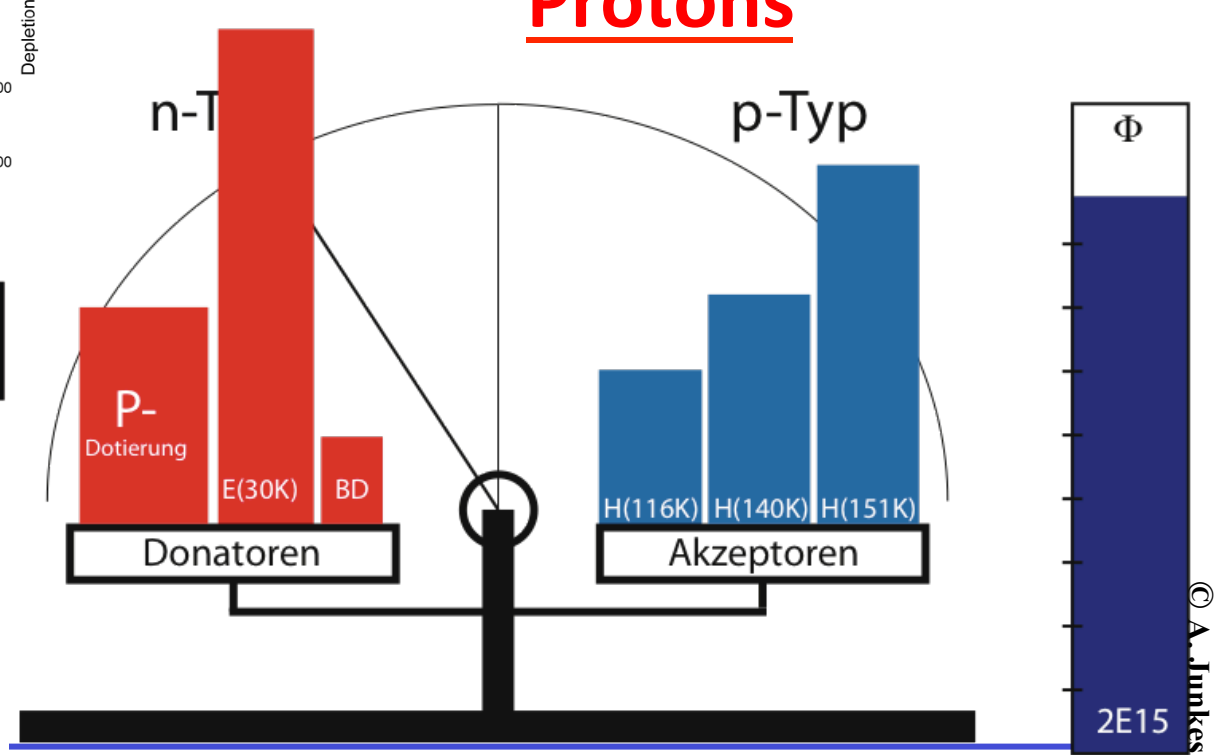
Epitaxial silicon (*EPI-DO, 72 μm, 170 Ωcm, diodes*) irradiated with 23 GeV Protons



N_{eff} : Proton irradiation



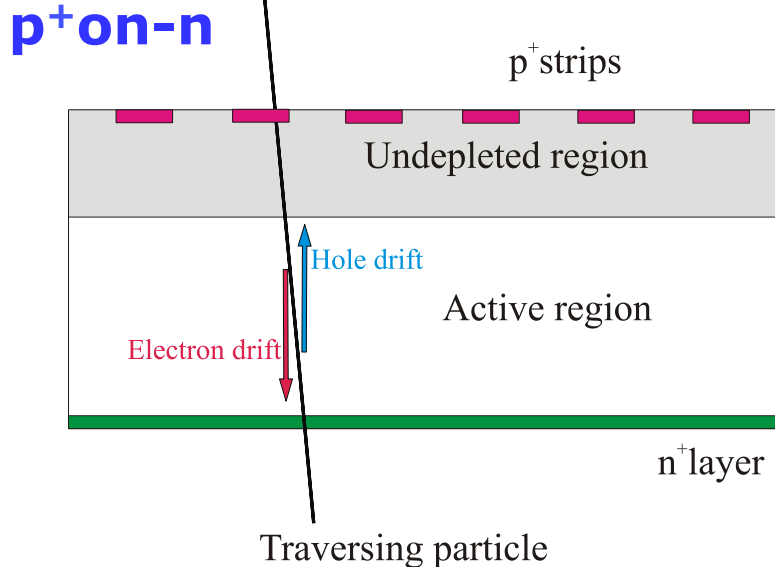
Epitaxial silicon (*EPI-DO, 72 μm, 170 Ωcm, diodes*) irradiated with 23 GeV Protons



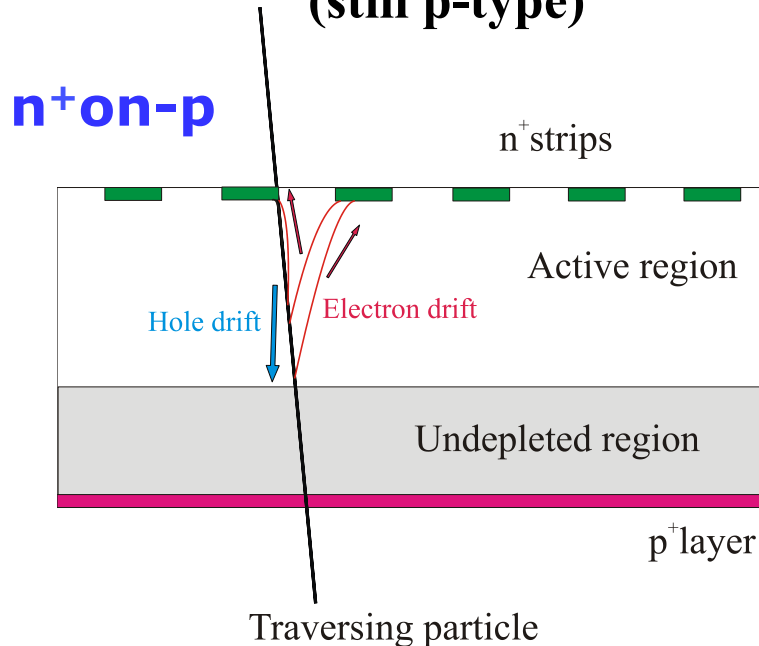
RD50: Device engineering

p-in-n versus n-in-p (or n-in-n) detectors

n-type silicon after high fluences: (type inverted)



p-type silicon after high fluences: (still p-type)



- Charge spread – degraded resolution
- Charge loss – reduced CCE

n-on-p silicon, under-depleted:

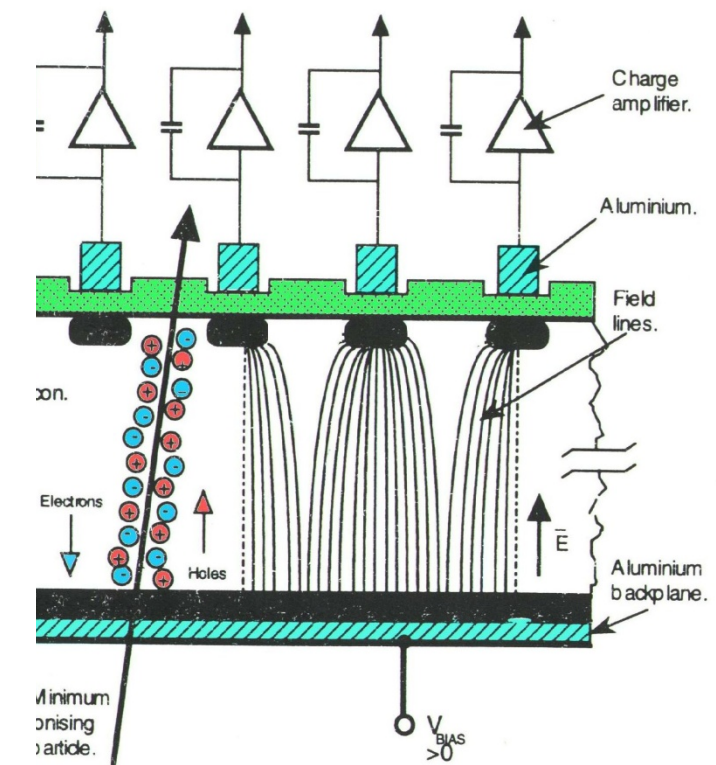
- Limited loss in CCE
- Less degradation with under-depletion
- Collect electrons (3 x faster than holes)

Charge Multiplication by impact ionization

Charge collected at electrodes in a semiconductor can not only be generated by ionising radiation of charge they high by fields, a phenomenon called impact ionization.

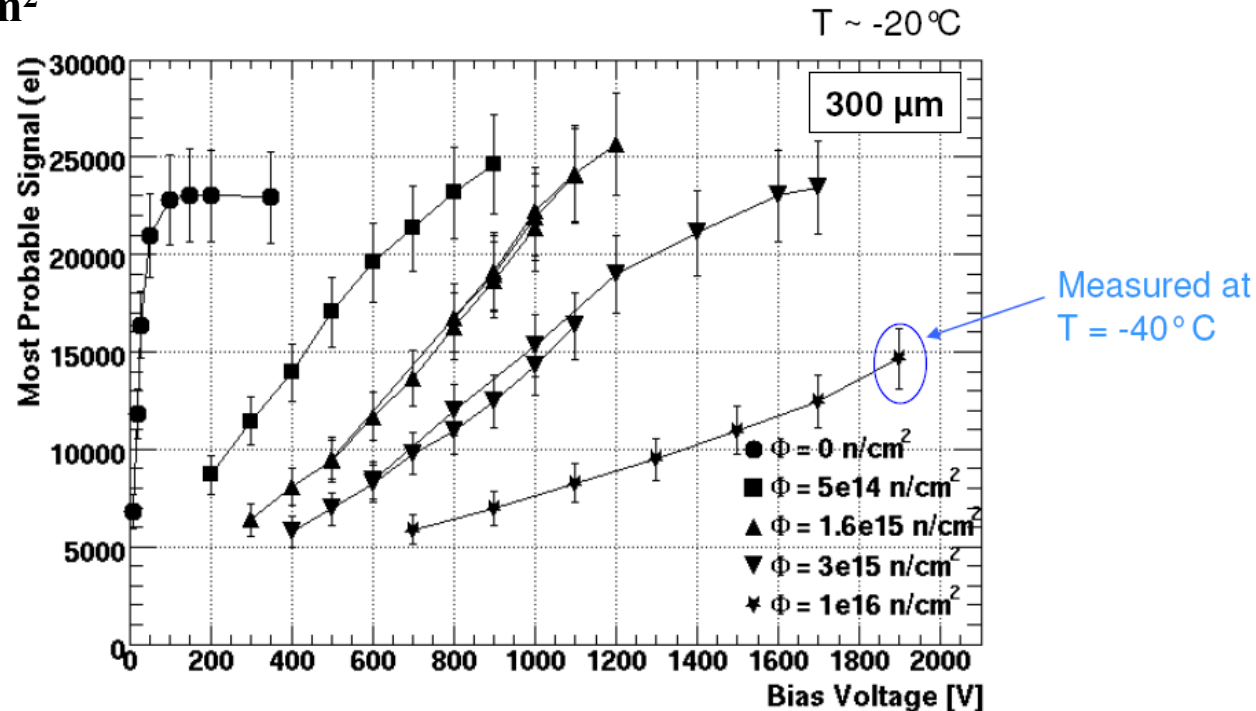
This way electrons and holes promoted in conduction/valence bands by ionising radiation (primary charge) attain enough energy to create new electron-hole pairs (secondary charge). This mechanism is also origin of current breakdown in diodes when very high reverse voltage are applied.

In a device electric field is increased in the nearby of collecting electrode due to accumulation of field lines. In irradiated devices the electric field is also enhanced by radiation induced defects



Charge Multiplication

CCE measured with p-type Si microstrip detectors at very high fluences shows evidence of a charge multiplication effect: 100% CCE seen after $3 \times 10^{15} \text{ n/cm}^2$, 15000 electrons after 10^{16} n/cm^2



I. Mandić, RESMDD08, Florence, Italy, 15th -17th October 2008

7



Increase of the electric field close to the strips causing impact ionization/carrier injection when high concentrations of effective acceptors are introduced at very high fluences.



Mara Bruzzi, Danno da radiazione in semiconduttori
Scuola Nazionale rivelatori ed elettronica per fisica delle alte energie , astrofisica 12 Aprile 2011,
Legnaro, Italy



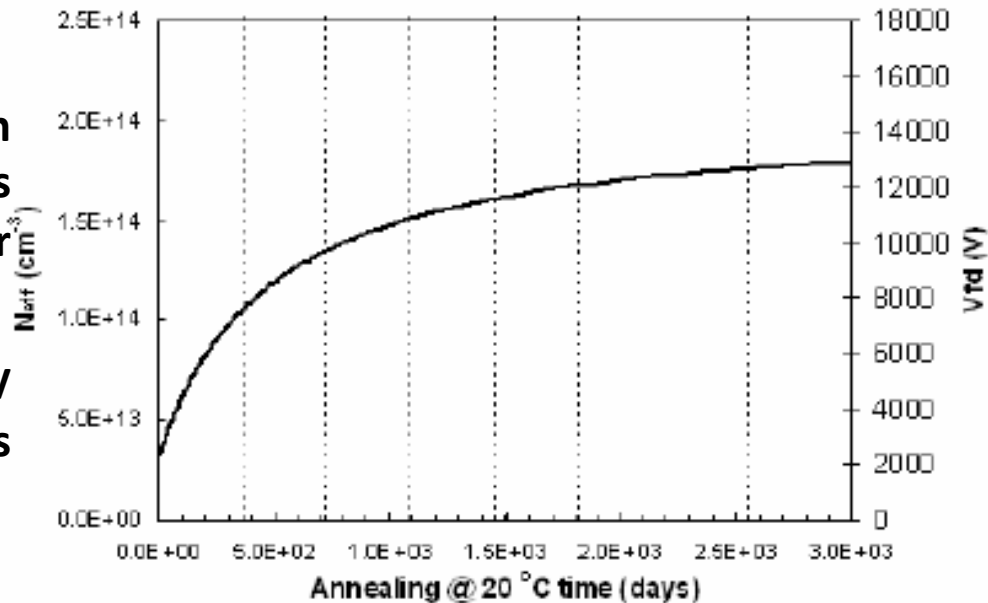
Annealing of irradiated microstrip detectors

Reverse annealing in irradiated Si microstrip detectors has been always considered as a possible cause of early failure in the experiments if not controlled by reasonable temperature

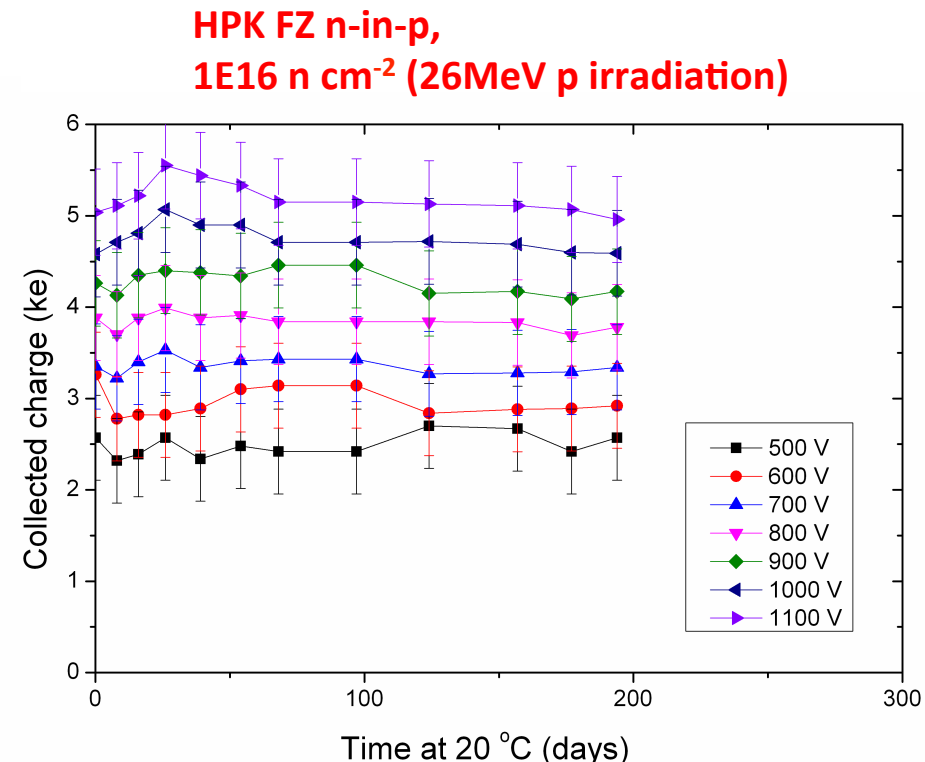
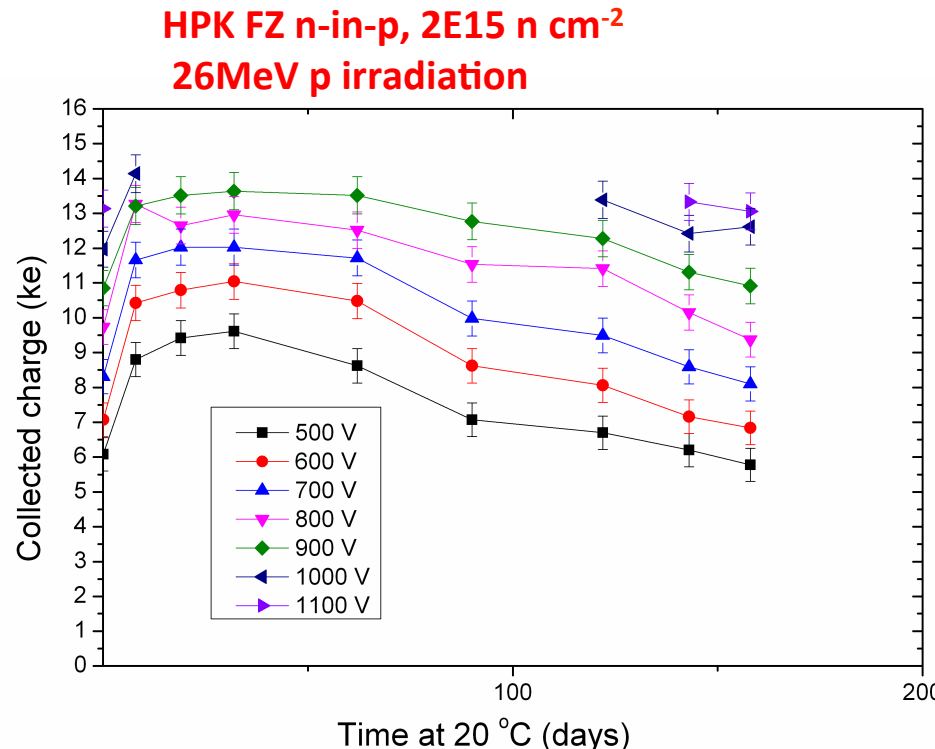
(not only during operations but also during maintenance/shut down periods). This was originated by accurate measurements of the annealing behavior of the full depletion

Expected changes of full depletion voltage with time after irradiation (as measured with the C-V method) for detector irradiated to $7.5 \times 10^{15} \text{ p cm}^{-2}$.

Please notice that according to CV measurements the so called V_{FD} changes from <3kV to >**12kV!**



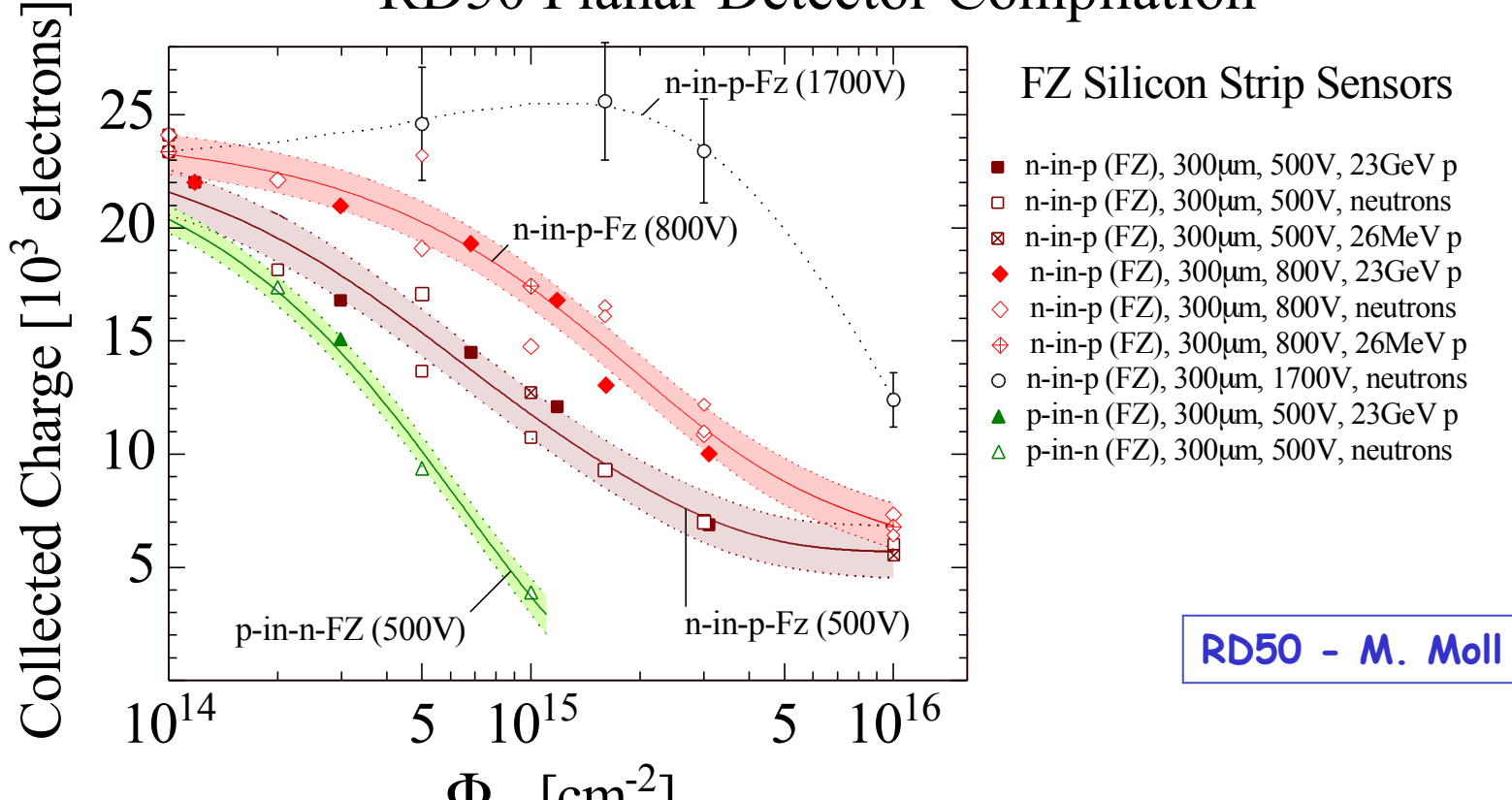
As a matter of fact, the annealing behaviour of the CCE measured with p-type Si microstrip detectors does not correspond to that measured by CV with diodes. No reverse annealing is visible in the CCE measurement.



Origin of observed behaviour :

- Charge Multiplication due to increased electric field close to strips as concentration of acceptors grows with time/temperature;
- Reduction of the effective trapping probability of electrons with annealing.

RD50 Planar Detector Compilation



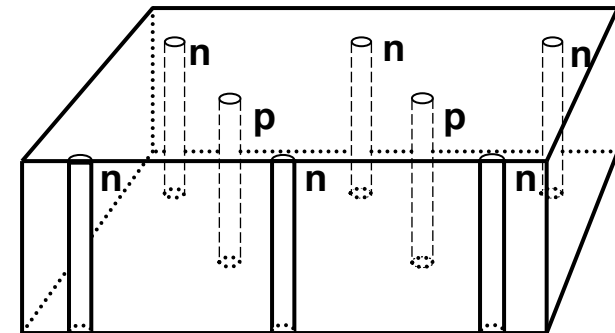
at 10^{16}N_{eq} at

- n-in-p benefits from charge multiplication at high bias voltages
- CM effect also seen for p-in-n (but less strong at high partial voltages)
- n-in-p (n-in-n) superior material for high radiation depletion mode)
superior material for high radiation environments



Device Engineering: 3D detectors

- Electrodes:
 - narrow columns along detector
 - narrow columns along detector thickness-“3D”
- diameter: $10\mu\text{m}$ distance: $50 - 100\mu\text{m}$
 - Lateral depletion:
 - fast signal
- Hole processing :
 - Dry etching, Laser drilling, Photo Electro Chemical

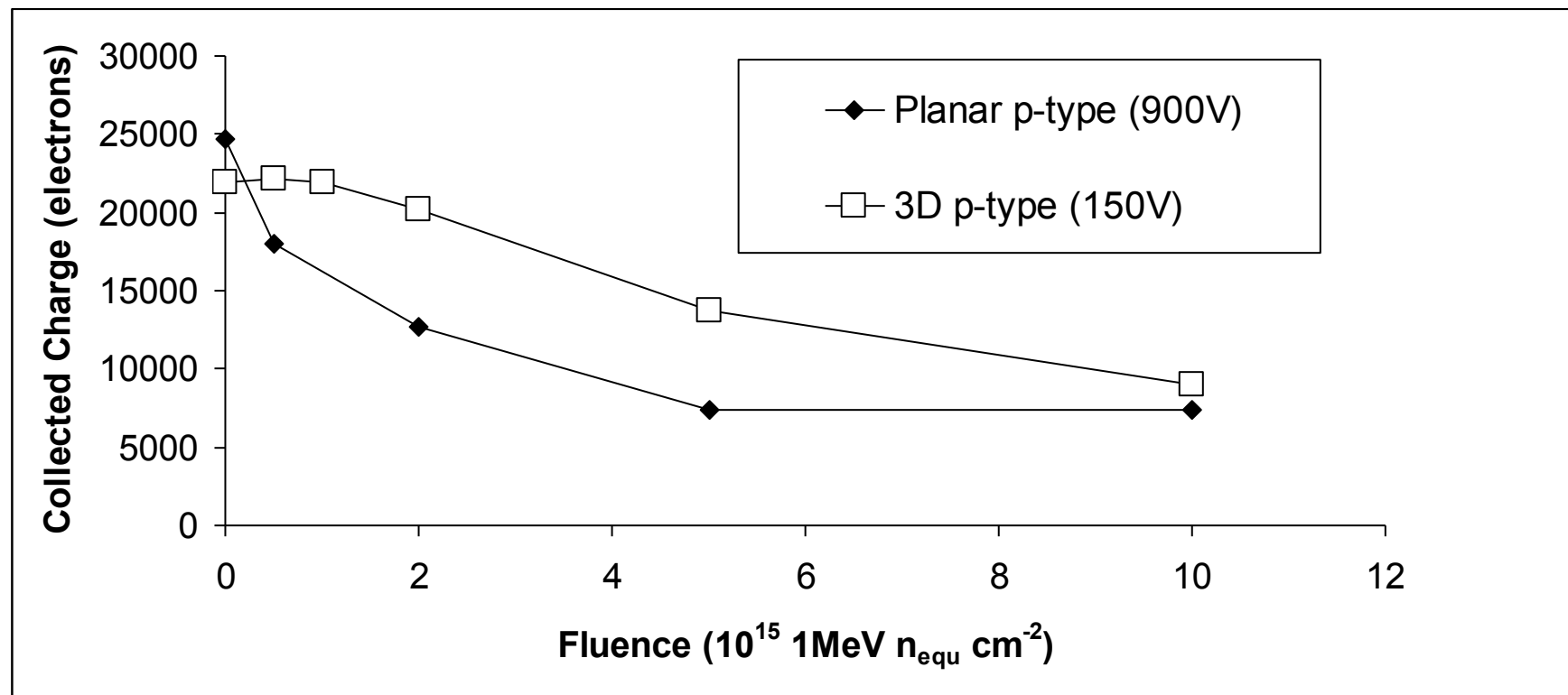


395 (1997) 328)



3D vs planar detectors

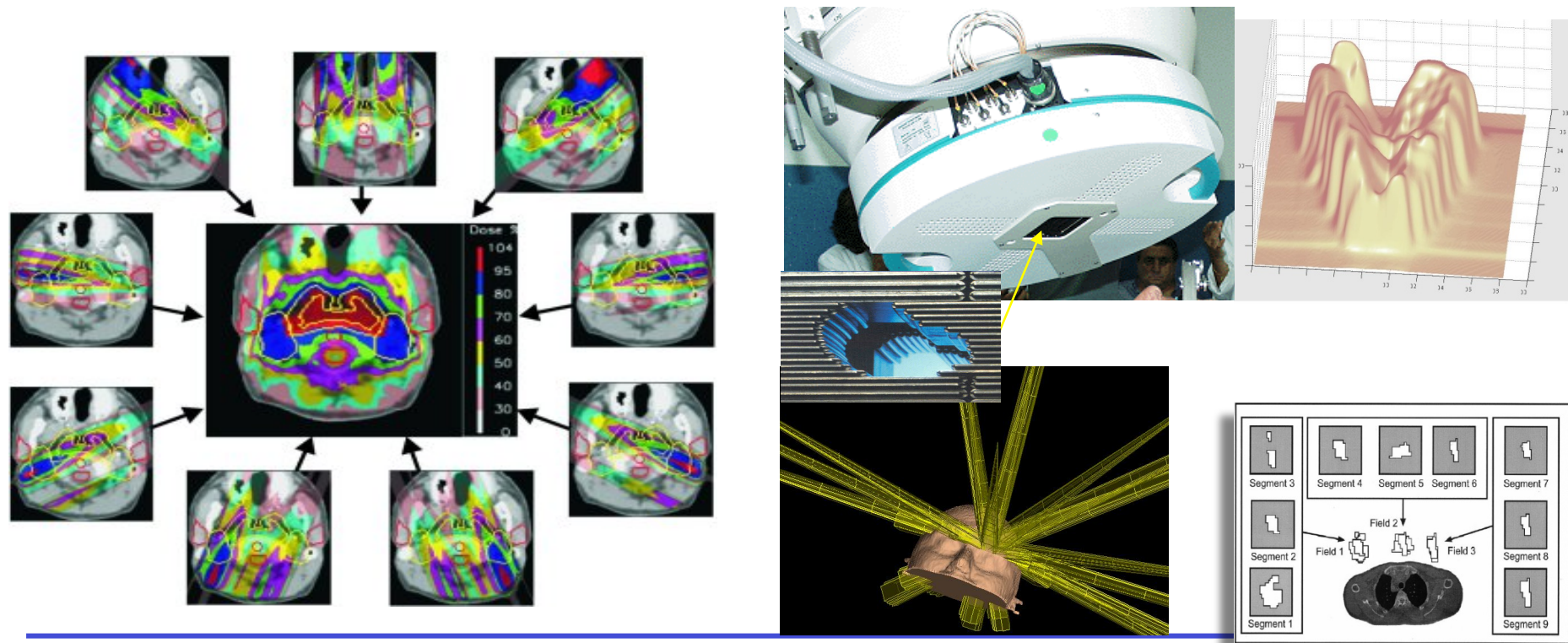
Collected charge as a function of fluence. Note 3D only 150V, high bias gets increase in charge due to multiplication



See next talk

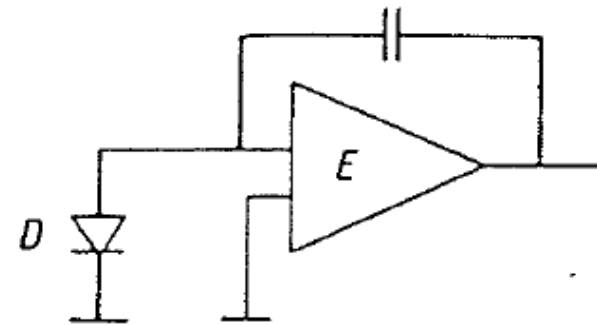
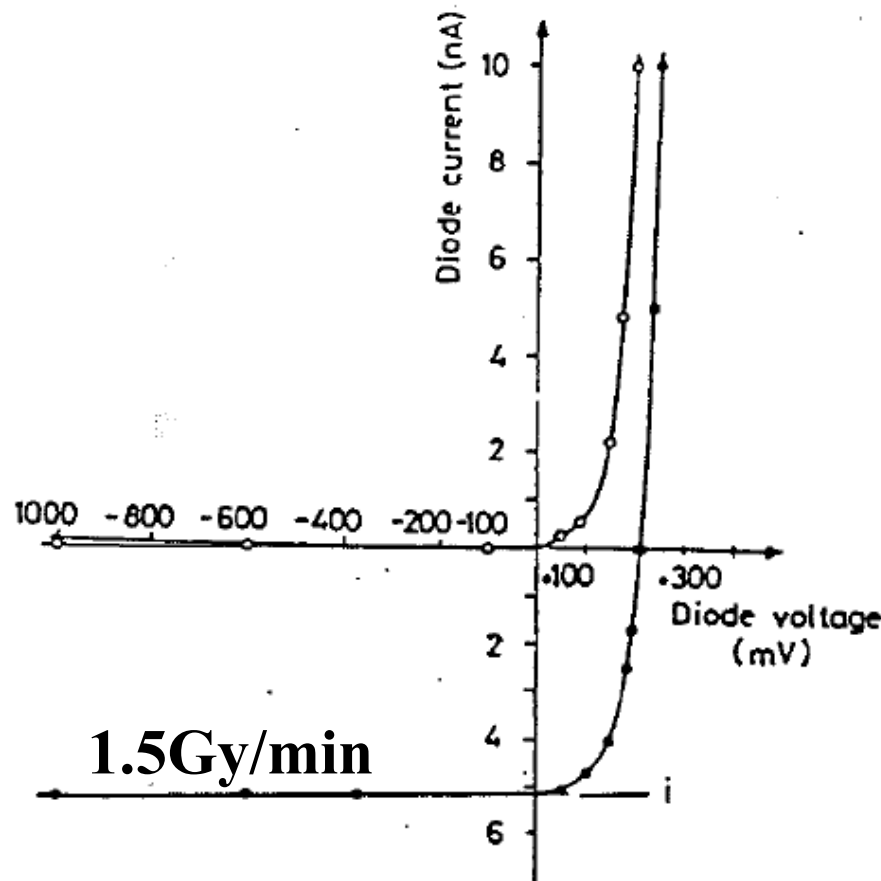
Another example: Semiconductor Devices in Clinical Radiotherapy

Clinical dosimetry in radiotherapy is well known matter but high conformal radiotherapy modalities (IMRT, Stereotactic treatments with photons and protons, IMPT) pose problems due to the **small radiation fields with high dose gradients**, to the **variation in space and time of the dose rate** and to the **variation in space and time of the beam energy spectrum**.



Mara Bruzzi, Danno da radiazione in semiconduttori
Scuola Nazionale rivelatori ed elettronica per fisica delle alte energie , astrofisica 12 Aprile 2011,
Legnaro, Italy

Si dosimeter working principle: Photovoltaic Mode



- a) null bias;
- b) DC coupling;
- c) Sampling time and reset fixed by digital electronics (usually $T \approx 10\text{ms}$);
- d) Only integrated charge measured.

Sensitivity of the device scales with diffusion length:

$$L_{e,h} = \sqrt{D_{e,h}\tau_{e,h}}$$

Sensitivity per unit area of the device is:

$$S = \frac{J}{R} = sL_e = \frac{q\rho_{Si}}{E_i} L_e.$$

$$S \approx \frac{q\rho_{Si}}{E_i} \sqrt{D_e \tau_e \left(1 + \frac{(\tau_h + \tau_e) G \rho_{Si}}{p_0 E_i} R \right)}$$

$\tau'(R)$ dependence introduces dose rate non-linearity, due to traps saturation.
Dose rate linearity is improved by:

- a) high doping (i.e. high p_0);
- b) short lifetime.

If a single trap dominates, neglecting R related term:

$$S = \frac{q\rho_{Si}}{E_i} \sqrt{\frac{D_e}{\sigma_e v_e N_t}} \propto N_t^{-1/2}.$$

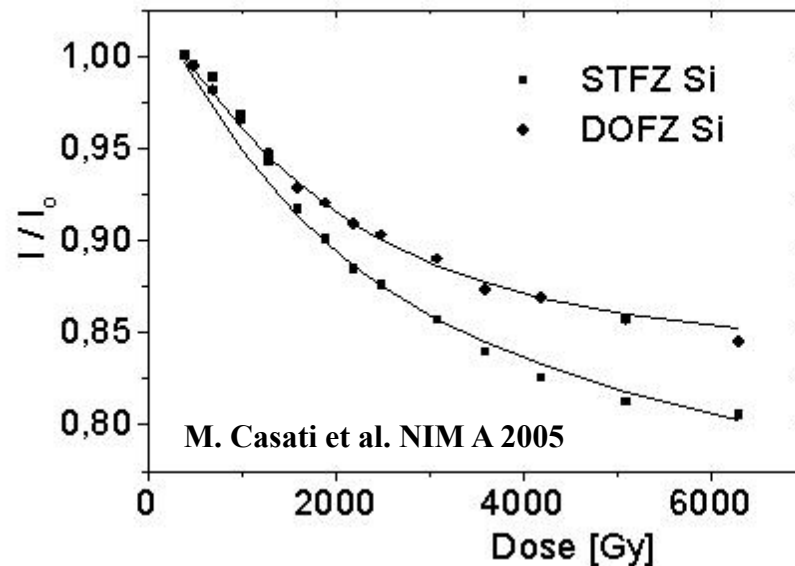


N_t grows with irradiation: τ_e and L_e decrease with accumulated dose.
This leads to a decrease in sensitivity S during device lifetime, and to the need of periodic recalibration.



Material engineering concepts have been applied also to Silicon dosimeters for radiotherapy

Improved radiation hardness of DOFZ Si



Decrease in sensitivity with the accumulated dose due to the generation of a dominant trap acting as lifetime killer.

$$1/\tau - 1/\tau_0 = \sigma v_{th} N_t, \quad N_t = a \phi; \quad a = \text{trap generation rate}$$

σ capture cross section ; v_{th} carrier thermal velocity. N_t trap concentration.

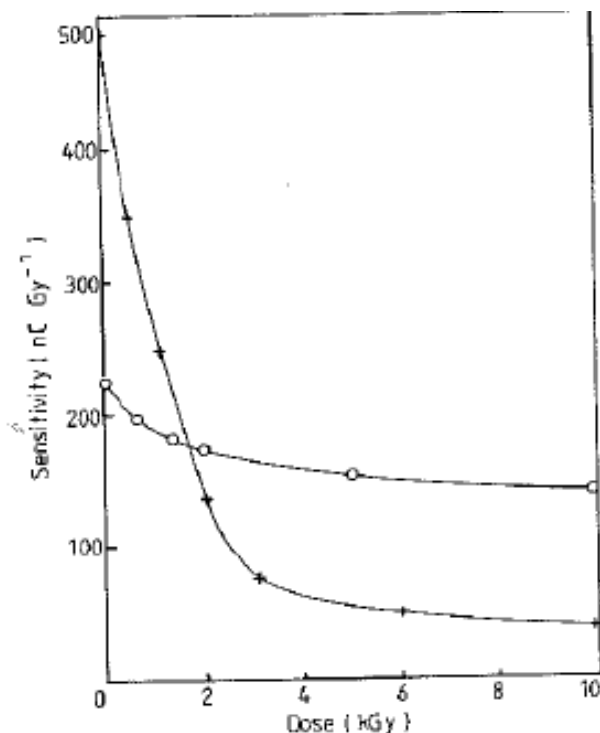
$a_{DOFZ} < a_{SFZ} \Rightarrow$ increased radiation hardness of the device to radiotherapeutic beams.

$$a_{DOFZ} = 5.0 \times 10^7 \text{ cm}^{-3}\text{Gy}^{-1}, \quad a_{SFZ} = 8.1 \times 10^7 \text{ cm}^{-3}\text{Gy}^{-1}$$

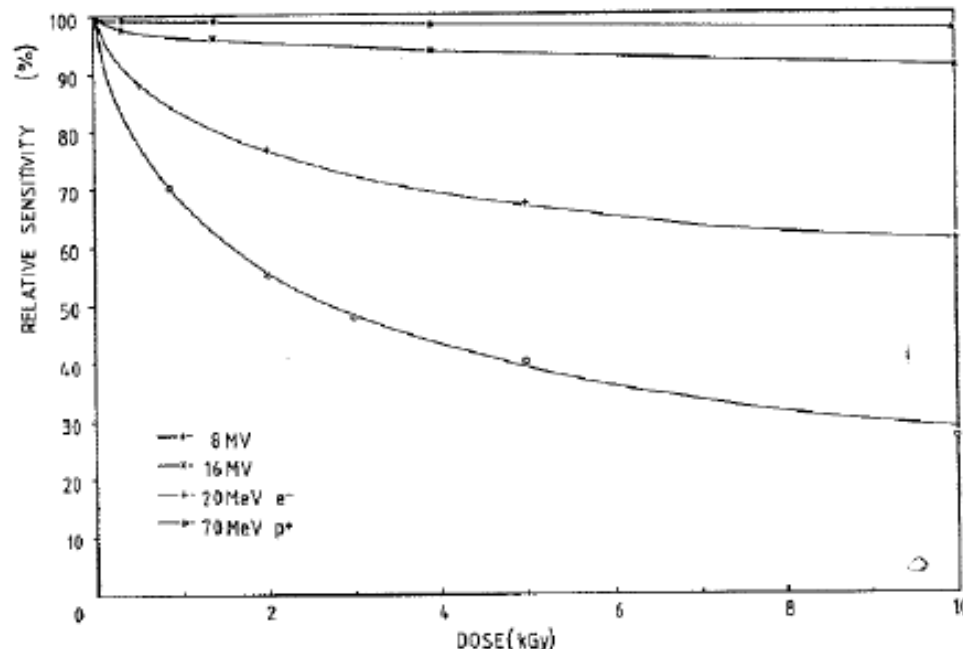


Radiation hardness of Si dosimeters

First radiation hardness solution (≈ 1980) has been pre-irradiation before use. In fact, since $S \propto N_t^{-1/2}$ pre-irradiation reduces the slope of sensitivity vs. dose curve. Usually 10kGy are adopted as a typical pre-irradiation.



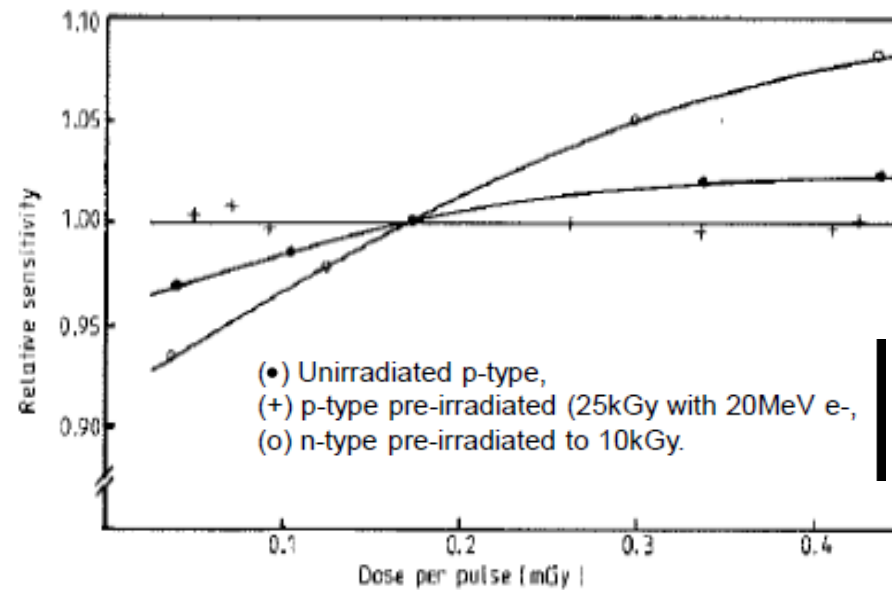
Sensitivity in a Co field of a p-type (o) and n-type (+) detectors, preirradiated with 20MeV electrons.
After Grusell and Rikner , 1984, Acta Radiologica Oncologica 23. 465-469.



Relative radiation damage effects caused by high energy radiation in p-Si detectors.
After Rikner G. et al., 1983, Nucl. Instr. and Meth. A, 217, 501-5.



Another radiation hardness solution (\approx 1980) was: working with p-type materials.



After Rikner G. and Grusell E., 1983, Phys. Med. Biol., 28, 1261-67.

In fact, dominant center produced by electron irradiation has cross sections:

$$\sigma_e = 1.62 \times 10^{-16} \text{ cm}^2,$$
$$\sigma_h = 8.66 \times 10^{-16} \text{ cm}^2.$$

see Shi J., Simon W. E., 2003, Med. Phys. 30, 2509-19
and cited refs.

This means that for this center is easier to capture holes. As diffusion is ruled by minority carriers, to get a transport less influenced by irradiation minority carriers must be electrons, thus material has to be p-type.

Material Engineering Recipe. Pt doping

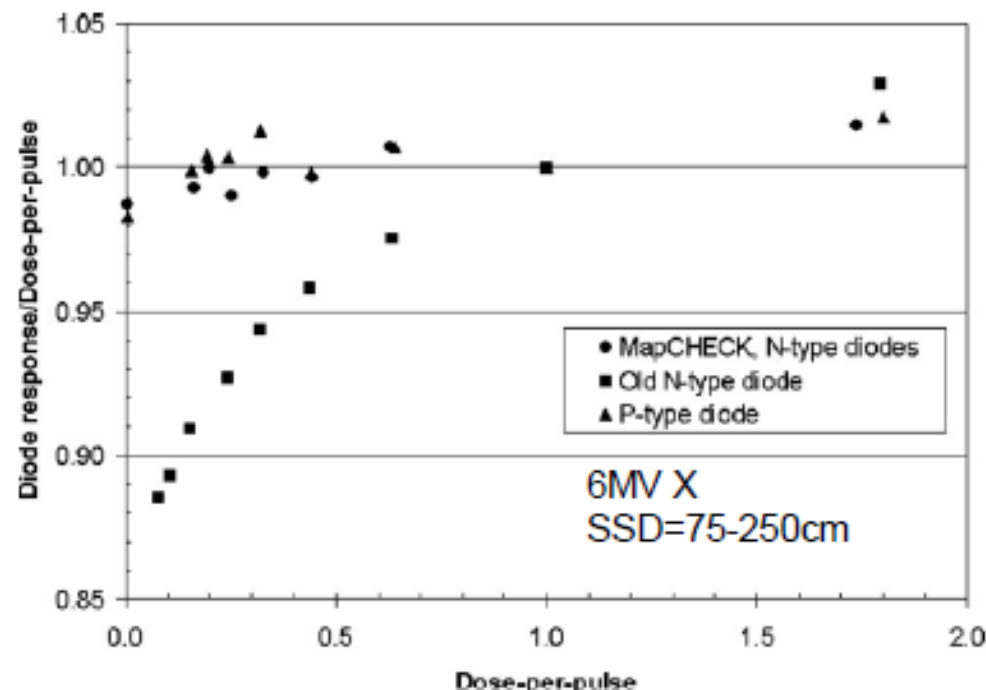
Platinum introduces a recombination level at (Baliga & Sun, 1977, IEEE Trans. Electron Devices 24, 685):

$$E_V + 0.42 \text{ eV},$$
$$\sigma_h = 2.7 \times 10^{-12} \text{ cm}^2$$
$$\sigma_e = 1.62 \times 10^{-16} \text{ cm}^2.$$

Large cross sections make Pt very effective in reducing minority carriers lifetime.

If Pt-related trap concentration is high enough:

- it dominates against radiation induced centers, and S is independent on accumulated dose;
- traps saturation and dose rate dependence are ruled out.



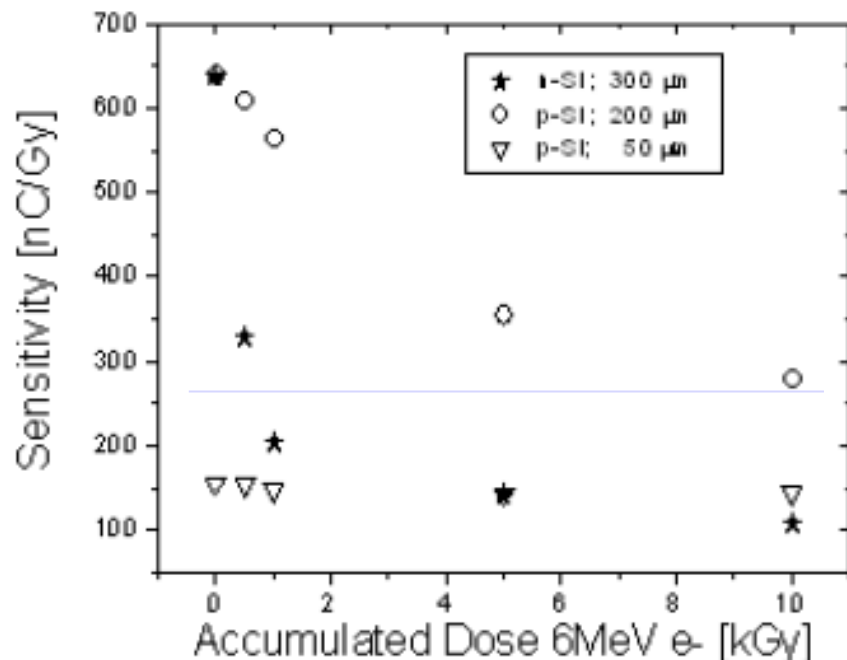
Old N-type: no Pt doping.
MapCHECK N-type: Pt doped
P-type: by Sun Nuclear

After Jursinic P. A. and Nelmsb B. E., 2003, Med. Phys. 30, 870-879.

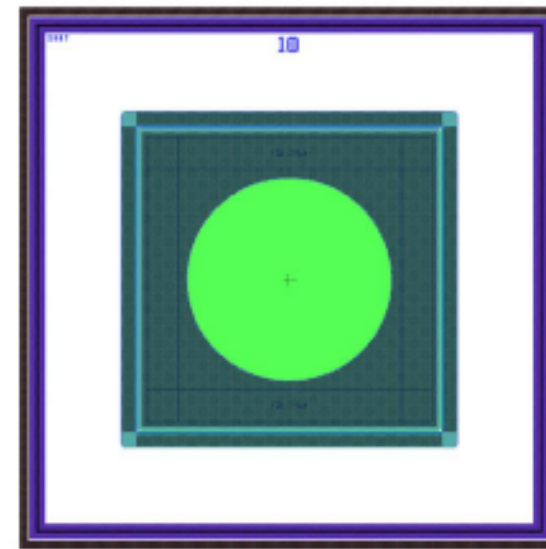


Our recipe: Low resistivity epitaxial p-type Si on MCz substrates

Concept: active region is limited in any direction to a value shorter than L_e at the highest dose of interest. Epitaxial Layer is used to limit active depth, guard-ring to limit active area.



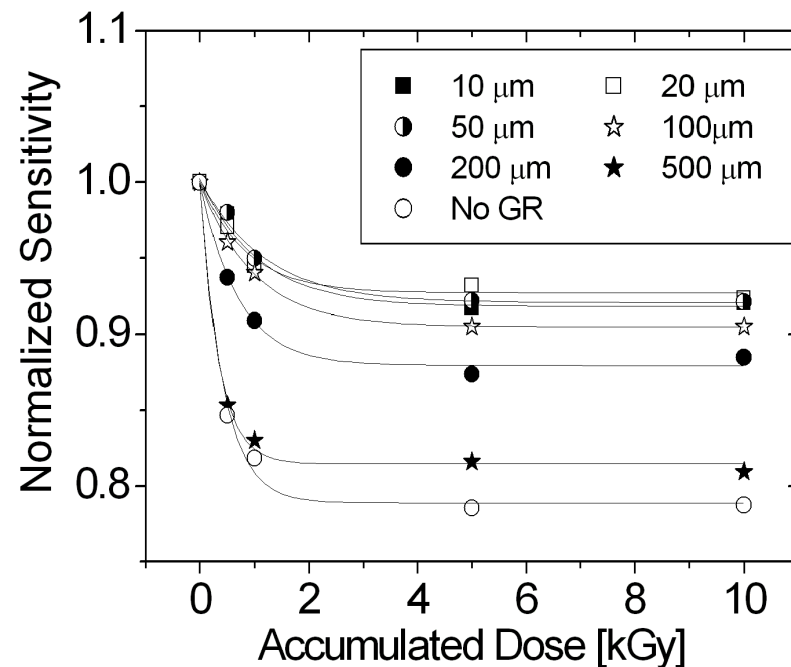
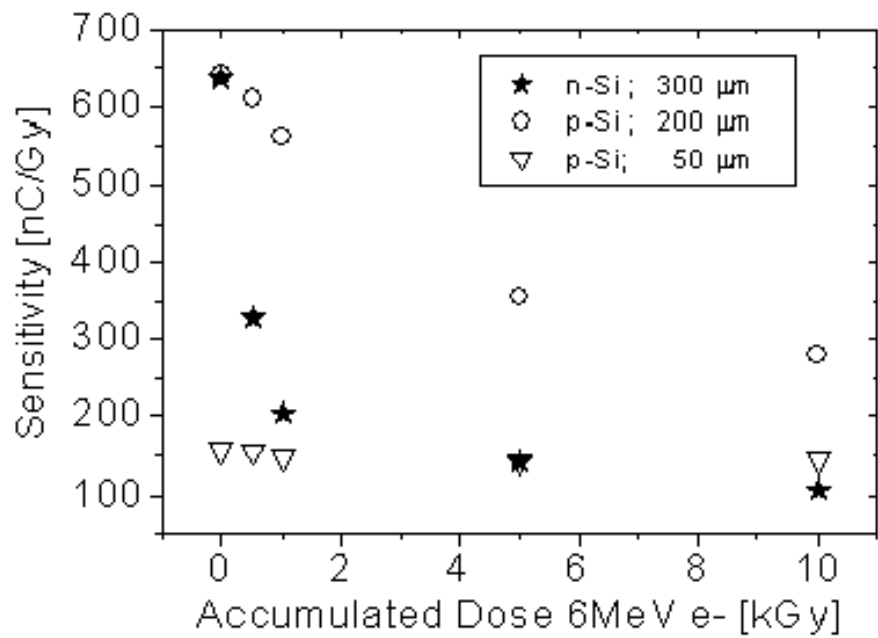
M. Bruzzi et al., "Epitaxial silicon devices for dosimetry applications," Appl. Phys. Lett., vol. 90 (2007) 172109 1-3.



Active area: ~9mm²
pad-grd distance: 10-500 μm
Epi layer: 50μm thickness
50Ωcm resistivity
p type



Improved stability of the sensitivity with the accumulated dose by using epitaxial Si (p-type) with guard ring to confine the active volume of the device



M. Bruzzi et al. App. Phys. Lett, 2007.

Italian patent No. FI2006A000166

Mara Bruzzi, Danno da radiazione in semiconduttori
Scuola Nazionale rivelatori ed elettronica per fisica delle alte energie , astrofisica 12 Aprile 2011,
Legnaro, Italy

Further Example: Solar cells in space radiation levels

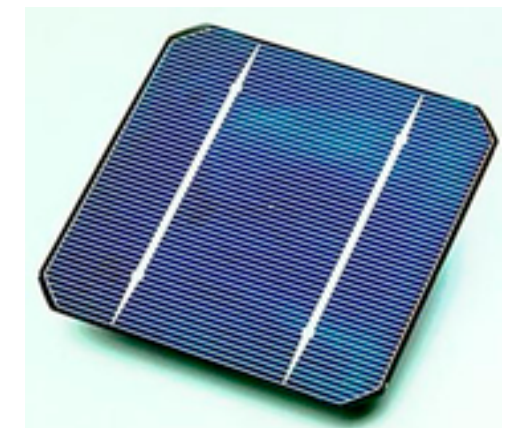
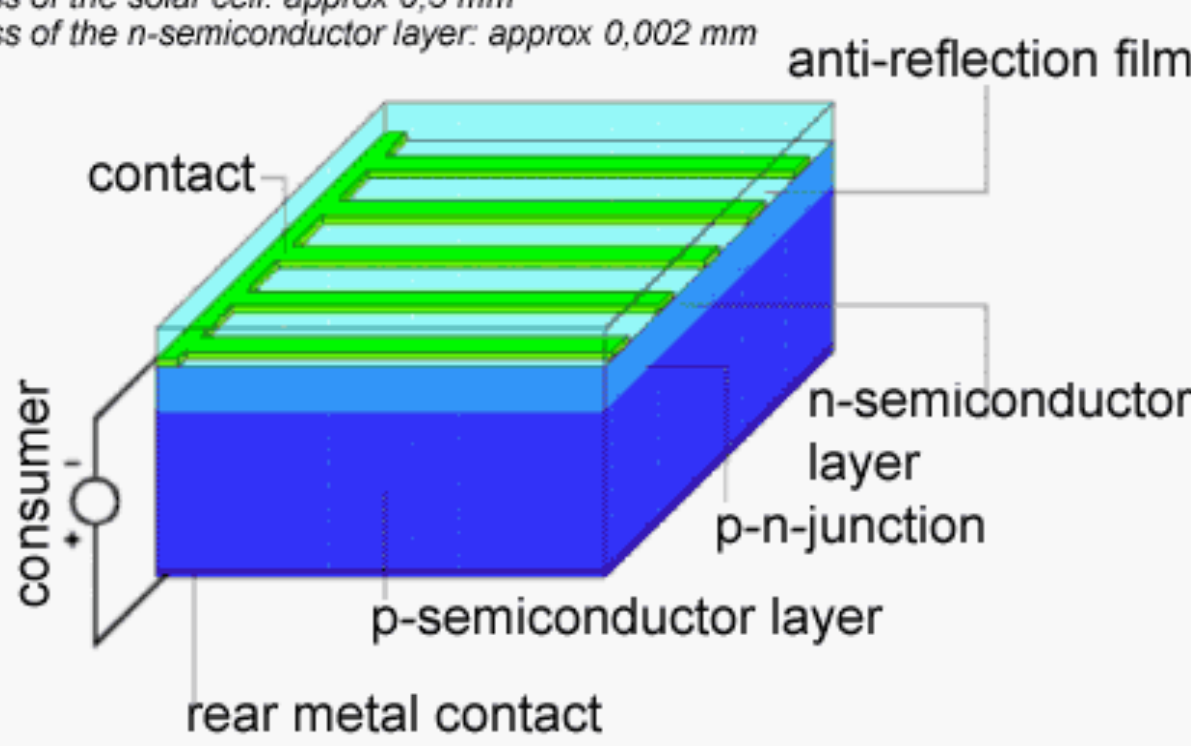
Main sources of radiation affecting PV modules are **protons and electrons trapped by the terrestrial magnetic field and protons coming from the Sun**, the particle flux depending on the orbit of the mission. Radiation damage in satellites at low altitude orbits (lower than 800 km) or in the high altitude ones (5000 km or higher) is mainly produced by protons (close to 90% of damage).

Most advantageous orbits for a global satellite network, both from cost and operational viewpoints, may be in Medium Earth Orbit (MEO), in the 2000–10 000 km range. Unfortunately, these orbits are in the midst of the Van Allen radiation belts, where the severe radiation environment causes a rapid degradation of the solar cells.

Working principle of a solar cell

Typical solar cell module is composed of n⁺/p/p⁺ junctions made on Silicon, used in photovoltaic mode. The built-in electric field leads to the separation of the charge carriers that are released by light. Silicon cells are approximately 10 cm by 10 cm large (recently also 15 cm by 15 cm). A transparent anti-reflection film protects the cell and decreases reflective loss on the cell surface.

*thickness of the solar cell: approx 0,3 mm
thickness of the n-semiconductor layer: approx 0,002 mm*



Solar cell efficiency factors

Maximum-power point

By increasing the resistive load on an irradiated cell continuously from zero (a *short circuit*) to a very high value (an *open circuit*) one can determine the maximum-power point, that is, the load for which the cell can deliver **maximum electrical power** at that level of irradiation. $V_m \times I_m = P_m$.

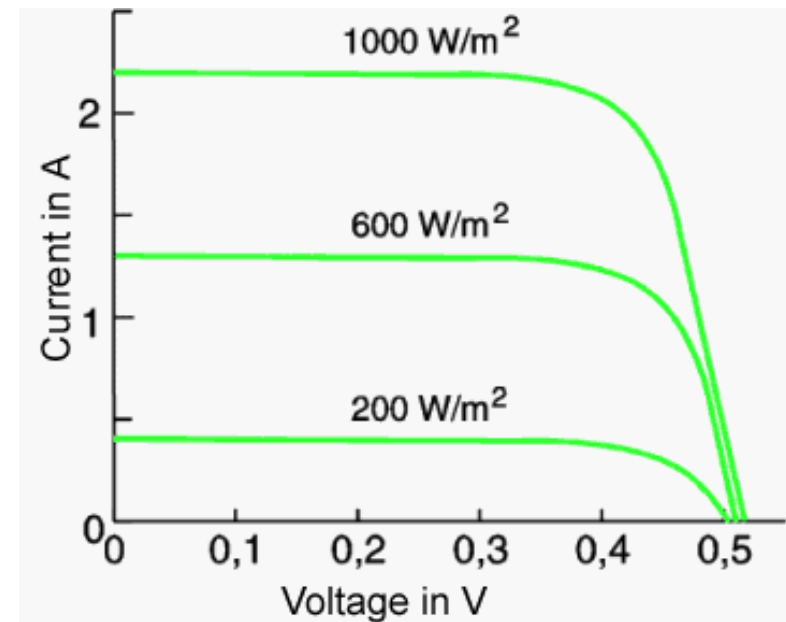
Energy conversion efficiency

A solar cell's *energy conversion efficiency* (η), is the percentage of power converted from absorbed light to electrical energy, calculated as P_m divided by the input light *irradiance* under "standard" test conditions (E , in W/m^2) and the *surface area* of the solar cell (A_c in m^2).

$$\eta = \frac{P_m}{E \times A_c}$$

Fill factor

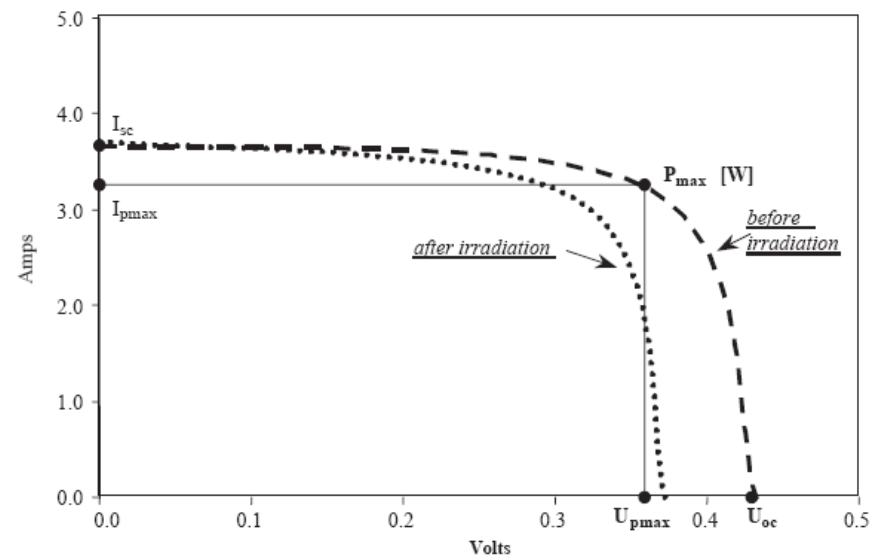
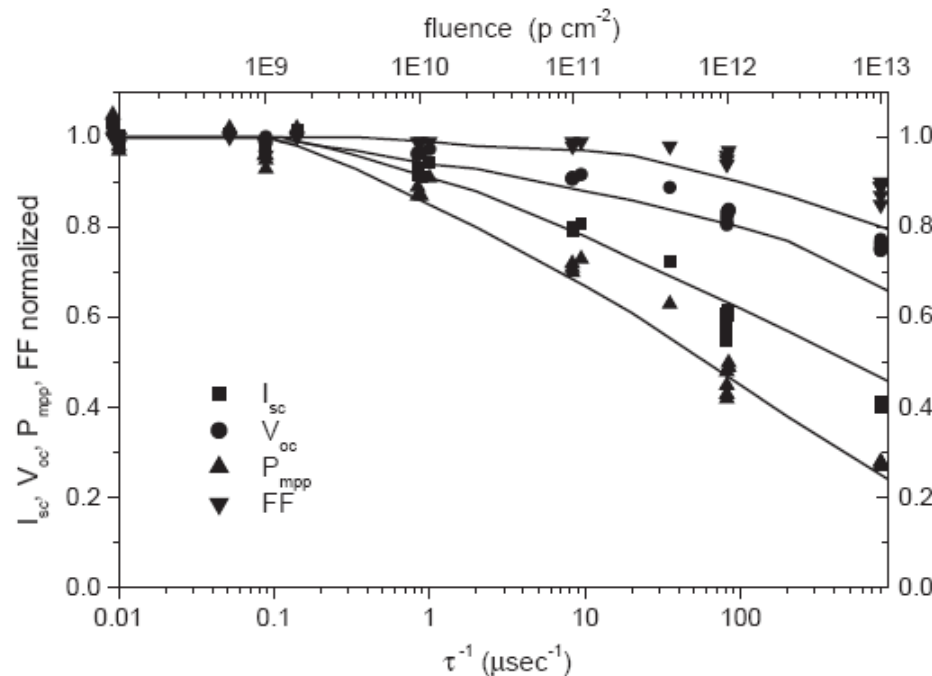
Another defining term in the overall behavior of a solar cell is the *fill factor* (FF). This is the ratio of the **maximum power divided by the open circuit voltage (V_{oc}) and the short circuit current (I_{sc})**:



$$FF = \frac{P_m}{V_{oc} \times I_{sc}} = \frac{\eta \times A_c \times E}{V_{oc} \times I_{sc}}$$

Radiation Damage in Si Solar cells

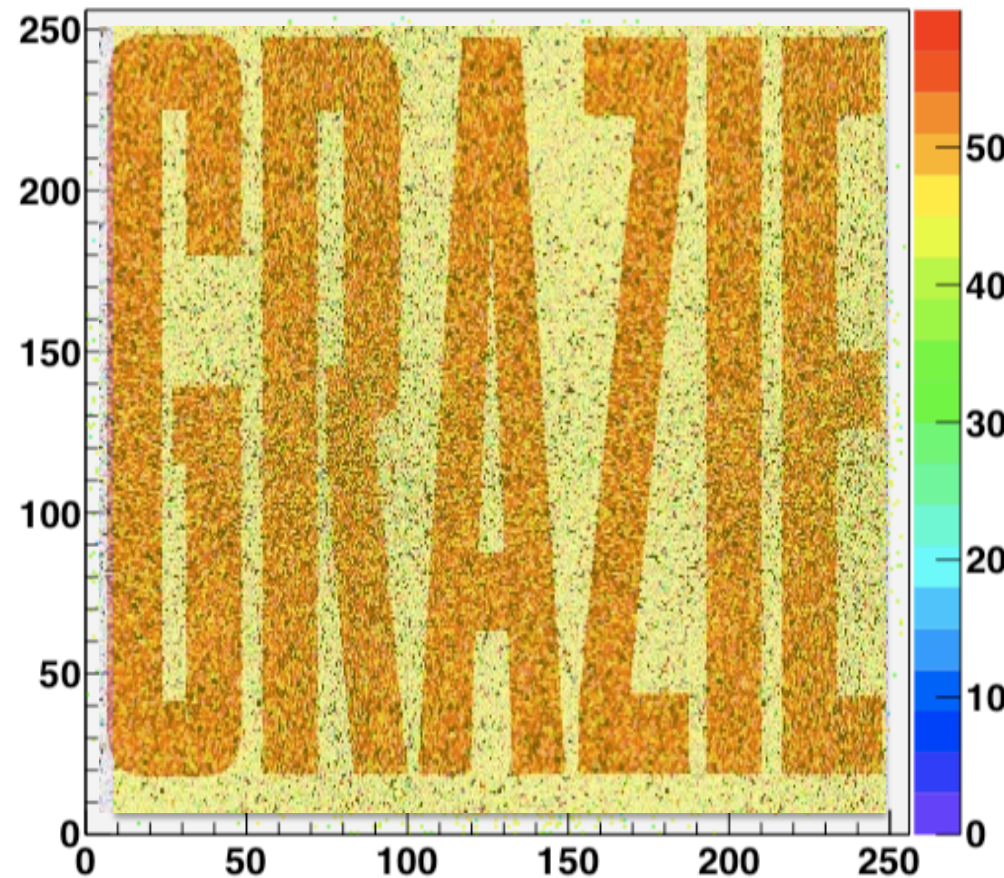
Deterioration of operative parameters of the solar cell due to the change of minority carrier lifetime



Conclusions

- Microscopic view of radiation Damage is a useful tool to quantitatively explain macroscopic radiation damage in semiconductor devices
- Material/Device Engineering successful
- Best to work on the subject interdisciplinarily
- RD50 forum for development of Ultra Radiation Hard Semiconductor Detectors

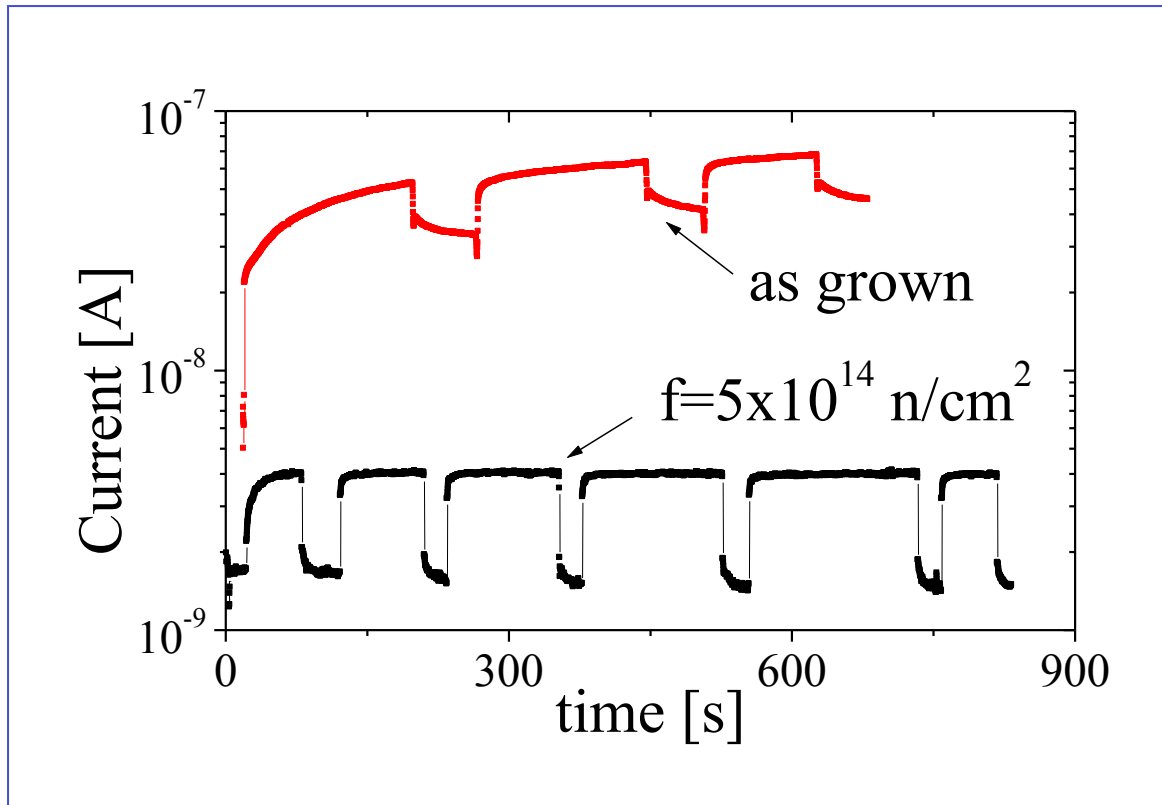




Mara Bruzzi, Danno da radiazione in semiconduttori
Scuola Nazionale rivelatori ed elettronica per fisica delle alte energie , astrofisica 12 Aprile 2011,
Legnaro, Italy



L'irraggiamento con elevate fluenze può anche migliorare le prestazioni del dispositivo: per esempio questo avviene nel dosimetro al diamante



Le proprieta' dosimetriche dopo irraggiamento con neutroni migliorano drasticamente a causa della rimozione di livelli energetici profondi

M. Bruzzi et al. App.Phys.Lett. (2002)

Forte diminuzione dei segnali TSC e PICTS relativi ai difetti responsabili della instabilità di corrente dopo irraggiamento con neutroni a tale fluenza

2

Appl. Phys. Lett., Vol. 81, No. 1, 1 July 2002

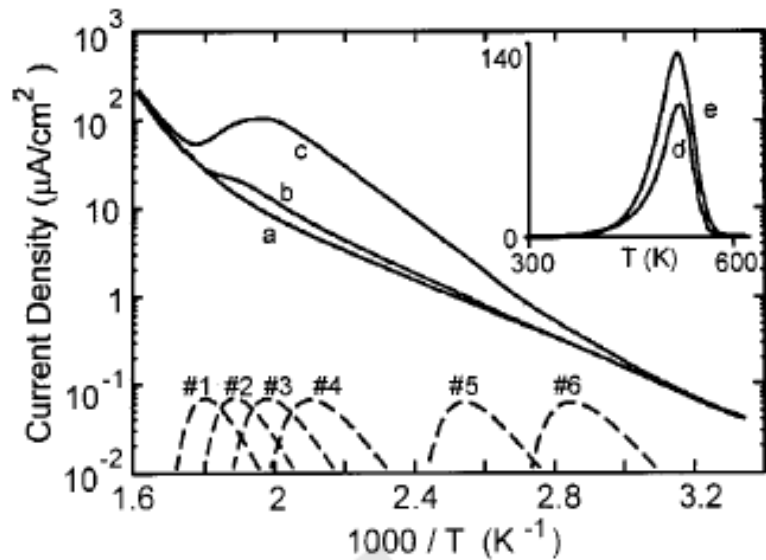


FIG. 1. TSC measurements performed with heating rate $\beta=0.15 \text{ K/s}$ and $V_{\text{bias}}=100 \text{ V}$. The background current (a) is measured without excitation. The other curves in the main plot correspond to measurements performed after a 30 min excitation using the Xe lamp, before (c) and after (b) NI. The contributions of fit components Nos. 1–6, calculated with arbitrary amplitudes, are shown in the bottom (dashed lines) for comparison. The spectra in the inset have been measured after a priming with a Co^{60} γ -source, up to a dose of 8 Gy; the signal measured after NI (d) is multiplied by ten for better comparison with the spectrum measured before NI (e).

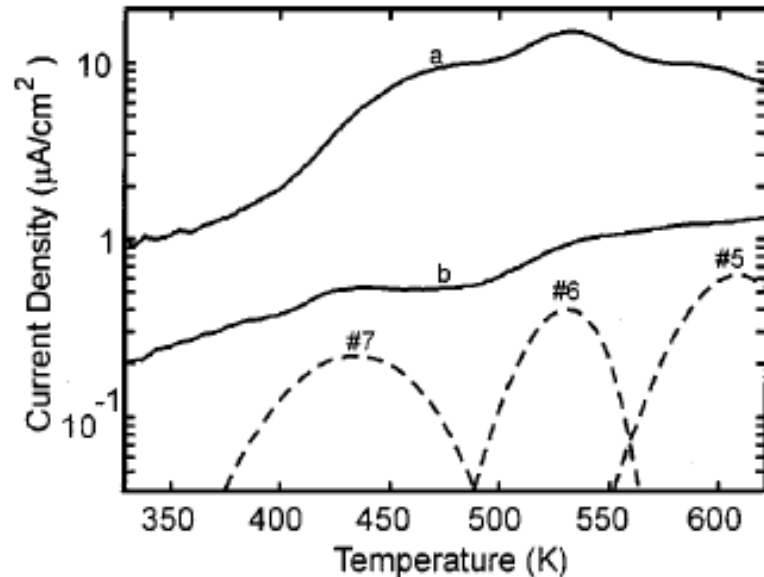
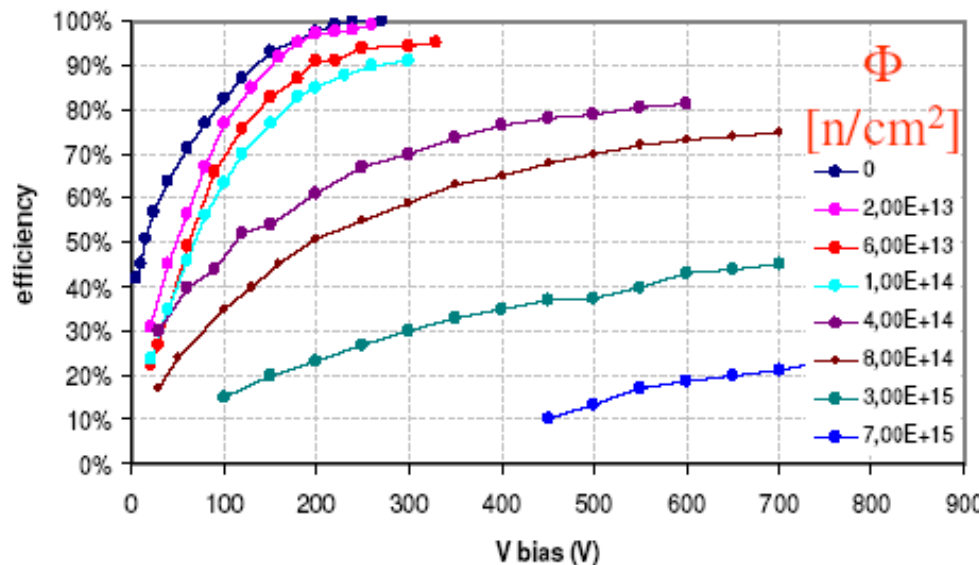


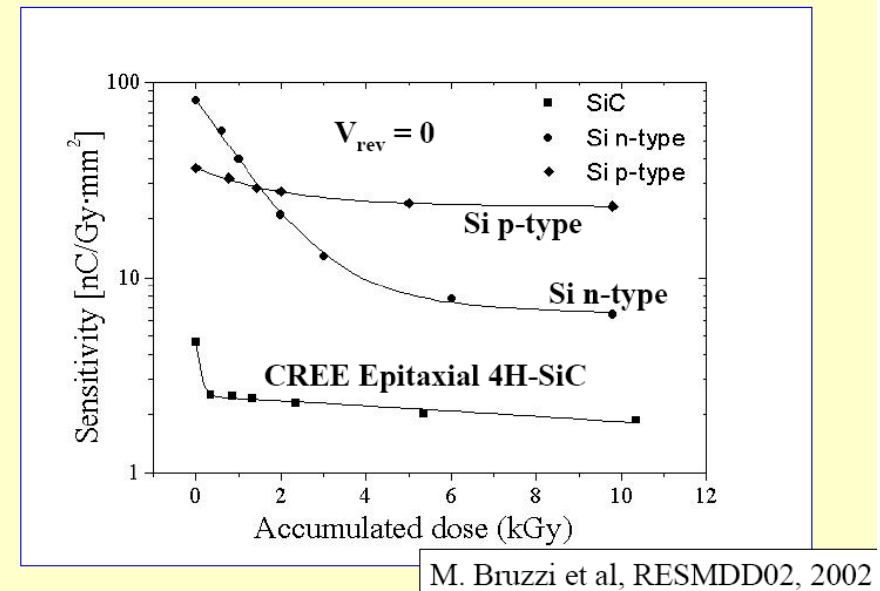
FIG. 2. PICTS spectra measured before (a) and after (b) NI. The calculated spectral lines corresponding to deep levels Nos. 5–7 are reported in the bottom (dashed lines), with arbitrary amplitude, for comparison.
COPY 054226APL

SiC: not radiation resistant as a high energy physics detector and a radiotherapy dosimeter.



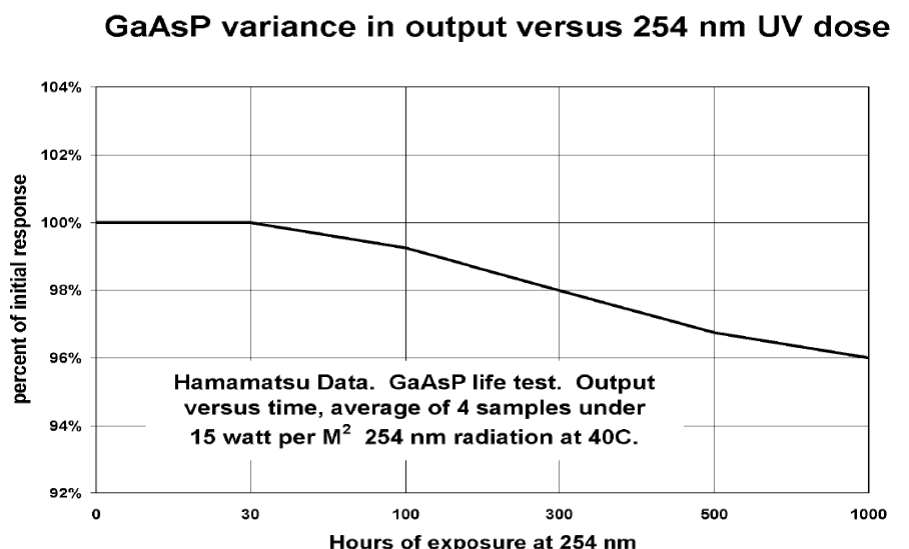
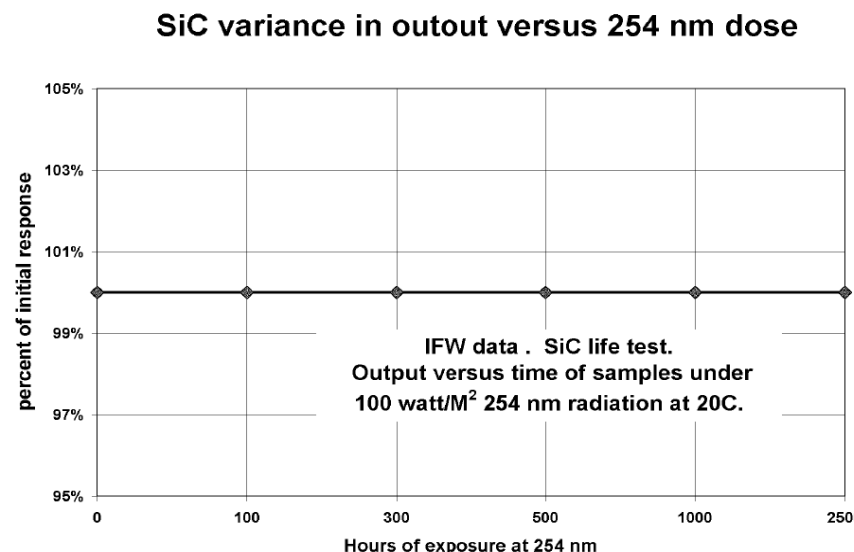
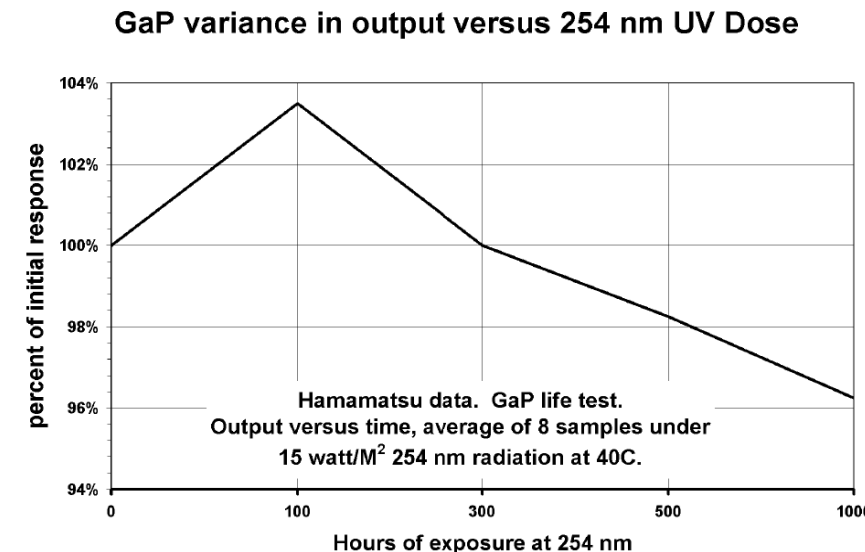
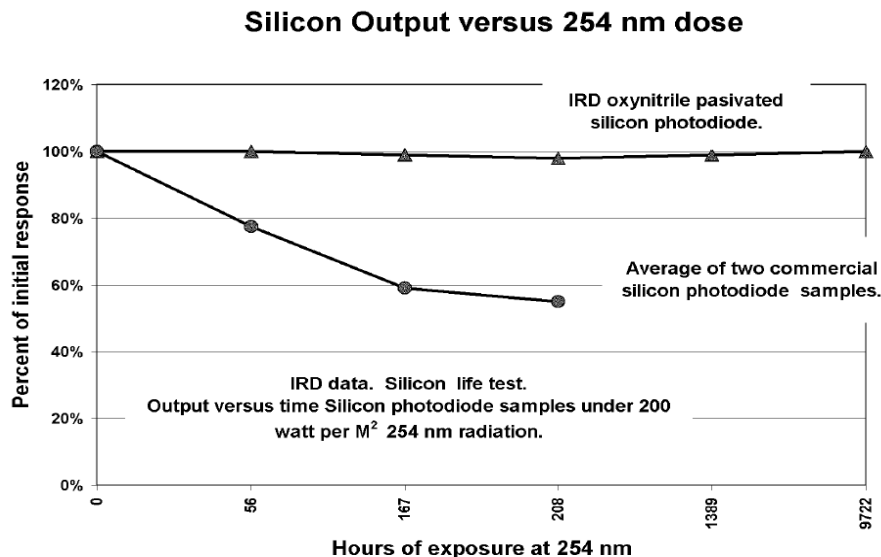
[F. Nava, INFN & University of Modena, Oct. 2004]

Sensitivity vs. Accumulated Dose after irradiation with Cs^{137}



M. Bruzzi et al, RESMDD02, 2002

But good radiation resistance as UV photodetector, extremely stable for long periods of time even when exposed to high doses of UV radiation of up to 100W/m²



Activation energy and apparent cross section

Thermodinamically, the ionization energy ΔE_t is defined as the chemical potential for the reaction forming one ionized defect and a free carrier. This is equal to the increase in the Gibbs free energy upon increasing the number of free carriers by one at constant temperature and pressure:

$$\Delta E_t = \Delta H_t - T \Delta S_t$$

The capture cross section is also temperature dependent according to the law:

$$\sigma_n(T) = \sigma_\infty \exp\left(-\frac{E_\sigma}{KT}\right)$$

and:

$$e_n = \gamma \sigma_{na} T^2 \exp\left(-\frac{\Delta H + E_\sigma}{KT}\right) = \gamma \sigma_{na} T^2 \exp\left(-\frac{E_{na}}{KT}\right)$$

Where the entropy term is included in σ_{na} (apparent cross section) and E_{na} represent the activation energy of the trap (electrons).



Mara Bruzzi, April 11, 2011

